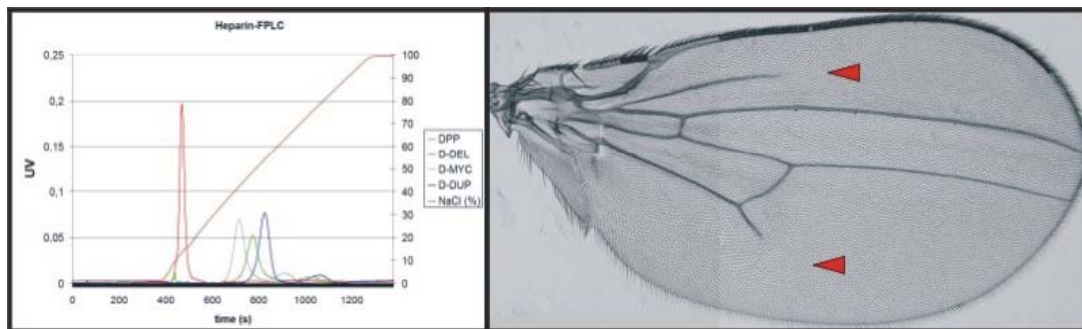




Functional and developmental characterisation of matrix binding sites in *decapentaplegic*



Dissertation zur Erlangung des
naturwissenschaftlichen Doktorgrades
der Bayerischen Julius-Maximilians-Universität Würzburg

vorgelegt von
Martin Roth
aus Würzburg

Würzburg 2003

The figures on the cover page represent biochemical and developmental approaches to understand matrix interactions of Decapentaplegic

Left: Graph of a heparin affinity chromatography performed with different DPP variants

Right: Wing preparation of *D.melanogaster*. Distal gaps in longitudinal veins (indicated by red arrowheads result from ubiquitous overexpression of a strong matrix binding DPP-variant in 3rd larvae wing imaginal disc.

eingereicht am:

Mitglieder der Promotionskommission:

Vorsitzender:

Gutachter: Prof. Dr. Gert O. Pflugfelder

Gutachter: Prof. Dr. Walter Sebald

Tag des Promotionskolloquiums:

Doktorurkunde ausgehändigt am:

Index

1 Introduction	1
1.1 Extracellular Matrix	2
1.1.1 Structural matrix proteins	2
1.1.2 Matrix carbohydrates	3
1.1.3 Proteoglycans and signaling	5
1.1.3.1 Glypicans and signaling	5
1.2 Decapentaplegic	6
1.2.1 The TGF- β superfamily and BMP-family	6
1.2.2 DPP structure and function	6
1.2.3 The DPP signaling pathway	7
1.2.4 DPP activation	8
1.2.5 DPP-interacting proteins	8
1.2.6 DPP receptors	8
1.2.6.1 Receptor interacting proteins	9
1.2.7 Smad proteins	9
1.2.7.1 Smad interacting proteins	10
1.2.8 DPP target gene regulation	11
1.3 DPP in development	12
1.3.1 DPP in dorsal-ventral axis patterning	12
1.3.2 Endoderm induction by DPP	13
1.3.3 DPP and tracheal development	13
1.3.4 Wing imaginal disc patterning via DPP	14
1.4 Aim of the project	16
2 Material and methods	17
2.1 Material and solutions	17
2.1.1 Solutions for cell lysis	17
2.1.2 Solutions for Western blotting	17
2.1.3 Solutions and equipment for protein purification	17
2.1.4 Solutions for viral expression of Tkv ectodomain in SF9 cells	18
2.1.5 Solutions for calcium phosphate transfection	19
2.1.6 Solutions for wing disc antibody staining	19
2.1.7 Solutions for embryo antibody staining	19
2.1.8 Solutions for limbbud assay	20
2.1.9 Protein markers	20
2.2 Methods	20
2.2.1 SDS-PAGE	20
2.2.2 Western blotting	20
2.2.3 Protein purification	21
2.2.4 Cell culture	22
2.2.5 Calcium phosphate transfection	22
2.2.5.1 Generation of stable cell lines	22
2.2.6 Viral expression of proteins	22
2.2.7 Biotinylation of ectodomains	23
2.2.8 Biacore measurements	23
2.2.9 Limbbud assay	24
2.2.10 Drosophila germline transformation	24
2.2.11 Larval heat shocks	24
2.2.12 Staining of wing imaginal discs	24
2.2.13 Staining of embryos	24
3 Results	26
3.1 Generation of DPP variants	26
3.2 Biochemical studies with recombinant DPP	27
3.2.1 Expression of DPP and DPP-variants in E.coli	27
3.2.2 Renaturation of DPP and DPP-variants	28
3.2.3 Purification of DPP and DPP-variants	28
3.2.4 Heparin affinity chromatography	29
3.2.5 Cloning and purification of the Tkv ectodomain	30

3.2.6	Biacore measurements with the Tkv ectodomain	32
3.2.7	The limbbud assay	33
3.3	Effects of ectopically expressed DPP-variants in Drosophila	34
3.3.1	Generation of transgenic flies	34
3.3.2	Testing the pUFWT system	34
3.3.3	Expression-test of pUAST-constructs	36
3.3.4	Clonal expression of UAS-DPP in the wing imaginal disc	37
3.3.5	Expression of DPP-variants in wing imaginal discs by various gal4-driver lines	38
3.3.6	Rescue of transheterozygous dpp^{dl2}/dpp^{dl4} flies by DPP-Variants	42
3.3.7	Expression of DPP-variants in the tracheal system	43
3.4	DPP-reporter systems	45
3.5	Influence of DPP and its receptors on Mad phosphorylation	47
4	Discussion	
4.1	Design of Variants	50
4.2	Expression and purification of recombinant DPP-variants	51
4.3	Biochemical properties of DPP-variants	51
4.3.1	Heparin affinity of DPP-variants	51
4.3.2	Receptor affinity of DPP-variants	51
4.3.3	Biological activity of DPP-variants	52
4.4	Design of expression systems in D. melanogaster	53
4.5	Moderate matrix-binding implications in DPP signaling in the wing imaginal disc	54
4.5.1	Overexpression of DPP-Variants in the endogenous DPP-domain	54
4.5.2	Overexpression of DPP-Variants in the Omb-domain	54
4.5.3	Ubiquitous overexpression of DPP-variants in the disc	55
4.5.4	Wing disc rescue by DPP-variants	56
4.6	Matrix-binding requirement of DPP in the tracheal system	56
4.7	Tissue specific relevance of matrix binding on DPP signaling	57
4.8	Matrix binding and gradient formation	58
4.9	DPP signaling in cell culture assays	60
5	References	62
6	Summary/Zusammenfassung	72
7	Abbreviations	74
8	Appendix	76
	Constructs	76
	Primer	77
	Fly stocks	80
	Cloning details	81
Publikationen		82
Lebenslauf		83
Erklärung		84
Danksagungen		85

1 Introduction

The Blind Men and the Elephant

Indian folktale retold in poetic form by Godfrey Saxe

It was six men of Indostan,
To learning much inclined,
Who went to see the elephant,
(Though all of them were blind),
That each by observation
Might satisfy his mind.

The first approached the elephant,
And happening to fall
Against his broad and sturdy side,
At once began to bawl:
"God bless me! But the elephant
Is very like a wall!"

The second, feeling of the tusk,
Cried: "Ho! What have we here,
So very round and smooth and sharp?
To me 'tis very clear,
This wonder of an elephant
Is very like a spear!"

The third approached the animal,
And happening to take
The squirming trunk within his hands,
Thus boldly up and spake:
"I see," quoth he, "the elephant
Is very like a snake!"

The fourth reached out an eager hand,
And felt about the knee.
"What most this wondrous beast is like
Is might plain," quoth he;
"'Tis clear enough the elephant
Is very like a tree."

The fifth, who chanced to touch the ear,
Said: "E'en the blindest man
Can tell what this resembles most:
Deny the fact who can,
This marvel of an elephant
Is very like a fan."

The sixth no sooner had begun
About the beast to grope,
Than seizing on the swinging tail
That fell within his scope,
"I see," quoth he, "the elephant
Is very like a rope."

And so these men of Indostan
Disputed loud and long,
Each in his own opinion
Exceeding stiff and strong,
Though each was partly right,
All were in the wrong.

1.1 The Extracellular Matrix

Extracellular matrix (ECM) defines the intricate network of macromolecules that fills large parts of the extracellular space. The matrix is composed of a variety of versatile proteins and polysaccharides that are secreted locally and assembled to an organized meshwork connected to the producing cells. As part of the architectural framework of vertebrate bodies extracellular matrix occupies the majority of space in connective tissues. To fulfill a variety of function in different tissues ECM can adopt a diversity of consistencies. In bones and teeth matrix occurs calcified and rock-like whereas in cartilage it is gellike and elastic. While built to compensate stretching forces in tendons the matrix in joints enables to withstand 100 atmospheres of pressure. Even the transparent cornea is nothing more than specialized ECM. Another appearance of matrix is the basallamina at the interface of epithelia and connective tissues.

In most connective tissues the matrix with all its diverse macromolecules is secreted by fibroblasts that are located within the matrix. There are two dominant types of secreted molecules: The polysaccharide chains called glycosaminoglycans and fibrous proteins with mainly structural function like collagen and elastin or mainly adhesive function like fibronectin and laminin [1-3].

1.1.1 Structural matrix proteins

Collagen contributes to about 25% of mammal protein mass and is one of the most abundant proteins on earth. There are at least 16 types of collagen, but 80-90% of the body's collagen consist of fibrillar collagen of type I, II and III. Type I collagen found in bone, skin and tendons consists of two $\alpha 1(I)$ chains and one $\alpha 2(I)$ chain which form the typical triple helix. To allow the close arrangement of three polypeptides in this helix nearly every third aminoacid in each strand is glycine, the smallest aminoacid. Two other frequent aminoacids proline and hydroxyproline stabilize the helix conformation because of their ring structure. Another unusual aminoacid, hydroxylysine is a target site for glycosylation in collagen. The collagen chains are synthesized with N- and C-terminal propeptides and secreted into ER and Golgi apparatus. Here after hydroxylation and glycosylation of sidechains three chains are linked in the C-terminal propeptides by cystin-bridges and the central part forms the triple helix. Because of solubility inside the cell the propeptides are removed after secretion by extracellular procollagen peptidases. The resulting roughly insoluble tropocollagen assembles to large fibrils stabilized by hydrogen bonds between hydroxyproline residues and covalent bonds between hydroxylysine residues. Collagen fibers are arranged to larger networks which can be thick parallel fibers like in tendons or as a wickerwork pattern in skin. This depends mostly on the type of fibril-associated collagen. Collagen IX has a nonhelical region that leads to a flexible kink inside the triple helix, also propeptides are not removed. Therefore collagen IX cannot form fibers but associates to type II fibrils and connects them in a crosslike pattern. To link type I fibrils to large fibers, collagen VI consists of thin triple helices with globular domains at each end. Association of these domains leads to long microfibrils that connect adjacent type I fibers.

Epithelial tissues and connective tissues are separated and connected by the **basal lamina**. Basal laminas can also have more specific functions e.g. as molecular filter between blood and urine in the kidney glomerulus or in covering muscle cells and the Schwann cells in the nervous system. Among other specialized matrix molecules collagen IV builds a stable sheetlike network. The collagen IV triple helix is interrupted several times by nonhelical segments and the C-terminus ends in a large globular domain. Lateral interactions between triple-helical segments and head to head interactions of globular domains enable the collagen IV to assemble to this unique planar network. Beneath collagen IV almost all basal laminas consist of the glycoproteins laminin and entactin and the proteoglycan perlecan. **Laminin** is a large molecule (~850kD) consisting of three single polypeptide chains: A, B1 and B2. There exist several isoforms of each chain leading to several types of laminin. Structurally, laminin is cross-shaped with a coiled-coil arrangement of all three chains in the central part, where the chains are crosslinked by disulfid bridges. Like other proteins in the ECM, laminin consists of many different domains: some bind to different collagen types, one to heparan sulfate, some to sulfated lipids and others to entactin and laminin receptors. Interactions between globular domains at the ends of the cross-arms lead like collagen IV to a feltlike sheet.

Many tissues like skin, blood vessels or lungs need to be not only strong but also elastic in order to function. Whereas strength is achieved by collagen, a fibernetwork made of elastin and microfibrillar proteins provides elasticity. **Elastin**, like collagen, has an unusual aminoacid composition: it consists of two types of short segments. One, rich in glycine, proline and valine can assemble to a unique structure only found in elastin, a random coiled structure. The other builds usual α -helices and is rich in alanine and lysine. The latter can, like in tropocollagen, be linked to other lysine residues by the extracellular enzyme lysyl-oxidase. Therefore an elastic fiber is composed of many crosslinked elastin molecules.

The cells producing the ECM need to keep in contact to the matrix. Therefore there are a number of adhesive proteins that have multiple specific binding sites for matrix macromolecules and cellsurface receptors. One

protein with stands as a prototype for this connective molecules is **fibronectin**, a large dimeric glycoprotein. Fibronectin mainly consists of many variations of three different motifs, each encoded by a single exon. The main motif, the type III fibronectin repeat, occurs at least 15 times in each fibronectin monomer and is also found in other matrix proteins. As fibronectin plays multiple rolls in different tissues like blood clotting, organization of the cytoskeleton or cell migration there exist at least 20 different isoforms of fibronectin resulting from alternative splicing between the 50 exons. Six specific domains were functionally characterized. There are two binding sites for fibrin (involved in blood clotting), two binding sites for the glycosaminoglycan heparan sulfate, one collagen binding site and one for the integrin family of cell surface receptors. This integrin binding site could be reduced mainly to a tripeptide sequence (Arg-Gly-Asp) therefore called RGD-sequence [1-4].

1.1.2 Matrix carbohydrates

In addition to the diverse group of matrix proteins there is the group of matrix carbohydrates, the glycosaminoglycans, which is in its molecular assembly very similar. **Glycosaminoglycans (GAGs)** are large unbranched sugarchains always occurring as repeating units of a simple disaccharide motif. Some are attached to coreproteins, then called proteoglycans, others are secreted. The GAGs can be ordered into four main groups, depending on the type of sugarmonomers and sidegroup modifications (see figure 1).

The most simple one, because never sulfated, is **hyaluronan**. It consists of alternating D-glucuronic acid and N-acetyl-D-glucosamine groups. There are up to 50.000 repeats of the disaccharide motif in one hyaluronan molecule. Hyaluronan only exists in secreted form and is not attached to cell surface coreproteins. Because of its anionic character through multiple repeating COO⁻ groups, hyaluronan attracts a lot of water and fills much more space than proteins of the same size. This leads in cartilage to a gellike structure that allows resisting to compression forces. In embryogenesis hyaluronan plays an important role in cell migration. Often when cell-free spaces develop, they are first filled with hyaluronan before cells migrate into it like in the developing heart, cornea and other organs. There are also many cell-surface and matrixproteins like CD44 that share the same hyaluronan binding domain. Through these interactions migrating and proliferating cells can cover themselves with an anionic hyaluronan coat that repells them from other cells.

In the more complex GAGs various positions in the repeating dimers are modified. These GAGs are with 15-250 repeats of the disaccharide unit much shorter than hyaluronan and in most cases attached to core proteins. GAGs are always attached to serine residues via a constant tetrasaccharide linker (xylose-galactose-galactose-glucuronic acid).

Chondroitin sulfate and **dermatan sulfate** consist of D-glucuronic acid and N-acetyl-D-galactosamine, the former is epimerized to L-iduronic acid in dermatan sulfate. Both are highly sulfated.

The most prominent and versatile GAG, **heparin/heparan sulfate**, is involved in a variety of biological phenomena including cell proliferation, differentiation, cell adhesion, angiogenesis, blood coagulation, lipid metabolism and bacterial/viral infections. It exists in secreted form and as attached sidechain in proteoglycans.

The secreted form heparin is produced in mast cells and the protein linked heparan sulfate is found associated with the cell surface of nearly every cell [5-7]. Heparin/heparan sulfate consists of D-glucuronic acid or L-iduronic acid and N-acetyl-D-glucosamine and is highly sulfated. Sulfation is not uniformly present at every disaccharide unit but starts at several points within the chain by substituting of N-acetyl groups by N-sulfo groups. From this start point sulfation spreads along the chain and leads to additional sulfation of selective 2-, 3- and 6-OH-groups, but there are always regions left unsulfated [5, 8]. Heparan sulfate is the most extensively examined GAG and there have been plenty of molecules identified that bind to heparan sulfate. In many cases also the biological activity is modulated by this interaction (see Table 1-1) [9].

The forth common GAG, keratan sulfate, consists of repeats of D-galactose and N-acetyl-D-glucosamine and is moderately sulfated [1, 2].

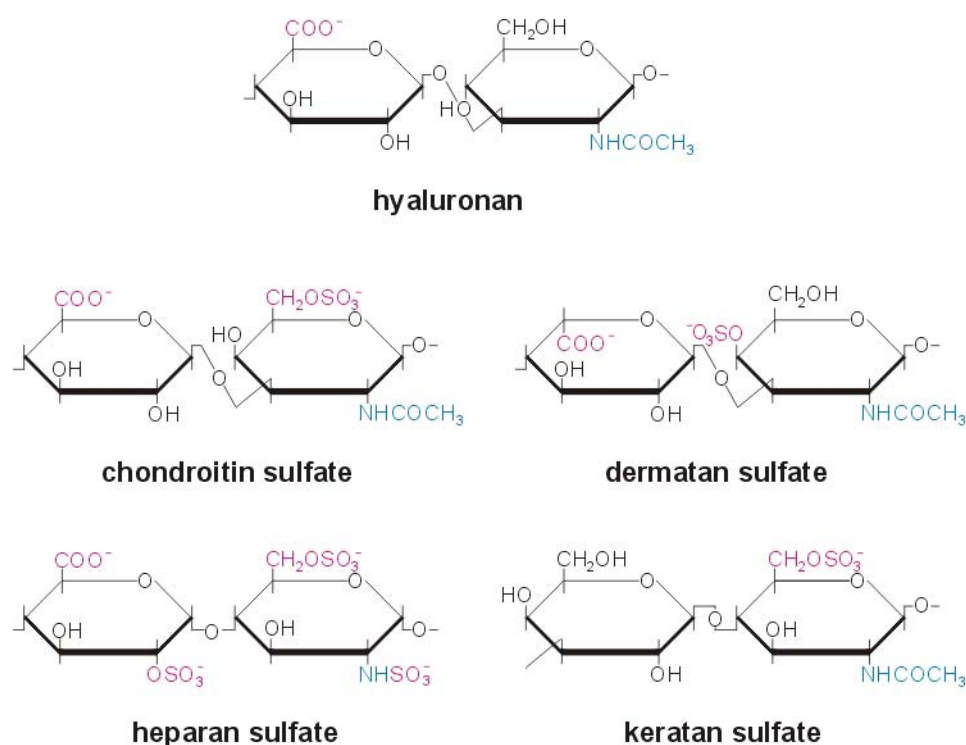


Figure 1-1: Dissaccharide units of major glycosaminoglycans
Negatively charged groups are shown in red, aminogroups in blue.

Angiogenesis: Angiostatin, endostatin, vascular endothelial growth factors

Cell-matrix interactions: laminin, fibronectin, thrombospondin, collagen types I,II and V, fibrillin, tenascin, vitronectin

Coagulation/fibrinolysis: Antithrombin III, heparin cofactor II, tissue factor pathway inhibitor, thrombin, protein C inhibitor, tissue plasminogen activator, plasminogen activator inhibitor-1

Growth factors/morphogens: Fibroblast growth factors (FGFs) and FGF receptors, Wingless (Wnt) factors, Hepatocyte growth factor (HGF, scatter factor) transforming growth factors (TGFs)β1 and 2, bone morphogenetic proteins (BMPs) 2,3,4 and 7, Hedgehog factors

Inflammation: Chemokines (e.g., MIP-1b); cytokines (e.g., IL-2, -3, -4, -5, -7, -8, and -12); L- and P-Selectins, Extracellular superoxide dismutase; antimicrobial peptides

Lipid metabolism: Lipoprotein lipase, hepatic lipase, apolipoprotein E

adopted from ref. [10]

Table 1-1: Examples of molecules whose biological activity is modulated by binding to heparan sulfate chains

Proteoglycans represent a large family of diverse cellular or secreted molecules found on or near every cell. They differ much from simple glycoproteins which contain 1-60% carbohydrates by weight. Whereas proteoglycans are in most cases also glycoproteins, their carbohydrate content can reach up to 95% because of their long sidechains. Also the number of sidechains can vary from one to over hundred. **Decorin**, carrying one heparan sulfate chain, has a molecular weight of ~ 40 kD and covers collagen fibers. The **aggrecan** coreprotein has 127 serine residues linked to 30 keratan sulfate chains and 97 chondroitin sulfate chains resulting in a molecule of around 2000 kD. In cartilage around 100 aggrecans are linked by small adaptor proteins to one hyaluronan chain resulting in a large biopolymer of around 200 000 kD, named “aggrecan aggregate”. This large complexes form a gellike matrix which can absorb in joints pressures of 100bar. **Perlecan**, a proteoglycan with

three heparan sulfate sidechains, exists in basal laminae. In the kidney glomeruli, the GAG chains build the molecular filter system.

Most cell anchored proteoglycans are assigned to two distinct families, the **glypicans** and the **syndecans**.

Glypicans are GPI-anchored cell surface proteins carrying only heparan sulfate sidechains in close proximity to the cell surface. Syndecans are transmembrane proteins and dimerize with their transmembrane regions. The cytosolic domains interact with cytoskeleton and PKC, whereas the extracellular part is decorated with several heparan or chondroitin sulfate chains. Thus besides other cellular receptors like integrins, syndecans are thought to be the main connections between cells and the ECM [11].

1.1.3 Proteoglycans and signaling

In the past years, it became more and more evident, that proteoglycans not only serve as structural matrix components but play key roles or have supporting functions in many developmental signaling processes. It is well established that heparan sulfate binds to all **fibroblast growth factors (FGFs)** identified to date and several in vitro experiments indicated a role for heparan sulfate proteoglycans (**HSPG**) as low affinity coreceptor in FGF signaling [12-17]. While the precise mechanism of HSPG involvement in FGF signaling still remains unclear, several studies suggest the induction or stabilization of a ternary complex between FGF, FGF receptor and HSPG [18-23]. The requirement of distinct 2-O and 6-O sulfate groups for ligand binding and receptor complex activation, respectively, underline the direct involvement of HSPG in FGF signaling [19, 24, 25]. Mutation experiments in *Drosophila* directly proofed a genetic interaction between FGF signaling and HSPG as mutations in HSPG synthesis (sulfateless, sugarless) mimic phenotypes of mutations in the FGF pathway [26]. Additionally, the *Drosophila* homolog of heparan sulfate 6-O-sulfotransferase (**dHS6ST**) shows a FGF-pathway specific expression pattern and mutations in dHS6ST are reminiscent of defects caused by FGF pathway mutations [27].

Since the demonstration that heparan sulfate proteoglycans are critical for FGF signaling, similar studies have shown a role for heparan sulfate in signaling mediated by **Wingless (Wg)**, heparin binding epidermal growth factor and hepatocyte growth factor [28-30]. Recent studies mainly in *Drosophila* also revealed an effect of mutations in glycosaminoglycan biosynthesis genes on a variety of growth factor patterning events. The **sugarless (sgl)** gene encodes the *Drosophila* UDP-glucose dehydrogenase, an enzyme essential for the biosynthesis of chondroitin sulfate, dermatan sulfate and heparan sulfate [31]. Mutations in *sgl* mimic *wg* mutations in various tissues and can be bypassed by *Wg* overexpression suggesting a role for PGs as low affinity *wg* coreceptors [32-34]. Detailed studies assigned heparan sulfate rather than chondroitin sulfate or dermatan sulfate to be responsible for *Wg* interactions. In weak *sgl* mutations that survive to late larval stages, *Hh*-like phenotypes are observed and as mentioned above, FGF signaling in tracheal development is dependent on *sgl* function. Surprisingly, DPP-like phenotypes were not found in *sgl* mutants, neither in *Dv* axis formation, nor in wing disc patterning.

With **tout-velu (ttv)** a *Drosophila* homolog of the vertebrate EXT1/2 genes was identified [35-37]. Like its homologs, *ttv* encodes for a heparan sulfate copolymerase, an enzyme responsible for heparan sulfate chain assembly [38]. Homozygous *ttv* mutant animals elicit disturbances in **Hedgehog (Hh)**-signaling and show a strong reduction in heparan sulfate content whereas other GAG levels remain unaffected. This selective *Hh*-signaling defects associated with loss of *ttv* contrasts with the widespread affects on *Wg*- and FGF-signaling in *sgl* mutants presumably indicating the existence of other HS-copolymerases in *Drosophila* [39, 40].

After chain polymerisation, some GAG chains get further modified. In HS for example, the initial step of modification is the exchange of the N-acetyl group to a N-sulfo group. This step is essential for all further modifications like epimerisation or 2-, 3- and 6-O sulfation (reviewed in [10]). In *Drosophila*, the **sulfateless (sfl)** gene encodes a N-deacetylase/N-sulfotransferase. Sulfateless was identified together with *sgl* in a screen for early zygotic lethal mutations and shows phenotypes reminiscent of *Hh* and *Wg* mutants [26, 32]. Comparable to *sgl*, the FGF-signaling dependent migration of mesodermal and tracheal cells is defective in *sfl* null mutants demonstrating the strong dependence of FGF signaling to selective modified HSPGs.

1.1.3.1 Glypicans and signaling

Among the disperse group of HSPG, the glypicans represent a remarkably homogenous group of GPI anchored cell surface proteins with six representatives in vertebrates and two in *Drosophila*. Common structural features are 14 highly conserved cysteins in the core proteins and several GAG attachment sites adjacent to the GPI anchor. Thus, the GAG sidechains are located close to the cell membrane and are exclusively of the heparan sulfate type (reviewed in [41]). Six members of the glypican family have been identified in mammals (GPC1-GPC6) [42-49], and two in *Drosophila* ([50, 51], reviewed in [52]). The Simpson-Golabi-Behmel syndrome (SGBS) has been proposed to be caused by the lack of functional GPC-3 protein [53-57]. SGBS is characterized by pre- and postnatal outgrowths. Clinical manifestations include macroglossia, cleft plate, syndactyly, polydactyly, supernumerary nipples, cystic and dysplastic kidneys, congenital heart defects and rib/vertebral abnormalities. GPC-3 knockout mice display several phenotypes of SGBS providing a strong support for

involvement of GPC-3 in SGBS [58]. Comparable clinical features of SGBS with Beckwith-Wiedemann syndrome suggest a role for GPC-3 in IGF-II signaling [54, 59]. Other studies showed an implication of GPC-3 in BMP-2/-4/-7 and FGF-7 signaling [60, 61].

In *Drosophila*, the glypican divison **abnormally** delayed (**dally**) was identified by virtue of its effect on cell division patterning in the visual system [50]. Further studies revealed genetic interactions between **dally** and **decapentaplegic (DPP)** in several adult tissues derived from imaginal discs namely the wings, eyes, antennae and genitalia [62].

Mutations in DPP strongly increase the penetrence of eye, antenna and genitalia defects caused by homozygous hypomorphic **dally** mutations. Surprisingly, DPP decreases the effect of **dally** mutations in the wing suggesting an antagonistic function. Nevertheless, DPP overexpression phenotypes in the wing are suppressed by **dally** mutants and **dally** overexpression potentiates the patterning activity of ectopic DPP. Supporting a positive correlation, **dally** is expressed at moderate levels in a small stripe of cells coincidently with DPP expression [63, 64]. While mutations in GAGs affect various cytokine pathways, DPP signaling remains mostly unaffected. This raises the question whether DPP interacts with **dally**'s heparan sulfate sidechains or with the core protein itself. More decoded is the interaction of **dally** with wingless. Early experiments clearly depicted the involvement of glycosaminoglycan sidechains in Wg signaling events [28, 32-34]. Transheterozygous combinations of **dally** alleles and RNAi experiments mimiced weak Wg phenotypes in early embryonic epidermis patterning [65]. Full wingless phenotypes were only obtained by simultaneous RNAi-mediated inhibition of **dally** and **dally-like**, the second *Drosophila* glypican [51, 66]. As **dally** and **dally-like** are expressed in nonoverlapping regions during embryonic epidermis patterning they might play different roles in extracellular distribution of Wg-protein. In wing development, **dally** is strongly expressed in a broad stripe along the DV compartment boundary and at moderate levels along the AP compartment boundary. This, together with genetic interactions of **dally** with Wg and the Wg receptor Frizzled-2 suggests a predominant role of **dally** in Wg signaling during wing disc patterning. Ectopic expression of **dally** is able to trap extracellular Wg ligands in regions distant to Wg expressing cells [51]. Comparison of early embryonic patterning with DPP with genitaliae disc development shows striking differences in **dally**-ligand interactions. Whereas **dally** interacts with Wg and not DPP in early embryogenesis, this is reversed in genitalia disc development. This opposite interactions are also discussed in the light of differences in HS-sidechain modifications which might lead to binding of selective ligands [65].

1.2 Decapentaplegic

1.2.1 The TGF- β superfamily and BMP-family

Decapentaplegic (DPP) belongs to a large group of more than 30 (in mammals; 7 in *Drosophila*) structurally related growth factors combined to the TGF β -superfamily [67]. In both, vertebrates and invertebrates, TGF- β superfamily members can direct a wide range of cellular responses including proliferation, cell fate specification and apoptosis. The range of biological activities is reflected by the variety of names given to members of the family: bone morphogenetic proteins (BMPs), activins or growth and differentiation factors. Due to structural and functional homology, Decapentaplegic is assigned together with two other *Drosophila* TGF- β superfamily members, screw (scw) and glass bottom boat (gbb) to the BMP-family [68-70].

1.2.2 DPP structure and function

Whereas the first mutation of the *dpp* genolocus was described in 1938 as "heldout" reflecting the unusual wing-phenotype [71], the second discovered mutation caused 15 different epidermal defects therefore named by the old-greek term decapenta(=15)plegic(=defects) [72]. Cloning of the *dpp* genolocus in 1987 revealed the gene product DPP as a typical TGF- β superfamily member, characterized by the rigid core structure of the cystein-knot and building a homodimer bridged by a seventh cystein [68]. Translated as a large precursor protein, the propeptide is cleaved off by means of furin-proteases leaving a homodimeric ligand of approximately 30kD and 2x132aa [73]. There is no other function for the DPP-prodomain reported than supporting the correct folding of the mature ligand [74]. While prodomains share only limited homology, human BMP-2/-4 and *Drosophila* DPP reach 75 percent aa identity in the mature ligands downstream of the first conserved cystein of the cystein knot (see figure 6-1). The N-terminal parts, although not very conserved, are similar by the appearance of clustered positive charged aas. Conferring to the high extent of homology, the resolved X-ray structure of BMP-2 [75] serves as satisfactory model also for DPP (see fig. 1-2).

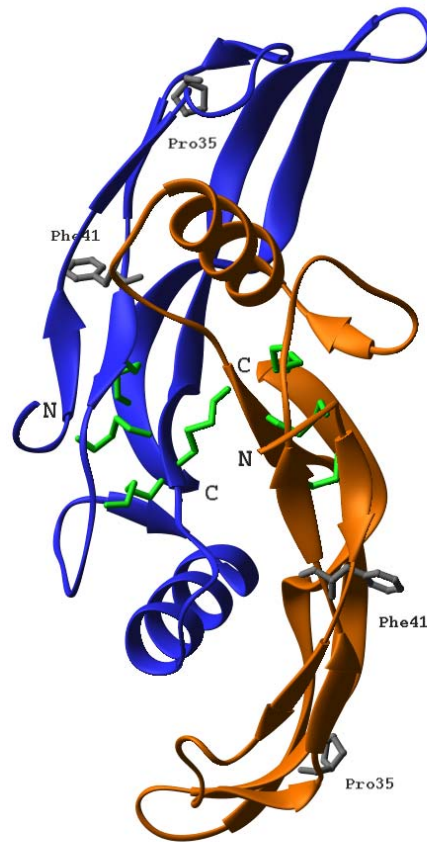


Figure 1-2: Structure of BMP-2

BMP-2 represents an antiparallel dimer of two identical monomers, depicted in blue and orange, respectively. β -sheets and α -helices are indicated. The cysteine-bridge connecting the two monomers and cysteine bridges of cysteine knot are indicated in green. (taken from ref. 234)

DPP plays a multifunctional role in *Drosophila* development, involved in several aspects of patterning the embryo and adult. During embryonic development, DPP is essential for formation of the dorsal-ventral axis [76-78], subdivision of the mesoderm into somatic versus visceral or cardiac components [79-81], induction between the visceral mesoderm and underlying endoderm in the developing gut [82, 83] and formation of trachea [84]. Further during adult development DPP is involved in growth of imaginal discs [85], patterning the anterior-posterior axis of imaginal discs such as the wing [86-88] and leg [89, 90], propagation of the morphogenetic furrow in the eye [91, 92], development of antennal structures [93], optic lobe development [94], oogenesis [95] and wing vein development in early pupae [96]. Selected dpp actions are described in more detail below.

1.2.3 The DPP Signaling pathway

Like other members of the TGF- β superfamily DPP signals via a heterooligomeric receptor complex composed of type II and type I serine/threonine receptor kinases. Following ligand binding, the type II receptor transphosphorylates the type I receptor at the GS-box, which then propagates the signal. Intracellularly, DPP signals are transduced by members of the Smad family. The Mad protein is transphosphorylated by the type I receptor at the C-terminal SSXS-motif and subsequently interacts with Medea to form a complex and to translocate to the nucleus. There Mad and Medea unveil their DNA-binding capacity and interact with cofactors to influence gene expression (reviewed in [97]).

1.2.4 DPP activation

DPP is initially synthesized as a precursor protein of 588 aa which is cleaved two times during secretion, leaving a large secreted prodomain and the active ligand as a homodimer of the last 132 aa. The prodomain is attributed to serve as “intramolecular chaperone” supporting the correct folding and cysteine bridging of the mature ligand. This view is confirmed by several mutations in the prodomain causing mild to severe DPP phenotypes [74]. Cleavage between the prodomain and the mature ligand is carried out by members of the proprotein convertase (PC) family of endoproteases [98, 99] also called **furin proteases**. Recent studies of BMP-4 revealed cleavage not only at the site reported so far but also more upstream thereby regulating BMP-4's bioactivity [100]. While the first theoretical cleavage site for mature DPP was confirmed by sequencing DPP produced in *Drosophila* S2 cells [73], like in BMP-4 also a second more upstream site is present [100, 101] which could in principle be also used to regulate DPPs bioactivity.

1.2.5 DPP-interacting proteins

In addition to the specific serine/threonine kinase receptors (see 1.4.3) several other proteins have been shown or postulated to interact directly with DPP. The *Drosophila* homolog of the vertebrate Chordin, **Short gastrulation (SOG)** is expressed in various developmental processes in cells adjacent to DPP sources [96, 102]. In two developmental processes, namely establishing dorsoventral axis and vein formation in the wing, SOG has been demonstrated to antagonize DPP signaling [96, 102]. While only weak biochemical interactions between SOG and DPP are detectable [103], these interactions were clearly demonstrated between the vertebrate homolog Chordin and BMP-4 [104, 105].

The inhibition of DPP by SOG binding is abolished through the cleavage of SOG by the metalloprotease **Tolloid (TLD)** [106]. This cleavage is strongly enhanced in the presence of DPP suggesting an interaction of TLD with the DPP-SOG complex. Whether TLD binds DPP directly remains unclear. Also in vertebrates the TLD homolog Xolloid cleaves Chordin thereby supporting BMP-4 signaling [107].

Twisted gastrulation (TSG) is also implicated in DV axis formation in vertebrates and invertebrates [103, 108-110]. Binding of TSG to vertebrate BMP-4 has been demonstrated [108] and the trimeric complex DPP-SOG-TSG is much more stable than DPP-SOG interactions [103]. TSG alone blocks DPP signaling at high concentrations and with SOG synergistically inhibits DPP signaling.

Thus, BMP/DPP activity in DV axis formation is posttranslationally regulated by several secreted factors which are highly conserved between invertebrates and vertebrates.

Morphogen properties of DPP in DV axis formation and wing disc patterning always coincide with the action of a second BMP ligand, SCW or GBB, respectively. This principally allows the formation of heterodimers in cells expressing both ligands. Notably, heterodimers between vertebrate BMP-2, BMP-4 and BMP-7 have been shown to be much more potent in induction of ventral mesoderm and bone induction than their respective homodimers [111, 112]. For SCW, the biological relevance of SCW-DPP heterodimers could be neglected since ventral misexpression of SCW in *Scw* null mutant embryos showed wildtype structures [113, 114]. In this approach, the ventral SCW misexpressing cells did not overlap with dorsal DPP expressing cells. Thus heterodimer formation between SCW and DPP was not necessary to induce dorsalmost structures. Also in the case of GBB, many overexpression experiments argue against a GBB-DPP heterodimer mechanism, and high levels of GBB in wing and eye/antennal disc are expressed reciprocally to DPP preventing efficient heterodimer formation [115, 116].

1.2.6 DPP receptors

The typical TGF- β superfamily receptor complex comprises two serine/threonine kinases named type II and type I receptor. For TGF- β s and Activins the type II receptor serves as high affinity receptor and can bind the ligands itself; the type I receptors are subsequently recruited into the ligand-type II receptor complex [117]. In contrast, BMPs show weak affinity for their type II receptors and first bind to their type I receptors [118, 119].

Additionally, BMP receptor complexes are found as preformed complexes at the cell surface binding the ligand synergistically [120]. The overall structures of type II and type I receptors are similar, and consist of small cysteine-rich extracellular parts, single transmembrane regions, and intracellular parts containing a serine/threonine kinase domain [121, 122]. Type II receptors represent constitutively active kinases and have, distal to their kinase domains, carboxy-terminal extensions of variable length. In contrast, type I receptors contain a serine-glycine rich domain in their intracellular juxtamembrane region designed as the “GS-Box” [121].

After identification and characterisation of TGF β -receptors, homology searches revealed the existence of five potential TGF- β receptors in *Drosophila*, meanwhile identified as type I receptors **thick veins (Tkv)**, **saxophone (Sax)** and **baboon (Bao)** and the type II receptors **punt (Put)** and **wishfull thinking (Wit)** [123-129]. Early experiments showed crosslinking of DPP to Tkv and BMP-2 to Tkv and Sax [126, 128] suggesting both to be type I receptors for DPP. These data were supported by genetic studies that demonstrated an absolute

requirement of *tkv* for all DPP actions examined [123, 125, 126]. Sax was also shown to be involved in DPP actions but with milder phenotypes than *tkv*. Initially, Sax was assigned as a receptor receiving peak levels of DPP since Sax mutations could at least in part be rescued through overexpression of *Tkv* or DPP [125, 128]. However, recent studies clearly demonstrated Sax to be the type I receptor for the two other BMP-ligands in *Drosophila*, Screw (*scw*) and Glass-bottom-boat (*gbb*) [69, 130, 131]. In dorsal-ventral patterning, screw augments DPP-signaling in defining the dorsal-most part of the embryo (see also 1.5.1) but Screw/Sax can not substitute for DPP/*Tkv* [113, 114]. Similar, GBB/Sax is involved in wing development to augment the DPP/*tkv* signal [115, 132]. In fact, overactivation of *tkv* can bypass the requirement for Sax, suggesting that the two receptors could use the same intracellular signaling machinery [131]. Ligand specificities for Sax and *Tkv* have also been established by determining which dominant negative receptor can block phenotypes caused by overexpression of ligands [115]. Thus, *Tkv* remains as the only type I receptor for DPP complemented by the type II receptor Punt, which has been shown to be required for DPP-signaling in vivo [123, 127] and to bind BMP-2/*Tkv* complexes in vitro [127]. The DPP-signaling cascade can also be activated ligand-independently by overexpressing *Tkv* and Put simultaneously [87] or by a constitutively active *Tkv* receptor *TkvQ253D* that comprises a kinase activating mutation [87, 133]. The high homology of DPP and BMP-signaling cascades is demonstrated by the ability of the constitutively active *Tkv* receptor to activate a BMP response element in mammalian cell culture [128].

1.2.6.1 Receptor interacting proteins

Whereas TGF- β signaling is supported by the type III receptor (betaglycan [134]), a proteoglycan facilitating the ligand access to the receptors, no such co-receptor has been reported for BMP-ligands so far. Nonetheless, the proteoglycan dally supports DPP signaling in many tissues [62] and although not shown yet, interactions between dally and dpp receptors might be possible.

The FYVE-domain protein **Sara** was shown to associate with Smads and anchor them to the cell membrane. C-terminally, Sara associates with TGF- β receptor and presents the substrate to the receptors kinase domain. Sara is also discussed to mask the Smad's nuclear localisation signal and thereby retaining Smads in cytoplasm [135, 136]. The *Drosophila* homolog of Sara was identified in a screen for interacting proteins of protein phosphatase 1 (PP1). Mutations in the PP1 binding domain of Sara as well as PP1 mutants resulted in overactivation of DPP signaling. This results suggest a role of Sara not only in presenting Smads to the receptors but also keeping Smads in unphosphorylated state through PP1 [137]. So far there are no mammalian phosphatases found to be involved in TGF β /BMP-signaling.

1.2.7 Smad proteins

Members of the Smad family were first identified in *Drosophila* through genetic screens to isolate dominant mutations that, if present in the maternal germline, exacerbated the *dpp* phenotype of the zygote [138, 139]. The first characterized gene therefore was named **mothers against dpp (Mad)**. Together with homolog genes in *C. elegans* *Sma-2*, *-3* and *-4* they were joined to the new protein family named "Smads". The other identified gene *Medea* had previously been described as gene required for imaginal disc growth [70]. Subsequently, vertebrate *mad* related proteins were identified and shown to be involved in BMP, Activin and TGF- β signal transduction [140-147].

Subsequent studies of Smad protein function in multiple systems contributed to the current model for TGF- β family signal transduction (see fig. 1-4). Smads are clustered into three functionally different groups: receptor-activated or R-Smads, common mediator or C-Smads and inhibitory or I-Smads. The R-Smads are the only proteins known so far to serve as direct substrates for type I receptor and directly transport the activation signal into the nucleus. Different R-Smads appear to specify the signal transduction cascade for BMP ligands versus TGF- β /activin ligands. Structurally, R-Smads can be divided into three parts: The N-terminal Mad homology 1 domain (MH1) containing intrinsic DNA-binding property and a nuclear localisation signal, a flexible linker part, and the C-terminal Mad homology 2 (MH2) domain with the receptor specificity bearing L3-loop and the SSXS motif at the C-terminus, which is substrate for the type I receptor kinase. MH2 domains also act as transcriptional activators and mediate formation of oligomeric complexes. After phosphorylation at the SSXS motif by the type I receptor, the R-Smads are able to interact with the C-Smads to form heterooligomeric complexes translocating to the nucleus. C-Smads, as R-Smads, comprise a MH1 and MH2 domain separated by a linker, but the MH2 domain of C-Smad lacks the SSXS motif and thereby is not a substrate for type I receptor kinases. In the nucleus, C-Smads elicit DNA-binding capacity and therefore might also regulate gene expression. The I-Smads antagonize signal transduction primarily by binding the type I receptor. They lack the whole MH1 domain and the SSXS motif, therefore can not be phosphorylated. I-Smads are immediate early response genes suggesting their function in limiting the signal response (reviewed in [97, 148-150]).

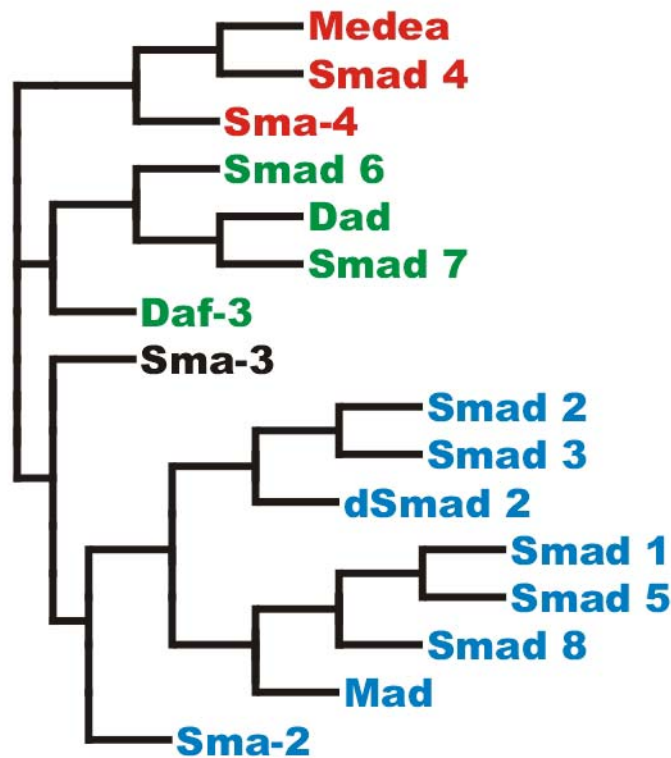


Figure 1-3: Phylogenetic tree showing the relationship of fly, human and nematode Smad family proteins (adopted from 91, 98). C-Smad subfamily members are shown in red, I-Smads in green and R-Smads in blue, respectively. Sma-3 function could not clearly determined so far.

Drosophila Mad has been shown to trigger all DPP signal transduction events examined to date [151-153]. The expression pattern of Mad is uniform in many tissues. Whereas Mad transfected into diverse cells has been shown to translocate efficiently into the nucleus through activation by DPP or constitutively active tkv, no remarkable amount of nuclear Mad could be detected in DPP-signal receiving cells in vivo [152, 154, 155] suggesting that only a small part of total cellular Mad becomes phosphorylated and shuttles between cytoplasm and nucleus. Mad binding sites in different promoters have been mapped by DNA-footprinting techniques and revealed the DNA-octamer GCCGNCGC as high affinity Mad binding site [156, 157]. Confirming the functional homology of BMP signaling cascades between invertebrates and vertebrates, this sequence has also been shown to work as Smad-1 binding BMP-response element in mammalian reporter assays [158].

A second R-Smad, dSmad-2, was described as part of an activin-like signaling pathway in *Drosophila*. dSmad-2 is activated through baboon, the *Drosophila* Activin-type I receptor, and punt and shuttles upon activation to the nucleus [128, 159]. Mutation analysis of baboon revealed a DPP independent function in development.

Medea was identified as the C-Smad in *Drosophila*. Homology comparison clearly assigns Medea as Smad-4 homolog confirmed by rescue experiments with hSmad4 [160]. Mutation analysis revealed implication of medea in embryonal and larval DPP signaling events [154, 160, 161]. For nuclear translocation of Medea, activated Mad is required [154, 161]. Based on footprint studies, DNA binding motifs similar to that for Mad have been identified for Medea [157].

Daughters against dpp (Dad) was characterized as an inhibitory Smad. DPP activates Dad thereby limiting its own signal [162]. Like other I-Smads, Dad binds to type I receptors and prevents interaction of this receptors with R-Smads [163].

Thus, all classes of Smads are found in *Drosophila* and various experiments demonstrated the functional homology of BMP signaling cascades between invertebrates and vertebrates (see fig. 1-3).

1.2.7.1 Smad interacting proteins

While in vertebrates a multitude of Smad binding proteins could be identified so far, the number of interacting proteins in *Drosophila* still remains limited. In addition to the Smad presenting protein Sara and the Smad

activating type I receptors, one nuclear factor, **Schnurri**, was identified to cooperate with Smads. Schnurri represents a member of the MBP family of zinc finger transcription factors. Mutation analysis revealed involvement of Schnurri in multiple patterning events that require dpp signaling. Schnurri phenotypes are very similar to the zygotic mutant phenotype of DPP receptors Tkv and Put [164-168]. Recent studies showed direct DNA-binding of Schnurri as a Mad cofactor. In reporter gene assays synergism between Mad and Schnurri in inducing target gene transcription was demonstrated [169, 170]. Moreover, Schnurri seems to play a key role in repressing the DPP target gene repressor brinker (see 1.4.7) as in brinker mutants, Schnurri is not required for DPP targetgene activation [171].

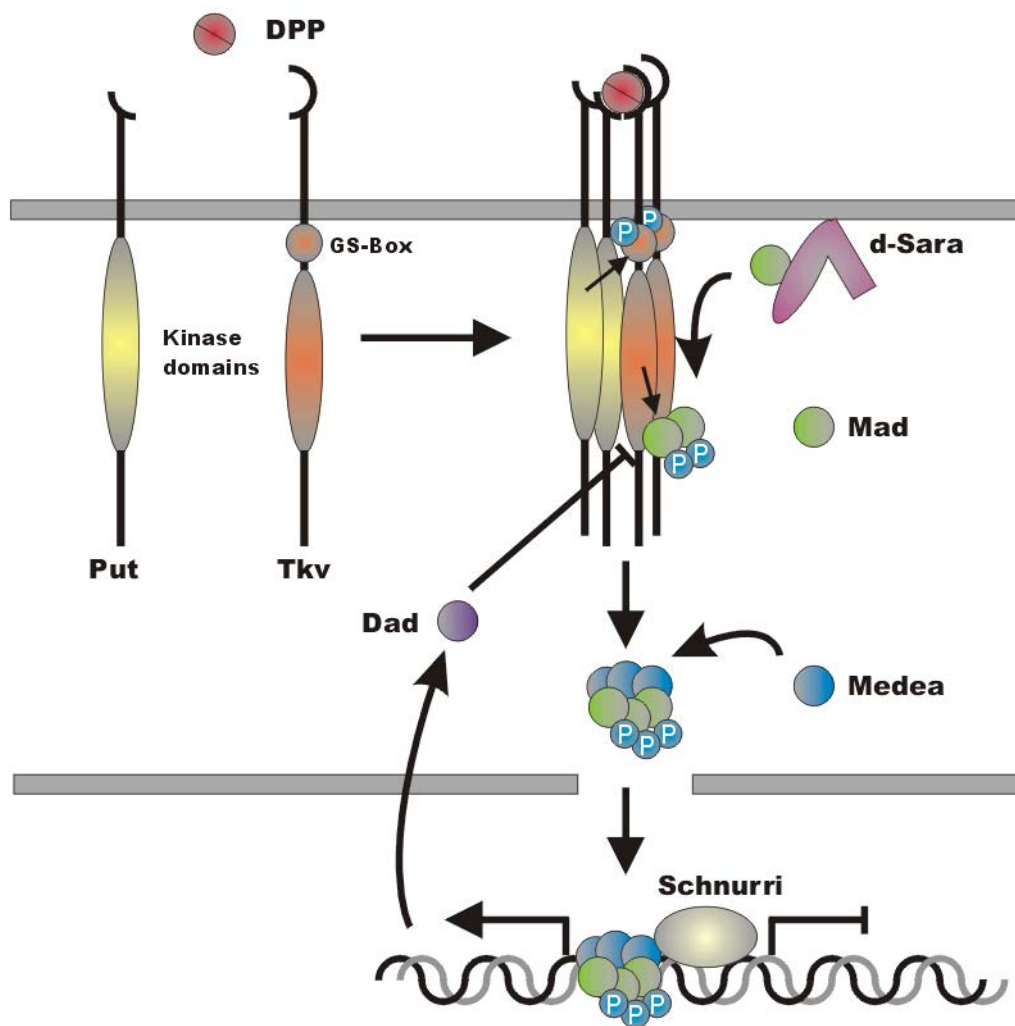


Figure 1-4: Model for DPP core signaling pathway

1.2.8 DPP target gene regulation

Several genes have been shown to be regulated by DPP [87, 156, 157, 162, 172-174]. Whereas for *Ultrabithorax*, *tinman*, *labial* and *vestigial* direct DNA-binding by Mad/Medea was demonstrated, regulation of other genes was unveiled by the discovery of **Brinker (Brk)**. Although no homolog is known to date, Brinker shows slight homology to repressor proteins. The expression pattern of Brk is reciprocal to that of DPP target genes suggesting a negative regulation of Brk by DPP. Indeed, Brk is able to repress DPP-target genes when overexpressed and DPP itself represses expression of brinker [175-177]. Generation of brk mutant clones directly activated some target genes whereas others need additional input signals. Detailed promoter studies unveiled a hexameric sequence GGCG c/t c/t as Brk consensus binding sequence. Interestingly, this sequence overlaps with Mad binding sequences in several DPP targetgene promoters [178-181]. For full repressor function, Brk requires corepressors like Groucho and CtBP depending on specific promoters [182]. Finally,

brinker has been shown to act different on promoters, either by competing with DPP dependent activators like Mad/Medea, or by strongly repressing DPP target genes, to allow only expression of the latter when efficiently repressed by DPP/Schnurri.

1.3 DPP in Development

1.3.1 DPP in dorsal-ventral axis patterning

Dorsal-ventral axis patterning is the first embryonic DPP function reported. DPP is expressed at uniform intensity throughout the dorsal 40% of embryonic circumference promoting dorsal cell fates such as amnioserosa and dorsal ectoderm and maintains its own expression through a positive feedback loop [183]. In DV axis formation, DPP fulfills the role of a typical morphogen since injection of different amounts of DPP mRNA induces different cell fates [102]. DPP activates target genes in different distance to the dorsal midline regulated through the brinker repression mechanism [176, 184]. Loss of dpp activity converts dorsal epidermis into neuroectoderm whereas DPP overexpression promotes the extension of dorsal epidermis into large areas of the presumptive neuroectoderm [131, 185]. In the dorsal 10% of the embryo highest BMP-like activity is achieved through combined action of DPP and **Screw (SCW)**, another BMP-family member. Whereas SCW and its type I receptor, **saxophone (Sax)**, are expressed at uniform levels throughout the embryo, mutation phenotypes only affect dorsal areas with high DPP activity. Under experimental conditions, however, DPP overexpression can compensate for loss of SCW, suggesting that SCW-SAX signaling synergizes with DPP-TKV signaling [113, 114]. In ventrolateral regions the DPP activity range is limited through expression of the **short gastrulation (SOG)** gene. SOG has been shown to promote neuroectodermal cell fate and to bind directly to DPP thereby blocking ligand activity. Recent studies also revealed a signaling promoting activity of SOG identified through the loss of amnioserosa cells in sog mutant embryos. Thus, SOG elicits antagonistic actions on DPP by high levels near SOG-producing cells but enhances DPP-signaling by low levels at distant sites [186]. In dorsal regions SOG is cleaved by **Tolloid (TLD)**, a metalloprotease expressed similar to DPP [106, 187]. This combination of SOG expressed in the lateral neuroectoderm and Tld degradation of SOG in the dorsal epidermis creates a lateral-dorsal SOG gradient. As SOG degradation leaves bound DPP from SOG fragments thereby reactivating DPP signaling capacity, a reciprocal DPP activity gradient is created with highest levels of DPP activity dorsally [186]. The effect of SOG on DPP signaling is enhanced by another secreted factor, **Twisted gastrulation (Tsg)**. Phenotypes of SOG and TSG mutants are very similar and experiments revealed a DPP inhibiting potency of TSG as well as TSG stabilizing the SOG-DPP complex [103]. Experimental data suggest TSG to function first as a potent DPP inhibitor building a trimeric complex with DPP and SOG and second as enhancer of dorsalmost DPP activity by redistributing the bound DPP and supporting the cleavage of SOG by TLD [103].

Evolutionary, this mechanism of modulating the activity and range of BMP-ligand signaling in defining dorsal ventral axis is highly conserved. Also in vertebrates development, as shown for *Xenopus*, BMP-ligands are involved in DV-axis formation. In early *Xenopus* development BMP-4 promotes ventral mesoderm formation and represses neural cell fate. From the Spemann organizer a couple of BMP-4 antagonists are secreted to limit the BMP-4 derived ventralisation. Chordin represents the vertebrate homolog of SOG and binds BMP-4 thereby preventing further receptor-binding of the ligand [188]. This complex is cleaved by Xolloid, the *Xenopus* tld-homolog, and other related proteases liberating the active form of BMP-4 [107]. A TSG-homolog, called xTSG was described as a ventralizing factor. As its fly-homolog, xTSG binds BMP-4 as well as Chordin-BMP-4 complexes and enhances the cleavage of these complexes by Xolloid-proteases. XTSG directs the cleavage of Chordin to specific sites and binds with higher affinity to BMP-4 than chordin fragments forcing their release from BMP-4 and reestablish ligands activity [103, 108, 109]. Other factors of Spemanns organizer not found in *Drosophila* development are noggin and follistatin. Whereas noggin like chordin complexes with BMP-4 and prevents receptor-binding, follistatin binds the ligand-receptor complex and prevents receptor activation [189, 190]. Thus, the posttranslational extracellular modulation of ligand activity in dorsal-ventral axis formation is conserved in details as it has been proven by the functional exchange of diverse antagonists between fly and frog [103, 191].

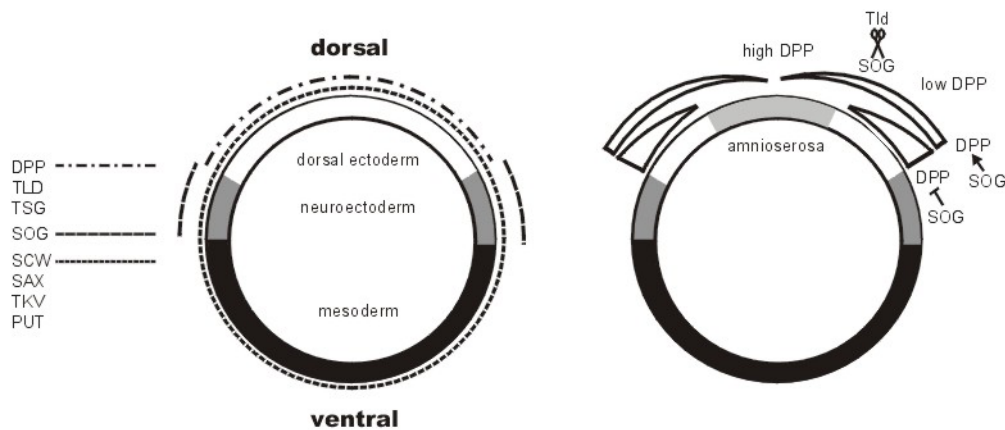


Figure 1-5: Dorsal-ventral patterning of *Drosophila* embryo

The left figure shows expression of ligands and receptors involved in patterning. The right panel shows refining of DPP gradient through dual action of SOG: SOG secreted from lateral cells diffuses dorsally and directly inhibits (together with TSG) DPP action. The DPP-SOG complexes allow long range diffusion of DPP. The cleavage of this complex in dorsalmost regions by TLD releases DPP in a SOG-free region thereby generating highest levels of DPP activity.

1.3.2 Endoderm induction by DPP

In *Drosophila* endoderm induction, DPP plays a prime function. The homeotic gene **Ultrabithorax (Ubx)** is active in parasegment (ps)7 of the visceral mesoderm, directly stimulating the expression of DPP within the same parasegment. Secreted DPP stimulates the expression of **Wingless (Wg)** in neighbouring ps8. Wg itself signals back to ps7 to stimulate Ubx expression, thereby building a "paracrine" feedback loop [173, 174, 192]. Both, DPP and Wg act on the subjacent endoderm to induce expression of the homeotic gene **labial (lab)** [193]. Whereas Wg stimulates or represses lab expression depending on its level, DPP only stimulates labial expression, shown by an expanded labial expression domain after ubiquitous DPP expression [194].

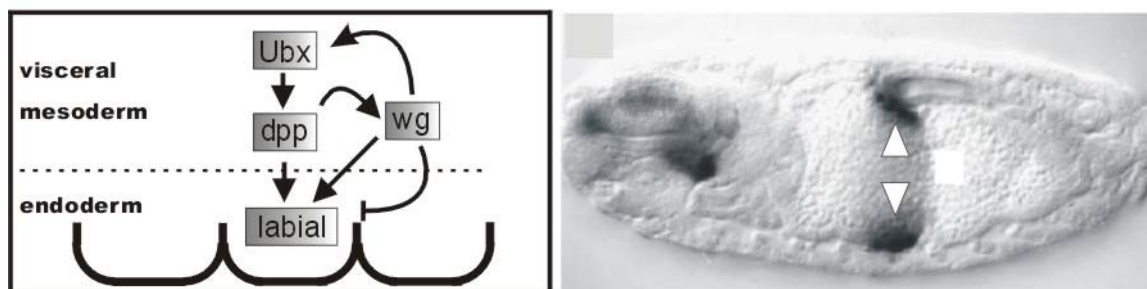


Figure 1-6: DPP in midgut induction

Left panel shows activation of labial through DPP and Wg. Right panel (taken from ref. 44) shows 12h-14h embryo stained against labial. White arrowheads indicate lab expression domain.

1.3.3 DPP and tracheal development

During development of tracheal tubes DPP is implicated in cell fate determination and cell migration. The tracheal precursor cells are separated early from dorsal ectoderm and invaginate to form 10 tracheal placodes on each side of the embryo. Each placode consists of a defined number of around 80 cells, which start to migrate into different directions to form 5 arms [195]. Cells are primed for migration in dorsal-ventral directions by DPP signaling and for anterior migration by EGF signaling [84]. DPP is expressed dorsally and ventrally of tracheal placodes and primes a subset of cells to become dorsal branches or lateral trunks. EGF is responsible for development of dorsal trunk and visceral branch [196]. Overexpression experiments revealed a dominance of the

DPP signal over EGF. If DPP or its constitutively activated receptor Tkv is ectopically expressed in all tracheal placode cells, dorsal trunks and visceral branches fail to develop whereas in *tkv* or put mutant embryos only these branches are formed [196, 197]. It is not clear whether DPP itself also provides the attractants, that directs the cells into their correct positions. The FGF-like ligand **Branchless** has been shown to be expressed in the tips of all developing branches and like its receptor **breathless** (*btl*) to be absolutely necessary for cell migration [198].

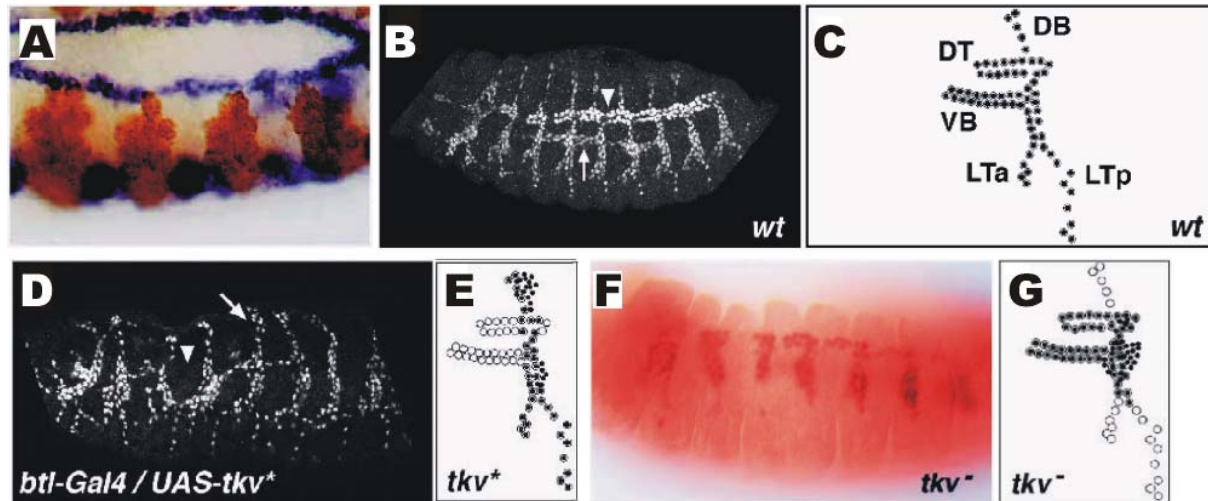


Figure 1-7: Influence of DPP on tracheal branching

a) shows DPP mRNA expression (blue) after invagination of tracheal placodes (marked in brown by 1-eve-1). Dpp expression abuts dorsally and ventrally the placode cells. In b) Wildtype branching pattern is shown (arrowhead: dorsal trunk, arrow: visceral branch). One parasegment of b is schematically shown in c (DB dorsal branch; DT dorsal trunk; VB visceral branch; LTa and LTp anterior and posterior lateral trunks). The constitutive activation of the DPP pathway by TkvQ253D in tracheal cells is shown in d+e ((arrowhead: dorsal trunk, arrow: visceral branch)). Cells preferentially migrate in DV direction. In f+g the *tkv* minus background is shown with cells migrating only in AP direction. b, d, f: by anti-trachealless antibody (a taken from [196], b-g taken from [84])

1.3.4 Wing imaginal disc patterning via DPP

The involvement of DPP in wing imaginal disc growth and patterning is the best examined DPP action so far. At least three DPP dependent processes have been described: Proliferation and cell survival, patterning and impartment of cell identity and wing vein formation.

The adult appendages of *Drosophila* are each subdivided into precisely defined regions, the anterior and posterior compartments, which derive from adjacent but immiscible cell populations established early in development. [199, 200]. The selector gene **engrailed** (*en*) plays an essential role both in the establishment of the parasegmental subdivision of the embryo and later in the maintenance of parasegmental borders in adult appendages giving posterior compartments their identity through inherited expression [201-203]. This results in a stable compartment border running straight through the center of the disc. Whereas **hedgehog** (*Hh*) is expressed through activation by engrailed in all posterior cells, *dpp* is directly repressed by the latter [204]. *Hh* secreted from cells of the posterior compartment crosses the compartment boundary and activates *dpp* expression in cells of the anterior compartment [205, 206]. The Gli-family protein **cubitus interruptus** (*ci*) is expressed ubiquitously in the anterior compartment, playing a dual role as transcriptional activator and repressor. In cells receiving no *Hh* signal, *Ci* is cleaved proteolytically leaving a 75kD fragment which has repressor function and downregulates *dpp*-expression [207]. In the case the *Hh* signal reaches anterior cells, *Hh* binds to the multi-transmembrane domain protein **patched** (*ptc*) [208, 209]. The role of *Ptc* is to inhibit the latent signaling activity of the G-protein coupled receptor **smoothed** (*smo*). The binding of *Hh* to *Ptc* reduces this inhibition and allows *Smo* to be active [210, 211]. In a poorly understood manner, *Smo* activity is transduced finally to *Ci* and prevents the cleavage of *Ci* to the repressor fragment (reviewed in [212]). The full-length *Ci* instead acts as transcriptional activator and augments DPP expression [213-215]. As the *Hh* receptor *Ptc* serves as a molecular filter and restricts the diffusion of *Hh* to several cell diameters, DPP expression is limited to a small stripe of cells in the anterior compartment adjacent to the compartment border [208].

Secreted DPP gives rise to a long range gradient with organizing influence on both compartments of the wing disc. Thereby DPP has the characteristics of a morphogen, evoking different cellular responses at different threshold concentrations. Whereas the target genes **spalt/spalt-related** (*sal/salr*) [216, 217] are expressed only in the wing pouch centered around the DPP expression stripe, the expression domain of **optomotor-blind**

(**omb**) [172] extends further than sal expression, both in the dorsal-ventral and in AP direction. Omb and the spalt-complex genes encode transcription factors. Omb has been shown to be required for proliferation and cell survival in the wing pouch and has ectopic wing inducing properties [172]. Sal/Salr in contrast contributes only partially to wing disc proliferation and is responsible for proper positioning of longitudinal veins L2, L3 and L5 [217-220]. Several experiments with ectopic DPP expression elicited evidence, that expression of sal/salr and omb in different AP distance to the DPP source, result from different sensitivities to a DPP-concentration gradient. Clones with moderate levels of ectopic DPP in lateral wing disc regions induced only expression of Omb, whereas clones with high levels of ectopic DPP induced both Sal and Omb with the latter extending further from the DPP source [87, 88]. Detailed analysis revealed a regulation of omb expression exclusively through the brinker repression mechanism (see 1.4.6) as brinker clones autonomously elicit Omb expression even in DPP-signaling deficient cells. Sal, in contrast, requires an additional direct DPP input signal together with abolishing the repression through brinker to elicit full expression levels ([176, 177], reviewed in [221]). Implicated in the establishment of the long range DPP morphogen gradient is the graded regulation of its receptor tkv. In peripheral regions of the disc, tkv is expressed at higher levels than in the central part. Experiments with clonal expression of DPP revealed a negative effect of DPP signaling on tkv levels in peripheral regions [222]. In the central part of the disc, tkv is regulated in a discrete pattern with low levels in the A compartment, lowest levels in DPP-producing cells and intermediate levels in the P compartment. This graded expression is mirrored by distribution of P-Mad, the activated form of the downstream mediator [223, 224]. Tkv-repression in the central part is mediated through **masters of tkv (mtv)**, a zinc finger protein with reciprocal expression pattern to tkv in the central domain, which is regulated by Hh and En [224]. Lowering the expression of tkv in the central disc region has been demonstrated to have several consequences. First, it extends the DPP gradient in the AP direction, as high levels of tkv sequester the DPP ligand and limit the diffusion range [115, 222]. Second, it enables cells at the edge of the DPP gradient to respond to low levels of DPP by increasing the receptor level. Third, it lowers the DPP signal in the DPP-expressing cells, as Hh plays the dominant role in patterning this central region [224, 225].

Beneath the distinct regulation of the receptor level, another mechanism supports the DPP morphogen gradient. Studies with hypomorphic alleles of GBB, another BMP-ligand, and modified expression of sax, the second BMP type I receptor in *Drosophila*, unveiled a supporting role of GBB and Sax signaling in the transduction of the DPP gradient. Coexpression studies and overexpression of ligands versus constitutively activated receptors clearly demonstrated the assignment of two ligand/receptor pairs: GBB signals via Sax and DPP via Tkv [115, 116, 132]. Recent studies demonstrated also a Sax-independent function of GBB in wing development suggesting signaling of GBB also through Tkv, but clearly proved a relationship between DPP and GBB signaling [226]. Thus, DPP morphogen gradient action is always accompanied by a second BMP-ligand: Screw in DV-patterning in the embryo and GBB in wing disc patterning.

Later, in early prepupae, the DPP expression along the AP compartment boundary disappears and expression of DPP is initiated in proximodistal stripes representing the vein primordia [96, 227]. The dpp expression is accompanied by elevated expression of the dpp receptor thickveins in neighboring cells and by expression of the DPP antagonist SOG in intervein tissue. DPP and Tkv expression influence each other negatively. This mechanism explains the curiosity of dpp and tkv mutants leading to thickening of veins in the case of hypomorphic tkv alleles and distal loss of veins in dpp-shortvein (*dpp^s*) mutants [227]. Nevertheless, in *dpp^s/tkv* double mutant combinations the tkv phenotype is suppressed and dpp phenotypes are strongly enhanced.

Comparable to the patterning of the DV axis, DPP has an autoactivation function during vein formation and SOG as a DPP antagonist might direct the wave of DPP autoactivation along the vein primordia [96]. As in wing disc patterning, GBB is also involved in vein specification. Detailed clonal analyses revealed, that local GBB action is necessary to specify the posterior crossvein and other vein areas [226]. Recently, **crossveinless-2 (cv-2)** was described to potentiate DPP/GBB signaling during early formation of the crossveins and sequence analysis turned out a secreted protein with cysteine-rich domains similar to SOG/Chordin suggesting a binding of cv-2 to DPP/GBB [228].

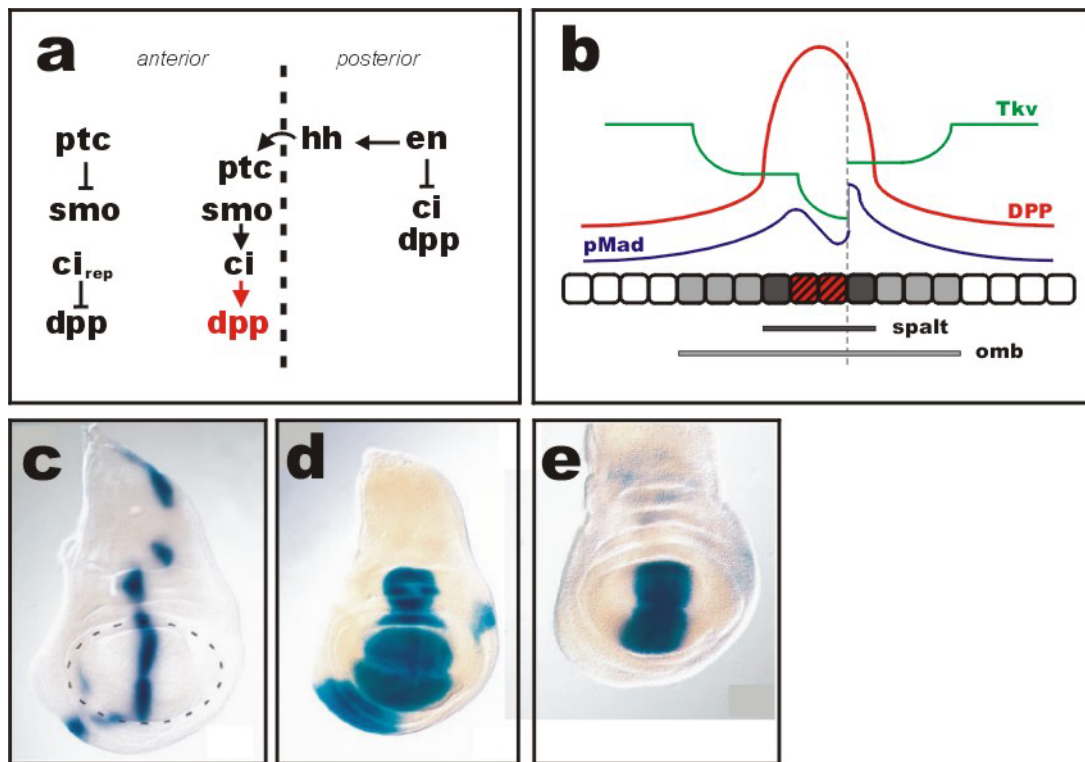


Figure 1-8: DPP-signaling in wing disc development

a) Ubiquitous repression and local restricted activation of *dpp* by short range induction via Hedgehog adjacent to the compartment boundary (dotted line). b) The resulting DPP-gradient induces targetgenes *omb* and *spalt* at different threshold levels. c-e) Expression patterns revealed by lacZ reporters BS3.0 (*dpp*), X35 (*omb*) and A405.1M2 (*spalt*), respectively (taken from [87]). Dotted line in c) indicates the wing pouch. Late 3rd instar wing discs are shown with anterior to the left and dorsal side up.

1.4 Aim of the project

Many genes involved in glycosaminoglycan biosynthesis have been identified so far. Due to their pleiotropic effects it was in most cases not possible to examine cytokine-matrix interactions of distinct ligands.

In the present work, the relevance of matrix ligand interactions should be investigated by mutating potential matrix binding sites in the mature ligand. As model system, DPP was chosen because of its high homology to BMP-2. The *Drosophila* system offers a lot of manipulatory genetic tools and *dpp* is one of the best-studied genes in *Drosophila* so far. Additionally, preliminary studies on BMP-2 revealed a matrix binding site in its N-terminal region which does not interfere with BMP-receptor interactions. Analysing DPP in biochemical approaches should show the specific bioactivity of mutated DPP as well as an unchanged receptor affinity. In vivo experiments with transgenic flies on the other hand should directly disclose the biological relevance of DPPs matrix binding in different developmental processes.

2 Material and methods

2-1 Material and solutions

2-1-1 Solutions for cell lysis

TNE-buffer (used for Smad western blots):

20mM Tris/HCl pH 7.5
 150mM NaCl
 1mM EDTA
 1% Triton-X 100
 freshly added :
 50mM NaF
 10mM Na₄P₂O₇
 1mM Na₃VO₄
 1mM PMSF
 1/25 Proteaseinhibitor complete solution (Roche)

2x SDS sample buffer (used for receptors, ligands):

125mM Tris/HCl
 4% SDS
 0.02% bromphenolplue
 eventually supplemented by 10% β-mercaptoethanol (reduced conditions)

2-1-2 Solutions for western blotting

Transfer buffer: 25mM Tris
 190mM glycine
 20% methanol

Wash buffer: 10mM Tris/HCl (pH 8.0)
 150mM NaCl
 0.5% Tween 20

Blocking solution: 3% low fat dry milk powder (Fluka) or BSA in wash buffer

Luminol: 2.5mM 3-aminophthalhydrazide
 1% DMSO
 0.1M Tris/HCl pH 8.5

Antibodies: anti-Myc (9E10) 1:300 in wash buffer (preparation by T. Lutz)
 anti-HA (12CA5) 1:100 in wash buffer (preparation by T. Lutz)
 anti-Tkv 1:1000 in wash buffer (raised against AA 43-59, eurogentec)
 anti-P-Smad 1:1000 in wash buffer (gift from P. ten Dijke [223, 229])
 anti-DPP 1:5000 in wash buffer (gift from M. Affolter [73])
 anti-His 1:2000 in TBS (blocking and first washes also in TBS; sigma)
 anti-Sal 1:20 in wash buffer (gift from R. Schuh [216])

TBS: 50mM Tris/HCl pH 7.4
 150mM NaCl

2-1-3 Solutions and equipment for protein purification

TBSE: 10mM Tris-HCl pH 8.0, 150mM NaCl, 1mM EDTA, 0.1%v/v 2-mercaptoethanol
 prior to use added PMSF at a final concentration of 0.5mM (dissolved as 0.5M stock in EtOH)

6M GUTE: 6M guanidinihydrochloride, 100mM Tris-HCl pH 8.0, 0.1mM EDTA,
 0.1%v/v 2-mercaptoethanol

Renaturation-buffer: 50mM Tris-HCl pH 8.0, 5mM EDTA, 1M NaCl, 2mM glutathione (red.), 1mM glutathione (ox.), 25mM CHAPS

Gel-filtration chromatography:

column: Pharmacia XK 50/100
 column-material: Sephacryl-S300 high resolution (Pharmacia)
 solvent: 6M GUTE, 1mM DTT
 pump: LKB 2232 Microperpex S Peristaltic pump
 detection: LKB 2238 Uvicord, Linear Instrument Recorder
 probe collector: ISCO Retriever II

FPLC-column : SO₃⁻-EMD-Fractogel (purification)
 Heparin-EMD-Fractogel (analysis)

Buffer P1: 300ml renaturation buffer containing refolded protein
 6M urea, 0.1M NaCl, 2mM EDTA, 50mM Tris
 pH adjusted to 8.0 with 1M HCl

Buffer P2: 6M urea, 2mM EDTA, 50mM Tris
 pH adjusted to 8.0 with 1M HCl

Buffer P3: 6M urea, 1M NaCl, 2mM EDTA, 50mM Tris
 pH adjusted to 8.0 with 1M HCl

Buffer F1: as buffer P1
 except 50mM Na-Formiat instead of Tris
 and pH adjusted to 4.0

Buffer F2: as buffer P2
 except 50mM Na-Formiat instead of Tris
 and pH adjusted to 4.0

Buffer F3: as buffer P3
 except 50mM Na-Formiat instead of Tris
 and pH adjusted to 4.0

HPLC (reversed phase):

column: Vydac C4
 pump: LKB Bromma HPLC pump 2150
 detection: merck hitacchi UV monitor 655A
 probe collector: LKB Bromma 2211 superrack

 flowrate: 0.7ml/min
 fraction: 1.4ml
 TFA-solution 0.1% FA in millipore-water, steril filtrated
 gradient: 0-30% acetonitril in 5 min
 30-40% acetonitril in 45 min
 40-100% acetonitril in 10 min

2-1-4 Solutions for viral expression of Tkv-ectodomain in SF-9 cells

IPL-41 HyQ IPL-41 (HyClone) solved in dH₂O

FBS Gibco

IPL-41-Medium: 760ml IPL-41 + 40ml FBS

BaculoGold™ transfection kit	(Pharmingen BD-Biosciences)
1.3x Xpress medium	SF900-Medium 1.3x (Gibco)
Ni-NTA-Sepharose	Quiagen
Ni-Buffer:	50mM NaH ₂ PO ₄ , 10mM imidazole, 300mM NaCl, pH adjusted to 8.3 (NaOH)
Ni-Elutionbuffer:	50mM NaH ₂ PO ₄ , 300mM imidazole, 300mM NaCl, pH adjusted to 8.3 (NaOH)
TMAE-buffer:	10mM Hepes, 3.4mM EDTA, pH adjusted to 7.5

2-1-5 Solutions for calcium phosphate transfection

transfection solution A: 33µl 2M CaCl₂
 18µg DNA (+ 1µg pUC-Hygro (invitrogen) for stable transfections)
 ad 270µl H₂O

transfection solution B: 270µl 2x HBS

2-1-6 Solutions for wing disc antibody-staining

PLP	3.7% p-formaldehyde 70mM glycine 30mM NaPO ₄ pH 6.8 10mM Na ₂ O ₅
PBS:	170mM NaCl 3.3 mM KCl 10mM Na ₂ HPO ₄ 1.8mM KH ₂ PO ₄
PBT 0.3%:	PBS, 0.3% Triton X-100
PBT 0.1%:	PBS, 0.1% Triton X-100
Blocking solution:	1.5% normal goat serum (sigma) in PBT 0.1%
1 st antibody solution:	anti CD2 1:100 anti β-galactosidase (cappel) 1:1000 anti sal 1:20 in blocking solution
2nd antibody solution:	FITC-goat-anti mouse (CD2) 1:250 (sigma) Cy3-goat-anti rabbit (β-gal, sal) 1:250 (sigma) in blocking solution

2-1-7 Solutions for embryo antibody-staining

PBT 0.3%:	PBS, 0.3% Triton X-100
PBT 0.1%:	PBS, 0.1% Triton X-100
Blocking solution:	1.5% normal goat serum + 5% BSA in PBT 0.1%
1 st antibody	anti β-galactosidase (cappel) 1:1000
2nd antibody solution:	Cy3-goat-anti rabbit 1:250 (sigma) in blocking solution

2-1-8 Solutions for limbbud assay

Growth medium:	Coon's F12 (biochrom) + 5% FBS
Starving medium:	Coon's F12 + 0.5% FBS
FBS:	Gibco
Na ₂ ³⁵ SO ₄ -solution:	1.5mCi Na ₂ ³⁵ SO ₄ (ICN)/ml PBS
NaAc-solution:	50mM NaAc 0.5% Triton X-100 pH adjusted to 5.8
Alcian blue solution:	0.2% Alcian blue 50mM NaAc 85mM MgCl ₂ pH adjusted to 5.8 (filtered, store for max. 2 weeks)
Wash-buffer:	50mM NaAc 100mM Na ₂ SO ₄ 50mM MgCl ₂ pH adjusted to 5.8

2-1-9 Protein markers

SDS-7B (Sigma) prestained:	protein	molecular weight
	α_2 -macroglobulin	205kD
	β -galactosidase	130kD
	fructose-6-phosphate kinase	90kD
	pyruvate kinase	64kD
	fumarase	53kD
	lactic dehydrogenase	37kD
	triosephosphate isomerase	32kD
PM selfmade by Ch. Söder:	protein	molecular weight
	phosphorylase b	94kD
	albumine	67kD
	ovalbumin	43kD
	carboanhydrase	30kD
	trypsine-inhibitor	20.1kD
	lactalbumine	14.4kD

2-2 Methods

All molecular biology and protein chemistry methods were performed according to standard protocols if not mentioned otherwise.

2-2-1 SDS-PAGE

SDS-Polyacrylamid-Gel-Electrophoresis was performed as described in [230]. stacking gel was of 3.75% and resolving gel of 10% (for receptors, Smads and immature ligands) and of 12% (for recombinant ligands).

2-2-2 Western blotting

Following separation of proteins by SDS-PAGE in a Mini-V8.10 chamber (Life technologies), proteins were transferred to nitrocellulose membrane (Schleicher&Schüll) in the same chamber with blot module in transfer buffer für 1h at 120V. The membrane was blocked with blocking solution for 30' at RT and incubated with first antibody in 10ml wash buffer overnight at 4°C, gently shaking. The antibody-solution was removed and the membrane was washed three times with wash buffer. An appropriate HRP-conjugated second antibody was

added in 1:20000 dilution in 10ml wash buffer for 2h at RT. Finally, the membrane wash was washed again three times with wash buffer and a premix of 2ml luminol supplemented by 9µl 90mM p-cumaric acid and 2ml 0.1M Tris-HCl pH 8.5 supplemented by 1.2µl 30% H₂O₂ was added and membranes were exposed for adequate time intervals to X-Ray films.

2-2-3 Protein purification

Preparation of DPP, D-DEL, D-MYC and D-DUP

E.coli bacteria cultures of the strain BL21DE3 containing the different pET-3d-DPP constructs were incubated overnight in 800ml LB-media with 100µg/ml Ampicillin. Next day eleven erlenmeyer-2l containing 800ml LB-Media/Ampicillin were inoculated with 50ml starting culture. At OD₅₅₀ of 0.5-0.7 expression was induced by addition of 1mM isopropyl-thio-β-D-galactopyranoside. After 3h induction cells were pelleted (Beckmann J2-21/JA-10 rotor/6000rpm/20°/4°C), resuspended in 5-fold volume cold 50mM Tris-HCl pH 8.0 pelleted (Beckmann J2-21/JA-10 rotor/6000rpm/20°/4°C), weighed and resuspended in 10ml/g icecold TBSE. To prepare inclusion bodies, cells were sonified at 300W for 5 min in wet ice with 30'' cooling pause after every minute sonification. The suspension was pelleted (Beckmann J2-21/JA-14 rotor/11500rpm/20°/4°C) and resuspended in icecold TBSE. Sonification and pelleting was repeated and after weighing and resuspending in 10ml/g TBSE, inclusion body suspension was frozen at -20°C.

Inclusion bodies were thawed, washed with TBSE and centrifuged for 45min (Beckmann J2-21/JA-14 rotor/11500rpm/4°C). Pellet was carefully resuspended in 60ml 6M GUTE. The solution was stirred for 2h at room temperature and pelleted by ultracentrifugation (Beckmann L8-70M/45ti rotor/30000rpm/90°/18°C). Clear supernatant was recovered and loaded on gelfiltration column (Pharmacia XK 50/100, Sephacryl-S300 high resolution) and eluted with 6M GUTE. The flowthrough was fractionated and analyzed photospectrometrically. Fractions containing protein of interest were pooled and concentrated by pressure filtration (Amicon / YM-10 membrane/3bar) to 8mg/ml.

The concentrated protein solution was diluted to a final concentration of 0.2 OD₂₈₀ /ml renaturation buffer. Renaturation was performed in 1liter samples at RT in the dark for 7 days.

Purification of DPP and D-MYC

2.5g of heparin-gel-powder (merck) was swelled with 50ml H₂O for 15min. Supernatant was removed carefully and gelmatrix (~10ml) was mixed with 20ml of buffer P2 and transferred to column (...). Samples were eluted and column was washed with 20ml P2.

Renaturation solution was desalted and pH-adjusted (1mM HCl) through 5 rounds of ultrafiltration steps: 1 liter renaturation solution was concentrated to 300ml and supplemented with 700ml 1mM HCl. After a final filtration step 300ml protein solution were recovered and added to 500ml of solution P1. This was carefully loaded onto the heparin column by gravity. Proteins were eluted by a NaCl gradient mixing 40ml of P2 with 40ml of P3. Monomeric DPP/DPPDUP was recovered around 0.25M NaCl, dimeric DPP/DPPDUP at 0.4M NaCl and higher aggregates with around 1M NaCl. Protein-containing fractions were analyzed by SDS-PAGE and dimeric fractions were dialysed against 5 liter H₂O, centrifuged (Bacifuge/400rpm/10°/4°C) and finally purified by HPLC. Dimeric DPP- or DPPMYC-containing fractions were pooled, aliquoted, lyophilized and stored at -20°C.

Purification of D-DEL

Renaturation solution was desalted and pH-adjusted (1mM HCl) through 5 rounds of ultrafiltration steps: 1 liter renaturation solution was concentrated to 300ml and 700ml 1mM HCl was added. After a final filtration step 300ml protein solution were recovered and completed to 500ml of solution F1. This was loaded onto the FPLC-column. Proteins were eluted by a NaCl-gradient, mixing solutions F2 and F3 according to the following scheme:

FPLC-gradient:	0-30% Buffer F3 (=100-70% Buffer F2)	in 15'
	30-75% Buffer F3	in 60'
	75-100% Buffer F3	in 15'
	buffer flow 1ml/min	

Protein fractions were analyzed by SDS-PAGE and dimeric fractions were dialysed against 5 liter H₂O, centrifuged (Bacifuge/400rpm/10°/4°C) and finally purified by HPLC. Dimeric DPPDEL-containing fractions were combined, aliquoted, lyophilized and stored at -20°C.

Purification of D-DUP

Renaturation solution was desalted and pH-adjusted (1mM HCl) through 5 rounds of ultrafiltration steps: 1 liter renaturation solution was concentrated to 300ml and 700ml 1mM HCl was added. After a final filtration step 300ml protein solution were recovered and completed to 500ml of solution P1. This was loaded onto the FPLC-column. Proteins were eluted by a NaCl-gradient, mixing solutions P2 and P3 according to the following scheme:

FPLC-gradient:	0-30% Buffer P3 (=100-70% Buffer P2)	in 15'
	30-75% Buffer P3	in 60'
	75-100% Buffer P3	in 15'
	buffer flow 1ml/min	

Protein fractions were analyzed by SDS-PAGE and dimeric fractions were dialysed against 5 liter H₂O, centrifuged (Bacifuge/400rpm/10'/4°C) and finally purified by HPLC. Dimeric DPPDUP-containing fractions were unified, aliquoted, lyophilized and stored at -20°C.

2-2-4 Cell culture

Drosophila S2 cells (invitrogen) were cultivated in DES (invitrogen) or Drosophila Schneider's Medium (gibco) supplemented by 8-10% FBS (gibco) and antibiotics. All standard techniques were carried out according to invitrogens DES-manual.

SF-9 cells were cultivated in IPL-41 medium supplemented by 5% FBS. Cells were cultivated in 75cm² flasks (nunc) and transferred to 11 roller bottles (greiner) for viral transfections.

2-2-5 Calcium phosphate transfection

3 x 10⁶ S2 cells were seeded per well of a 6-well plate and incubated overnight at 25°C. The next day transfection solutions A + B were mixed thoroughly by air-bubbling and incubated for 10' at RT. Cell supernatant was removed and transfection mixture carefully added. Cells were incubated with mixture for 16h at 25°C. Transfection mixture was removed and cells were washed twice with 2ml medium and further incubated 48h prior to lysis or generation of stable cell lines.

2-2-5-1 Generation of stable cell lines

Cells were cotransfected with 1µg of pUC-Hygro (Invitrogen) coding for the hygromycin resistant gene. 48h after transfection, cells were removed by pipetting and removed to a 25cm² flask. After first splitting, 15µl of 100mg/ml hygromycin-b are added to 5ml of medium. This step was repeated with every splitting for 4 weeks until no dead cells are found in flasks after 3-4 day incubation. Stable cell lines were frozen in 1ml aliquots (7.5% DMSO in FBS, 10⁷ cells/ml).

2-2-6 Viral expression of proteins

Virus transfection

SF-9 cells were adjusted to 0.8 x 10⁶ cells/ml and 1ml of cells were seeded per well of a 6-well plate. After addition of 1ml medium, the cells were grown for at least 1h at 27°C for proper attachment to the surface. Then medium was replaced by 500µl of transfer buffer A (Baculo-Gold® transfection kit). 1.5µg of DNA-construct was mixed with 2µl of Baculo-Gold® DNA, incubated for 5' at RT. After addition of 500µl of transfer buffer B to the DNA solution, the mixture was slowly pipetted onto the cells. The transfection was incubated for 4h at 27°C, washed twice with IPL-41 medium and incubated with 2ml of fresh media for 4-5 days at 27°C.

Plaque assay

Cells were adjusted to 1.2 x 10⁶ cells/ml and 1ml of cells were seeded per well of a 6-well plate. 1ml IPL-41 medium was added and cells were grown for at least 1h at 27°C to allow attachment to surface. The virus stock was diluted after the following scheme with IPL-41 medium:

10 ⁻¹ dilution:	mix 100µl of virus stock with 900µl medium
10 ⁻² dilution:	120µl of 10 ⁻¹ dilution / 1080µl medium
10 ⁻³ dilution:	120µl of 10 ⁻² dilution / 1080µl medium
*	*
*	*
10 ⁻⁸ dilution:	120µl of 10 ⁻⁷ dilution / 1080µl medium

Medium was removed from cells and virus dilution (10^{-4} till 10^{-8}) was added to the cells. The 6th well remained without virus as positive control. The cells were incubated exactly for 1h at 27°C. Meanwhile 10ml of 2.7% low melting agarose were boiled and slowly cooled at RT. 6.6ml of 1.3x Xpress medium were mixed with 3.3ml hand warm 2.7% agarose and 700µl FBS. Immediately after removing medium from wells, 1.5ml of the mixture was slowly applied to each well. Open plates were kept under flow hood for 10' to let low melting agarose harden. The plates were closed and sealed with parafilm®, given into a wet chamber and incubated at 27°C for 4 days. To stain cells, 1ml of 0.1% MTT solution was added to each well for 1h and then carefully removed. Virus plaques remained as bright spots in the dark-stained confluent cell-layer.

Virus amplification

The cell culture supernatant of transfected SF-9 cells was collected and a full-sterile plaque-assay was performed. From the wells with detectable single clones ($10^{-4}/10^{-5}$) 9 clones were punched out by pipette tips and given in new 6-wells with SF-9 cells. After four days supernatants were collected again and analyzed by α -His western-blotting. Clones with highest expression were further amplified. Second virus amplification was performed in 75cm² flasks. 20ml cell culture were infected with 1ml of original virus stock. After four days supernatant was collected, spun down (Haereus Megafuge/1000rpm/10'), and a plaque assay was performed to count virus titer. Next round of amplification was performed in 1l roller bottles(greiner). Three confluent 175cm² flasks were harvested and cells given with 150ml medium into one roller bottle. After four days cells were counted and adjusted to 1.5×10^6 cells/ml. Cells were infected with 0.3 MOI/cell and incubated for four days. Again cells were pelleted, supernatant was collected and a plaque assay was performed to check virus titer. Eventually, 4th and 5th round of virus amplification were performed until virus stocks with titer $>5 \times 10^7$ MOI were obtained.

Viral expression and protein purification

Roller bottles containing 300-600ml of 1.5×10^6 cells/ml were infected with 3 MOI/cell and incubated for three days. Cells were centrifuged (Beckmann J2-21/JA-14/10000rpm/30') and supernatant was dialysed twice against 5l Ni-buffer. Solution was again centrifuged as before and loaded onto Ni-NTA-agarose column (1ml Ni-NTA-agarose solution (Quiagen) per 100ml supernatant) by gravity flow. Column was washed with 3-5 bed volumes of Ni-buffer and eluted 6x with one bed volume of Ni-elutionbuffer. Washing and elution fractions were collected and analyzed by SDS-PAGE. Protein containing fractions were pooled and dialysed against 1l TMAE-buffer. The resulting dialysate was loaded on a TMAE-column and eluted by a NaCl-gradient (0-1M). Collected fractions were analyzed by SDS-PAGE and fractions with monomeric receptor were finally purified over HPLC and lyophilized.

2-2-7 Biotinylation of ectodomains

200µl of NaHCO₃ and 10µl of 400µM Sulfo-NHS-LC-Biotin (pierce) was added to 100µg of protein resolved in dH₂O (1mg/ml). The reaction was filled to 1ml with 1x PBS and incubated at RT for 5h. To prepare the biotin-linked protein for chip-coupling, it was dialysed against low salt HBS (10mM HEPES pH 7.4, 150mM NaCl, 3.4mM EDTA) filled up to 10ml with low salt HBS and pressure filtrated to ~300µl to remove nonreacted biotin. The resulting solution was aliquoted in 10µg aliquots and stored at -80°C.

2-2-8 Biacore measurements

The BIA2000 system was used to record the binding of DPP variants to the immobilized receptor ectodomain. The biotinylated protein was fixed to streptavidin-coated matrix of a biosensor CM5 chip in flow cell 2 at a density of ~200 resonance units (RU) corresponding to 200pg of protein per mm². DPP variants at 15 to 180nM in low salt HBS buffer (10mM HEPES pH 7.4, 150mM NaCl, 3.4mM EDTA, 0.005% surfactant P20) were perfused over flow cells 1, 2, 3, 4 in series at a flow rate of 10µl/min at 25°C. Sensograms were recorded at a data sampling rate of 2.5 Hz. The association period was 600s and the dissociation period was set to 300s. Free receptor was regenerated between measurements by perfusion with 0.1M acetic acid, 1M NaCl for 30s. The background sensogram recorded for flow cell 1 (streptavidin control) was subtracted from sensograms obtained for flow cells 2 (Tkv) and flow cell 3 (Act-RIIB). The differential sensograms were evaluated according to fitting routine 2 provided by the BIA evaluation 2.2.4 software (Biacore). Equilibrium binding of DPP variants was measured twice with a maximal SD of $\pm 25\%$. Because the true stoichiometry of complex formation

was not certain, all sensograms were evaluated on the basis of an unproven 1:1 association model, and therefore only apparent and not absolute constants are presented.

2-2-9 Limbbud-assay

20-40 fertilized chicken eggs were incubated in a brooding chamber for 6 days at 37°C. Eggs were opened, embryos (hamilton stage 27-29) were transferred into PBS and the distal part of the leg and wing primordia, the limbbuds, were cut off and transferred into a small 6cm plate with PBS. After collecting all buds the PBS was replaced by 2ml 0.2% trypsin and 2ml 0.25 collagenase. Through gently shaking for 30' at RT the tissue became loosened. Following two careful washing steps with 5ml PBS, 5ml of growth medium was added to the buds and they were pressed through a 100µm polyester membrane (hartenstein) to separate the cells. Cells were counted and adjusted to 1×10^7 cells/ml with growth medium. Cells were seeded into 24 well plates, placing a drop with 2×10^5 cells into the center of each well. To attach cells to surface they were incubated for 1h at 37°C. Ligands were diluted in starving medium and 1ml of starving medium with/without ligand was added to each well. After cells were incubated for 96h at 37°C/5% CO₂, 20µl Na₂³⁵SO₄-solution was added to each well and cells were incubated for additional 6h at 37°C/5% CO₂. The supernatant was carefully removed and cells were washed once with 1ml PBS. Cells were lysed by adding 400µl GUTE and by shaking sealed plates at RT for 12-60h. The lysates were transferred to eppendorf tubes and spun down for 10' (13000rpm). 25µl of cleared lysate was precipitated with 75µl NaAc-solution and 150µl Alcian-blue solution in a 96 well plate for 1h. Precipitate was transferred onto skatron® filtermat with skatron®-12 well semiautomatic cell harvester (buffer: washbuffer, adjustment: 0 5 0), dried for 30min and measured with raytest.

2-2-10 Drosophila germline transformation

Transgenic Drosophila lines were generated by transforming modified P-elements into the germline of Drosophila syncytial blastoderm stage embryos [231, 232]. 12µg of pUAST or pUFWT constructs and 4µg of pUCsπΔ2-3 helper vector [233] were coprecipitated and resuspended in 25µl injection buffer (5mM KCl, 0.1mM Na-PO₄ pH 6.8). Resuspended DNA was microinjected into w¹¹¹⁸ embryos. Injected flies were mated to w¹¹¹⁸ flies and transformants could be identified by the presence of the white⁺ marker of the pUAST/pUFWT vector. The transgenes were mapped on chromosomes by segregation analysis and stocks were established.

2-2-11 Larval heat shocks

Egg-laying flies were kept in standard medium glasses for 5 days and larvae were grown until first 3rd instar larvae started to climb for pupation. The larvae-containing medium was transferred to a glass erlenmeyer containing 200ml water and stirred until medium was totally suspended. Approx. 100g saccharose was added and suspension was stirred until larvae started floating. Larvae were collected with 50ml greiner-vials (50ml standard vial, bottom removed, aperture in lid) covered on the top side with a Ø200µm nylon membrane and washed several times to completely remove the sugar-solution. For heatshocks, greiner-vials were closed at the open end with a fly-glass stopper and hold with the membrane side down for 4' to 8' 32°C prewarmed Drosophila Ringer. Immediately after the heatshock larvae were could down in rinsing cold water and transferred into new standard medium glasses.

2-2-12 Staining of wing imaginal discs

3rd instar climbing larvae were collected and put in icecold Ringer for 20' to receive cold-stiffness. Males recognizable by genitalia were discarded and larvae were dissected and turned inside out. Following fixation with PLP on ice for 30' larvae were washed two times for 10' with PBT 0.3% and blocked for 30' at RT in blocking solution. Larvae were carefully transferred to nunclon® microwells 60x10 into wells containing ~10µl 1st antibody solution. After incubation at 4°C overnight in a wet chamber, larvae were washed three times with PBT 0.1% by transferring them into new wells and incubated in wells with 2nd antibody solution in darkness. Finally, larvae were washed for 1h in PBT 0.1% and wing discs were prepared, transferred to a slide into a drop of 12µl vectastain®, covered by coverslip and edges fixed with nail varnish. Slides were kept at 4°C in darkness until analysis with CLSM.

2-2-13 Staining of embryos

Eggs were collected for 30' on 1.2% agar plates supplemented with 25% apple juice. The plates were incubated at 25°C for 12h (to reach embryonal stage 14) followed by 4min treatment with 7% sodium-hypochloride. During incubation embryos were displaced from agar with a brush. The embryos were transferred to a 50ml greiner shell (50ml standard vial, bottom removed, aperture in lid) covered on the top side with a Ø200µm nylon

membrane and washed thoroughly with water. Embryos were transferred into small glass vials (5ml, Hartenstein), water was removed and the embryos were fixed for 30' with 3ml n-heptane and 3ml 3.7% formaldehyde in PBS, gently shaking. The lower phase (PBS) was removed and 3ml methanol were added. After 1min of thoroughly shaking, all decorionated and devitellinated embryos sink down. The complete supernatant was removed and the embryos washed 3x with PBT 0.3%. Afterwards the embryos were transferred with a pipetman 1000µl pipette to an Eppendorf Cap and incubated for 30 min in 100µl blocking solution. For antibody incubation 1µl 100x antibody in PBT was added and embryos incubated o/n at 4°C. Next day the antibody solution was removed and embryos washed 3x with PBS. The embryos were incubated for 2h at RT in 200µl of secondary antibody solution in the dark and washed again 3 times. To clear the embryos, they were kept for 2h at a time in 30%, 50% and 70% glycerol. Embryos were transferred in 70% glycerol to a slide with coverslips at each side as spacer, covered with one coverslip and sealed carefully with nail polish.

3 Results

3.1 Generation of DPP-Variants

The aim of this work was to determine the role of specific domains of DPP & BMP in signaling. Hereby the focus was on domains potentially relevant for the interaction with extracellular matrix which would be important for the establishment of morphogen gradients. Groups of basic aminoacids are found in the N-terminal region of mature *Drosophila* DPP as well as mammalian BMP-2/BMP-4. This clustered islands of positive charges have been shown to represent heparin binding sites in BMP-2 [234]).

To investigate the potential matrix-binding function of the basic aminoacid groups, different variants of *Drosophila melanogaster* DPP were generated. Expression of mature proteins was obtained in *E.coli* to perform biochemical experiments. The full-length protein expressed in *Drosophila* was used for in vivo studies. In order to detect synthesized DPP by westernblotting, a myc-epitope tag (GEQKLISEEDL) was introduced between Glu462 and Gly463 (aa positions refer to immature protein sequence published in [68]).

The D-MYC variant corresponds to the wildtype DPP with the addition of the myc-epitope. To remove all potential matrix-binding sites, the deletion variant D-DEL, also carrying the myc-epitope and lacking the sequence from Lys466 to Lys481 (see table 3-1), was created. Thus, all basic aminoacids upstream of the first cysteine residue of the cysteine knot were deleted. D-DUP was generated as a “duplication variant” with potentially increased matrix binding. In D-DUP, the sequence from Lys471 to Lys481, which contains 63% basic aa residues, was introduced in a second copy after Gly460 followed by serine and glycine (see table 3-1). D-DUP also carries a myc-epitope after position Glu462.

For expression of recombinant DPP as well as the three variants D-DEL, D-MYC and D-DUP in *E.coli*, the different constructs were cloned into the expression vector pET-3d (stratagene)(for cloning details see [235]). Hence, the *E.coli* DPP-protein was not folded correctly and it had to be refolded in a suitable buffer solution (see 3.2.2). The proteins were expressed only in their mature form, i.e. starting with Asp457. The wildtype DPP-construct starts with the sequence MAPT, which has been shown to work as efficient translation start in the BMP-2 variant EHBMP-2 [234]. Thereby, the first two aa's of mature DPP [73, 187], Asp457 and Val458 had been removed [236]. The variants D-DEL, D-MYC and D-DUP start with the aminoacid triplet MAP followed by Asp457, the regular first aminoacid of mature DPP (see table 3-1).

<i>E.coli</i> expression	
DPP	MAPT-----SGGE-----GGGKGGRNKRQPRRPTRRKNHDDTC...
D-DEL	MAP-----GEQKLISEEDLGGG-----NHDDTC...
D-MYC	MAPDV-----SGGEGEQKLISEEDLGGGKGGRNKRQPRRPTRRKNHDDTC...
D-DUP	MAPDVSGKRQPRRPTRRKSGGEGEQKLISEEDLGGGKGGRNKRQPRRPTRRKNHDDTC...
<i>D.mel.</i> expression	
D-DEL	...DV-----SGGEGEQKLISEEDLGGG-----NHDDTC...
D-MYC	...DV-----SGGEGEQKLISEEDLGGGKGGRNKRQPRRPTRRKNHDDTC...
D-DUP	...DVSGKRQPRRPTRRKSGGEGEQKLISEEDLGGGKGGRNKRQPRRPTRRKNHDDTC...

Table 3-1: N-terminal regions of mature DPP-Variants

Basic aminoacids are shown in red, myc-epitope in blue and non-DPP sequences in grey. All constructs contain C-terminal from the cystein 101 additional aminoacids. Fly constructs start with the regular propeptide of 456 aminoacids, not shown. Note that the myc-epitope carries one basic and four acidic residues.

3.2 Biochemical studies with recombinant DPP

3.2.1 Expression of DPP and DPP-Variants in E.coli

The expression of recombinant DPP has previously been described [235-237]. The pET-3d vector includes a promoter for T7-RNA-polymerase upstream of the BamHI/NcoI cloning site. PET-3d is used for expression in E.coli strain BL21DE3. This E.coli strain contains a chromosomal integrated T7-polymerase gene under the control of a lac-operator. The lac-operator (lacUV5) represses T7 polymerase expression. The operator is activated by feeding bacteria with galactose or the stable analogon IPTG. BL21DE3 bacterias were transformed with pET-3d-DPP-X (DPP-X representing wildtype DPP and the three variants D-DEL, D-MYC and D-DUP) and 5 clones of each construct were tested for high protein expression after induction with IPTG for 3h. This step was necessary because recultivation of frozen BL21DE3 stocks often led to loss of inducibility. High expression clones were grown and induced as described in chapter 2-2-3. Immediately prior to induction and then every hour a 1ml aliquot was collected for analysis. Cells were harvested, sonified and finally frozen at -20°C.

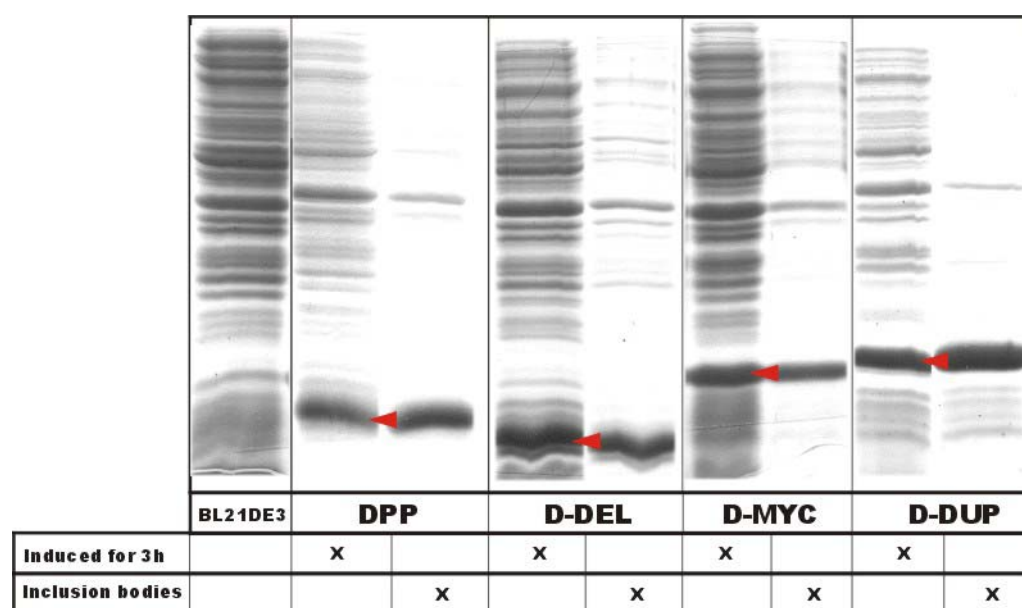


Figure 3-1: Expression of DPP and DPP-Variants

Coomassie stained 12% SDS-gel run under reduced conditions. Lanes with uninduced or induced cells were loaded with pellet of 100µl bacteria culture. Lanes indicated with inclusion bodies were loaded with 1µl final inclusion body suspension. Red arrowheads indicate induced proteins. Expected MW is 14.9, 14.2, 16.2 and 17.8kD, respectively.

Analysis by SDS-PAGE showed expression of all four proteins in high amounts of up to 30% of total bacterial protein content (see figure 3-1, lanes 3,5,7,9). These simply could be separated from most soluble bacterial proteins by a centrifugation step leaving the DPP-X in over 70% purity (see figure 3-1, lanes 4,6,8,10). Because the DPP-X in inclusion bodies was not correctly folded, it was extracted with 6M guanidine hydrochloride (GuCl), an extremely potent chaotropic reagent. This treatment in combination with 0.1% β-mercapto-ethanol left the DPP-X in a total reduced and denaturated form, a prerequisite for correct refolding. After extraction, the denaturated protein mix was separated via size exclusion chromatography on a Sephacryl S300-column. The column material is made of porous sephacryl-beads, allowing small molecules to invade whereas large molecules are excluded. By means of this reverse filtration step, proteins varying drastic in size as well as remaining bacterial DNA were separated from the DPP-X fractions. To decrease the high guanidine hydrochloride concentration in the following renaturation step, the solution was pressure-filtrated until the protein had reached a concentration of ~8mg/ml.

3.2.2 Renaturation of DPP and DPP-Variants

One advantage of bacterial expression of recombinant DPP compared to other methods like cell culture expression [73] is the large yield of protein. The disadvantage, however, is the renaturation required to achieve correct folding of the protein. As mentioned above, DPP is normally secreted as a cysteine-bridge linked homodimer with three intramolecular cysteine bridges in each monomer. To get a biologically active dimeric molecules, all four different types of cysteine bridges have to be connected in the right manner. Normally, in eucaryotic cells this correct linkage is supported a) by the large prodomain, which is thought to play a key role in correct prefolding of the ligand [74] and b) by the suitable chemical milieu in ER and Golgi-apparatus. The recombinant DPP was refolded in a suitable buffer system that contains high salt concentrations, CHAPS as a detergent and a redox system of reduced and oxidized glutathione. The latter helps cysteine bridges to form and to reopen until the correct ones have been built. Preliminary tests have shown that the best ratio between correctly folded dimer and presumable not correctly folded monomers was achieved at 18°C after 7 days. Figure 3-2 shows that all four DPP-Xs reached over 50% dimer share.

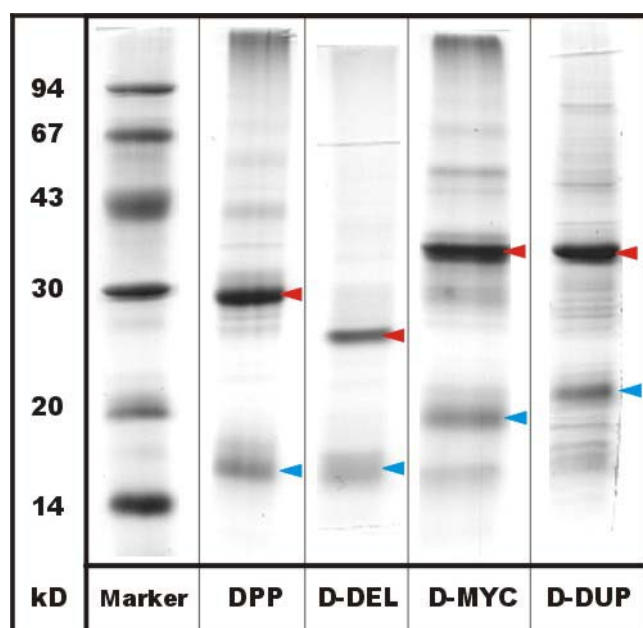


Figure 3-2: Renaturation of DPP and DPP-Variants

Coomassie stained 12% SDS-gel run under nonreduced conditions.

Loading for marker lane 1 µg/band, for other lanes 1 µg protein. Red arrowheads indicate dimer bands, blue arrowheads monomer bands.

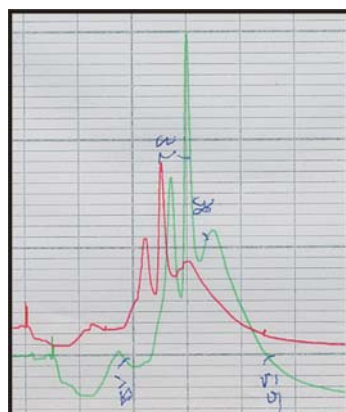
3.2.3. Purification of DPP and DPP-Variants

To separate the dimeric DPP from monomeric DPP, cation-exchange-chromatography has been shown to be the appropriate tool. In former attempts [235, 236] the renaturation probe was dialysed against 50mM NaOAc at pH 5.0. After addition of 30% v/v 2-propanol, the mixture was loaded onto a CM-Sepharose column and eluted by a NaCl-gradient as described for the purification of BMP-2 [234]. In contrast to BMP-2 the addition of 2-propanol to DPP-renaturation solution led to a drastic loss of material through clumping. Therefore the method was altered to that described in Groppe, J. et al. 1998 [237]. The renaturation solution was stepwise desalted by pressure filtration and the pH lowered to 3. Urea was added to a final concentration of 6M which stabilizes DPP and prevents aggregation and clumping. The recombinant DPP and the variant D-MYC were then loaded onto a heparin-sepharose column and eluted as described (see also Figure 3-3).



Figure 3-3: Elution profile of DPP from Heparin-column

Recorded at 280nm; green line shows higher signal amplification than red line (in shifted timescale), blue numbers indicate collection fractions.



As the D-DEL mutant should, according to the BMP-2 homolog EHBMP-2 [234] not bind to heparin, the purification of D-DEL through heparin-sepharose was not attempted. The system was changed to tentacel-FPLC (Fractogel EMD SO_3^-) with the 6M urea buffer adjusted to pH 4.0 by exchanging Tris-HCl to Na-Formiat because of the low pI of 4.67 of D-DEL. The separation of monomer and dimer was more efficient than with heparin-sepharose (compare fig. 3-4 to fig. 3-3). Therefore the same chromatography was chosen für D-DUP. Because of different pI (9.76) of D-DUP the buffer was changed to Tris-HCl and pH 8.0..

Figure 3-4: Elution profile of D-DEL from FPLC-column

Spectrum recorded at 280nm; green line shows higher signal amplification than red line (in shifted timescale), blue numbers indicate collection fractions.

The protein-containing fractions of each column were analysed by SDS-PAGE and fractions containing only dimeric DPP-X were pooled and dialysed against H_2O . After final purification by reverse phase HPLC the proteins were aliquoted and lyophilized. The resulting freeze-dried protein can be stored at -20°C for at least several months.

After the two purification steps the resulting proteins consist almost completely of the dimeric fraction (>95%) with only little share of multimers (see figure 3-5). The yield of the different DPP-Variants out of 10l induced bacterial culture varied from 4.8 mg to 32.1 mg finally purified and lyophilized protein (see table 3-2).

The amount of cells and the yield of inclusion bodies was comparable among all four preparations. Strikingly the purification over Heparin-column (DPP, D-MYC) was much more efficient than purification over FPLC (D-DEL, D-DUP).

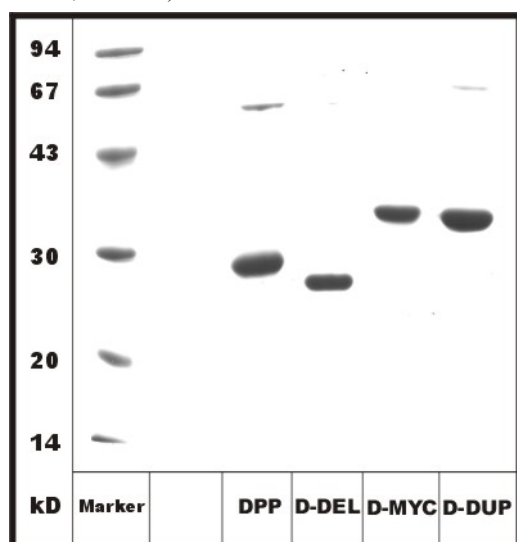


Figure 3-5: DPP and DPP-Variants after purification and resolution

Coomassie stained 12% SDS-gel run under nonreduced conditions. Loading of protein marker $1\mu\text{g}/\text{band}$, other lanes $2\mu\text{g}$ protein/lane.

Variant	wet pellet after harvesting in g	wet pellet inclusion bodies in g	final yield in mg
DPP	33.2	6.0	32.1
D-DEL	44.3	7.0	5.1
D-MYC	32.6	6.2	22.0
D-DUP	31.4	7.4	4.8

Table 3-2: Yield of purified DPP-variants

3.2.4 Heparin-affinity chromatography

To demonstrate the apparent affinity of the different DPP variants to heparin, 1mg of each variant was loaded on a heparin-EMD-fractogel column and eluted with a 0-1M NaCl gradient, in the presence of 6M urea. The absorbance at 280nm was detected together with the conductivity to visualize protein elution and NaCl gradient simultaneously. The elution profiles indicated increasing heparin affinities for the ligands (D-DEL < D-MYC <

DPP < D-DUP). Elution-peaks were at 0.15M NaCl (D-DEL), 0.4M NaCl (D-MYC), 0.5M NaCl (DPP) and 0.55M NaCl (D-DUP), respectively (see figure 3-6).

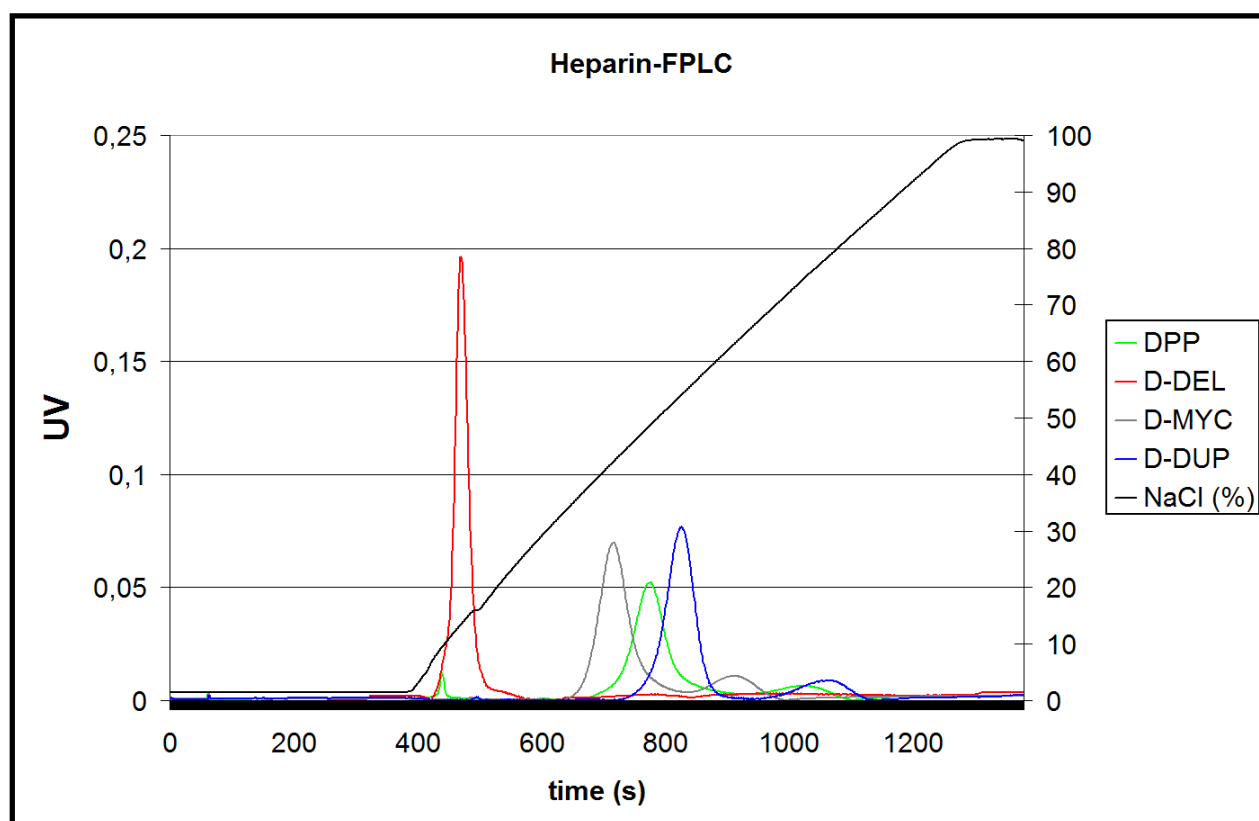


Figure 3-6: Elution profiles of DPP variants within a 0-1M NaCl gradient from heparin-fractogel

Elution profile at 280nm of DPP-variants, black line shows the recorded conductivity.

Elution points:

DPP	0.5M NaCl
D-DEL	0.15M NaCl
D-MYC	0.4M NaCl
D-DUP	0.55M NaCl

3.2.5 Cloning, expression and purification of the Tkv-ectodomain

According to ExpASY database (www.expasy.ch; accession number Q9VMT1) and Brummel et al. 1994 [124] the tkv ectodomain includes the first 179 aminoacids of the polypeptide chain. The 20 most N-terminal aminoacids represent the signalpeptide sequence [124, 126]. Therefore, the DNA-sequence from Glu21 to Thr179 (aa positions refer to protein sequence published in [124]) was amplified by PCR using primers tkv-7 and tkv-8a. With these primers BamHI-sites were introduced "in frame" at both ends. The resulting PCR-product was cloned via BamHI into pAcGP67/B-TH (provided by J.Nickel). This vector provides a signalpeptide, a thrombin cleavage site and C-terminal a 6x His-tag in frame with Bam HI. The clone "pAcGP67/B-TH-tkv" was verified by sequencing and used in baculovirus cotransfection to produce tkv-ectodomain secreting viruses.

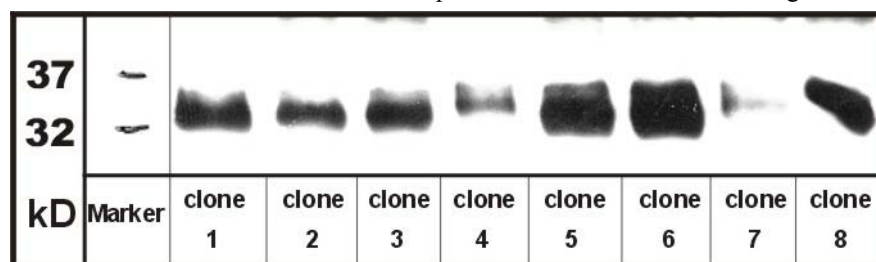


Figure 3-7: Tkv-ectodomain expressing clones

10% SDS-PAGE with 10µl cell culture supernatant under nonreduced conditions followed by Westernblot with anti-His-tag antibody.

Out of the 8 examined clones shown in figure 3-7, clone 5 was chosen for further amplification because of its relatively high expression level. After three rounds of amplification, a virusstock with sufficient virus titer (6×10^7 MOI/ml) was established and protein expression was performed. The elution fractions from two virus expressions (350ml + 800ml), which contained a protein of slightly smaller than 30kD (see figure 3-8 lanes 5-7) were pooled and further purified by TMAE-anion-exchange-chromatography (see figure 3-9). All fractions expressing the expected 30kD protein also contained a prominent band at ~50kD. This band was immunoreactive with α -His antibody and could not be reduced by β -mercapto-ethanol.

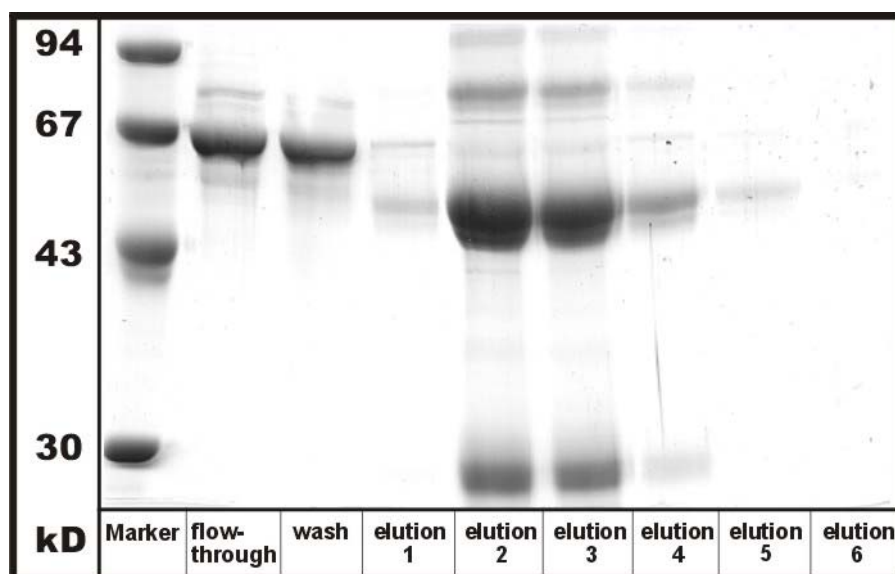


Figure 3-8: Elution of tkv-ectodomain from Ni-NTA-column (800ml expression)

(10% SDS-gel run under nonreducing conditions; protein of interest (27kD) is detected in lanes 5-7; the most prominent band at ~50kD is also present under reducing conditions and detectable by α -His-westernblot (data not shown))

After dialysis against Hepes-buffer the solution was loaded onto a TMAE-column. Other receptor-ectodomains like Alk-6 or ActIIB did not bind to TMAE-matrix, in contrast to their multimers (J.Nickel, pers. comm.), which provided a tool for purification. Surprisingly, the Tkv-ectodomain bound to the column and could be eluted by a NaCl-gradient (see figures 3-9 & 3-10).

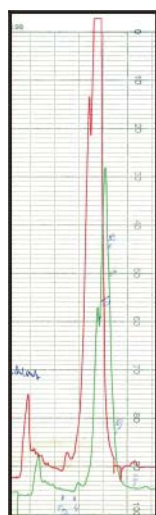


Figure 3-9: Elution of Tkv-ectodomain from TMAE- column

Recorded at 280nm; red line shows higher signal amplification than green line.

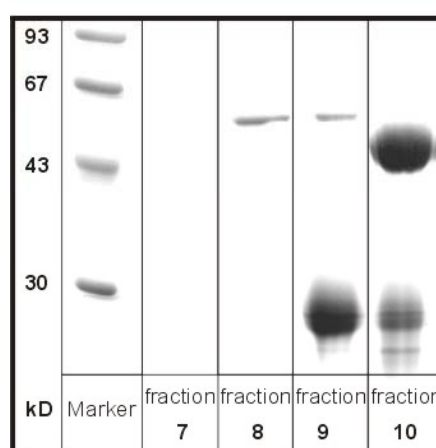


Figure 3-10: TMAE-elution fractions of Tkv- ectodomain
Coomassie stained 10% SDS gel run under nonreduced conditions. Loading lanes 7-10: 10 μ l

As seen in figure 3-10 the monomeric tkv (~27kD) was well separated from the more prominent 50kD protein. Fraction 9 was further purified by HPLC and lyophilized. The final yield from 1.15 liter SF-9 culture was 1.2 mg purified monomeric tkv-ectodomain. This extracellular receptor fragment was further used for ligand-receptor affinity determination with biosensor-measurements (see 3.2.6).

3.2.6 Biacore-measurements with the Tkv-ectodomain

In BMP-2, the N-terminal region prior to the first cystein does not contribute to receptor binding [75, 238, 239]. Due to conserved binding residues and the ability of BMP-2 to phosphorylate Drosophila Mad in S2-cells (see fig 3-32) this might also hold true for DPP. The DPP-variants generated for this work, thus, should not show altered receptor binding. To verify this assumption, biacore-experiments were performed with the ectodomain of the Tkv-receptor bound to a CM5 sensorchip. This method makes use of the phenomenon, that light reflection at a boundary layer depends to some extent on the mass of the layer. Thus, in this experiment, the ectodomain of Tkv was coupled to a chip with a thin gold layer and the changes in light reflection after ligand binding resulted in different resonance units. A solution with 100ng/ml of the biotinylated receptor was applied to one cell of the streptavidin coupled chip until 200 resonance units per mm² (RU) were bound. A second cell was coated with 200 RU of ActRIIB as a control. The formation and dissociation of the receptor/ligand complex was measured in real time during perfusion for 600s with buffer in the presence of the different ligands and for further 300s with the buffer alone. The traces in fig 3-11 represent measurements with 180nM of each ligand. Higher ligand concentrations were not tested since in one of two measurements, D-DUP precipitated in the initial 240nM buffer mix. After rapid binding in the first 20s, the curves reach steady state conditions after 100-200s. The K_d values were calculated from dose dependent equilibrium binding in the concentration range from 15 to 180nM (see table 3-3).

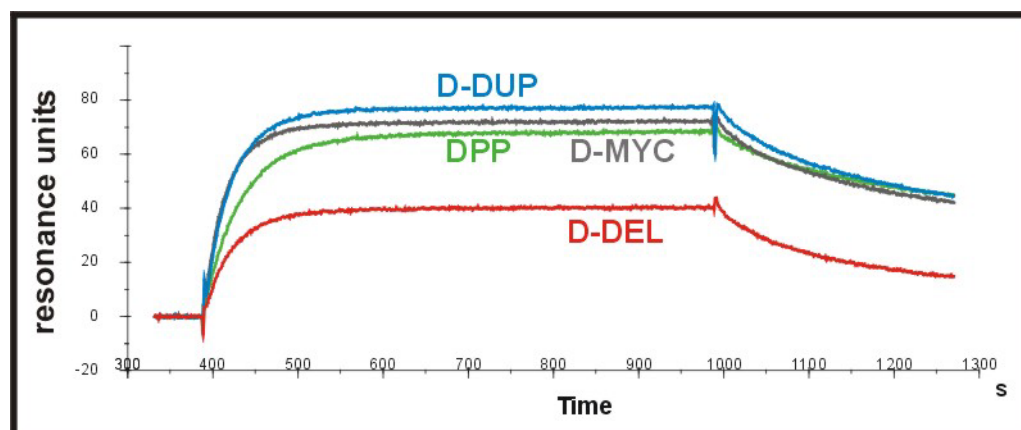


Figure 3-11: Resonance profiles of different DPP-variants at 180nM (resonance curves for each ligand shown in different colour; different maximum resonances correspond to different molar masses of DPP-variants)

ligand	KD (eq) 1 st measurement (15/30/45/60/120/180nM)	KD (eq) 2 nd measurement (30/60/90/60/120/180nM)	mean
DPP	24nM	21nM	22nM ±2
D-DEL	24nM	27nM	25nM ±2
D-MYC	11nM	18nM	14nM ±4
D-DUP	18nM	14nM	16nM ±2
BMP-2	32nM	47nM	39nM ±8

Table 3-3: KD values of different DPP-variants to tkv calculated through equilibrium conditions (Sensograms were evaluated on the basis of an unproven 1:1 association model, and therefore only apparent and not absolute constants are presented due to lack of complex stoichiometry data)

The KD-values of the different DPP-variants ranged all from 14nM to 25nM with a difference of factor 1.7 between D-DEL and both D-MYC and D-DUP. Thus, the potential matrix-binding deficient variant D-DEL elicits a slight decrease in receptor affinity, but mean variations are too high to take significant differences into consideration.

3.2.7 The limbbud-assay

The cell culture system using mesodermal embryonic chick limbbud cells has often been described [240-242]. It is used to characterize the differentiation of mesenchymal stem cells to cartilage and bone tissue. In the course of this, the synthesis of proteoglycans, which starts 2d after stimulation with appropriate growth factors and reaches its maximum after 4-5 days, is taken as an indication for ongoing chondrogenic and osteoblastic differentiation programs. The synthesis rate of proteoglycans is measured through incorporation of radioactively labeled sulfate into newly synthesised GAG-sidechains. This assay has been modified and optimized for BMP-2 to result in a dose-response curve that reaches a saturation level [234]. This allows to determine the concentration of ligand at the halfmaximal response, the EC_{50} value, as a measure of biological activity of the ligands.

In the limbbud-assay a micromass cellculture is incubated with varying concentrations of ligands for 96h. The production of matrix is measured through the incorporation of radioactive labeled sulfate groups into the glycosaminoglycan sidechains of the growing matrix. After another 6h cocultivation with $Na_2^{35}SO_4$, cells are lysed with 6M guanidine-hydrochloride and the proteoglycans are precipitated with 0.2% alcian blue and washed on a filtermat to be analysed for incorporation of the radioactive label.

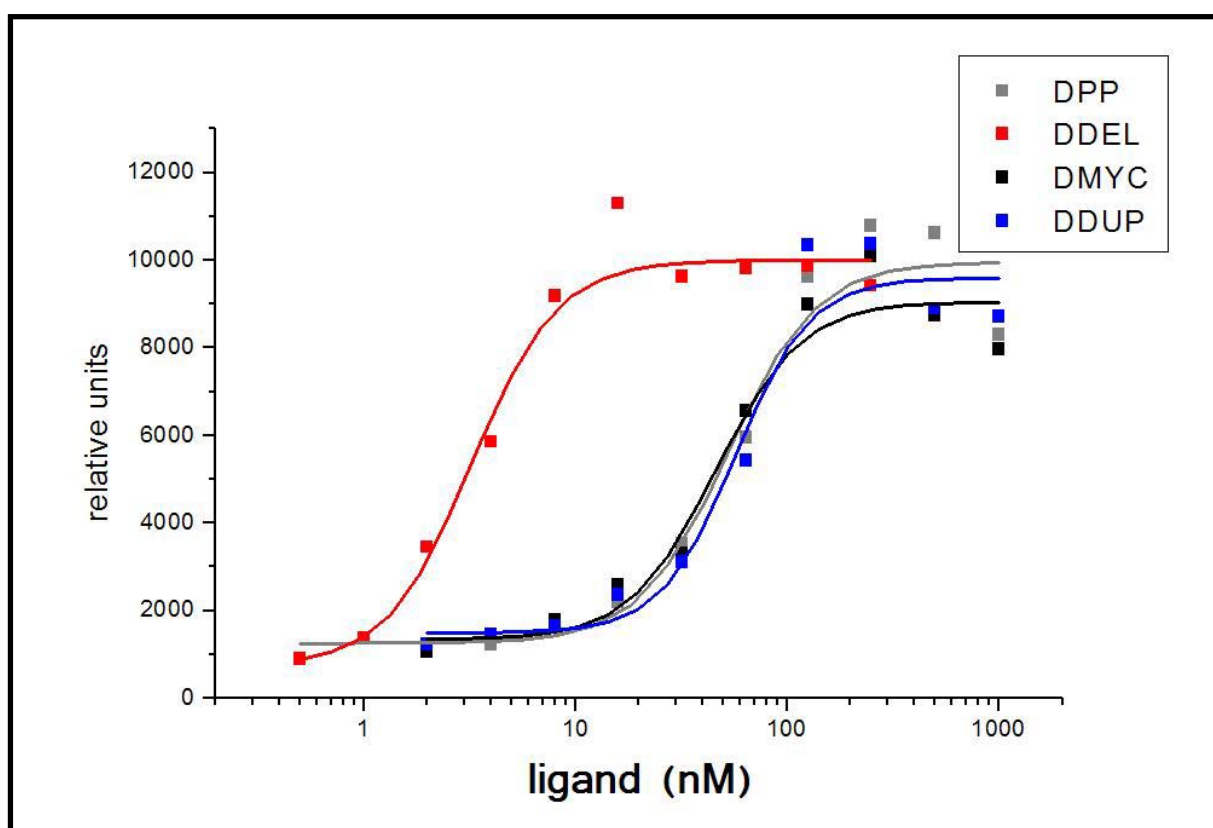


Figure 3-12: Comparison of biological activity of the four DPP-Variants

Relative units reflect the results from two independent experiments, each performed in triplicate. EC_{50} values represent ligand concentration at halfmaximal response.

Two independent limbbudtests in triplicate measurements revealed the activity differences as seen in figure 3-12: the deletion variant D-DEL with an EC_{50} of 4-5nM was much more active than wildtype DPP, D-MYC and the duplication variant D-DUP, which all shared an EC_{50} value of 50-60nM. The difference between D-DEL and DPP/D-MYC is consistent with the findings between BMP-2 and EHBMP-2 [234]. Interestingly, the addition of potential matrix binding sites in D-DUP does not lower the activity in the limbbud experiments. Also the MYC-epitope in D-MYC, containing four negative and one positive charges, compared to wildtype DPP does not noticeable interfere with DPP activity.

3.3 Effects of ectopically expressed DPP-variants in *Drosophila*

3.3.1 Generation of transgenic flies

To allow expression of the three DPP variants in *Drosophila*, cDNAs coding for the full-length proteins including the large propeptide of 456 aminoacids, were cloned into *Drosophila* expression vectors pUFWT and pUAST (for cloning details see Figure 6-1). Both vectors contain a UAS binding site for the yeast transcription factor Gal4. The variants were cloned as Not-I fragments [235] into the unique Not I site downstream of 6xUAS in pUAST. For the pUFWT-vector system initially also a subset of deletion variants (D-DEL-1/-2/-3/-4) was generated, which stepwise truncate the region deleted in D-DEL. All constructs have been verified by sequencing. As experiments with these constructs have not been performed beyond the first expression tests (see figure 3-15) they are not described in detail here. In case of the pUFWT vector, the NotI-fragments were cloned into the unique NotI-site, which is separated from the UAS-site by a CD2-cassette, flanked by two FRT-Sites (see figure 3-13). All constructs were germline injected into white¹¹¹⁸ flies and for each construct ~10 independent lines were established.

3.3.2 Testing the pUFWT-system

The pUFWT-vector system was chosen because of its utility in generation of small clones expressing ectopic DPP. In the transgene, the DPP-gene is totally inactive because transcripts starting from the UAS-promoter are terminated behind the CD2 gene. Incrossed Gal4-lines can only give rise to expression of the CD2 gene. To activate the DPP-gene, a yeast flippase is needed. This flippase is crossed in as a heatshock-promoter construct. By applying heat shocks to the animal, the heatshock promoter activates the flippase gene. Next the expressed flippase-enzyme can bind to the flippase recognition target (FRT) sites and catalyze a somatic homologous recombination event. Thereby the CD2-cassette is cut out and the UAS-promoter comes into proximity of the DPP-gene, only separated by one left FRT site. In this situation the UAS-promoter gains influence over the DPP-gene and expression of the DPP-construct can be achieved by the transactivator Gal4.

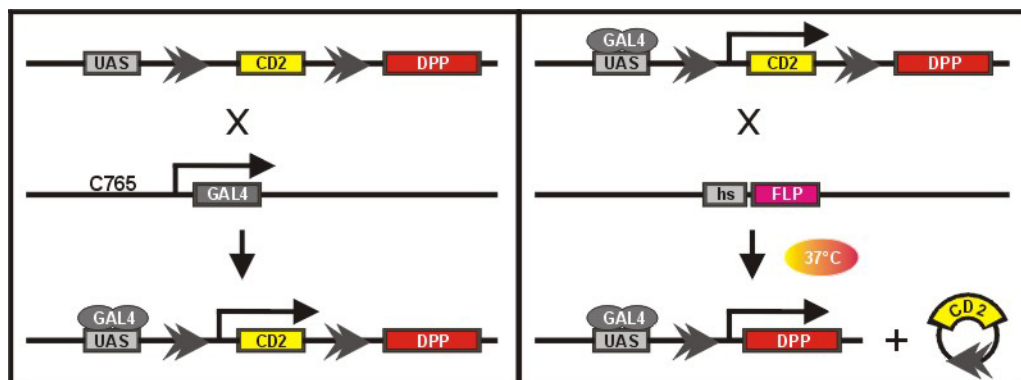


Figure 3-13: Gal4-driven expression of CD2 before heatshock (left panel) and DPP-construct after heatshock (right panel). Double arrows represent FRT sites.

The intensity of the heatshock can be varied by temperature and time. Whereas strong heatshocks (37°C/1h) activate the flippase and lead to flipping in all suitable cells, mild heatshocks (32°C/4') give only rise to randomly distributed single DPP expressing cells. If the heatshock is applied during embryogenesis or larval stages, the single DPP-expressing cells undergo several rounds of proliferation and lead to clones of DPP-expression. Nonflipped cells keep expressing the rat CD2 gene, that serves as a cell surface marker and can be stained with specific antibodies. The flipped, DPP-expressing cells are recognized as dark spots because of lack of the CD2-staining.

Since the wing imaginal disc is a cell-monolayer and sensitive to DPP in a dose-dependent manner [87], it has been chosen to analyse the effect of clonal ectopic expression of the DPP-variants. The target genes *optomotor-blind* and *spalt*, which are regulated by low and high doses of DPP respectively [87, 243], should serve as readout for the activity of the different variants.

Test series with differences in duration and temperature of heatshocks revealed, that shocking early 3rd instar larvae for 4'-8' at 32°C elicited small numbers (~1-10) of flipped, DPP-expressing clones randomly spread over the wing disc (see figure 3-14a). In the P-element line X35, a P-element within the *omb*-locus expresses β -galactosidase in the endogenous *omb*-expression pattern [172]. Staining for β -galactosidase detected ectopic expression of *omb* in a circular domain around the DPP-secreting clone (see figure 3-13b). This demonstrated the function of the pUFWT-based expression system.

To ensure that observed differences in omb-expression were caused by differences in the activity of the variants and not by different levels of expression, lines of each construct with comparable expression level had to be collected for further analysis. The circumstance, that the construct needed to flip in order to be active, made it necessary to generate equal numbers of flipping events in every transgenic line. This could principally work with very strong heatshocks. These heatshocks activated dpp in all cells sensitive to the flippase enzyme and also led to large amounts of expressed DPP, that should be detected by western blotting. Early larvae from several lines were treated with a strong heatshock lasting for 60' at 37°C. Immediately, the larvae were brought back to standard growth conditions for 48h and then analysed by α -CD2-staining for heatshock-efficiency (see figure 3-14a-f). Apparently the strong heatshock did not result in comparable rates of flipping in different transgenic fly lines.

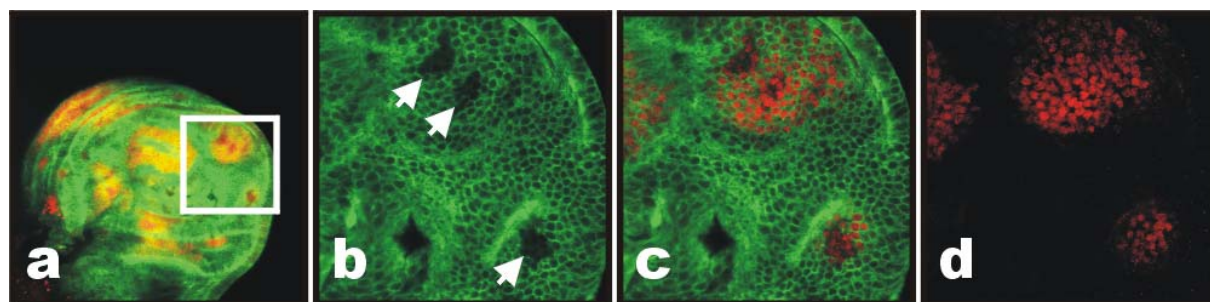


Figure 3-14: Induced ectopic clones expressing D-MYC

a: Optical cross-section through a 3rd instar wing imaginal disc (green: CD2; red: β -Gal). The inset is shown in higher magnification in b-d. b: D-MYC-expressing cell clones are seen as black spots in CD2-staining marked by arrows. c: overlay of CD2 and β -gal staining shows that D-MYC induces expressing of omb-lacZ(X35) also in cells surrounding the clones. d: β -Gal staining represents omb-expressing cells.

All discs shown in this and subsequent figures are wing imaginal discs. Anterior is always to the left, if clearly discernible, and dorsal is to the bottom.

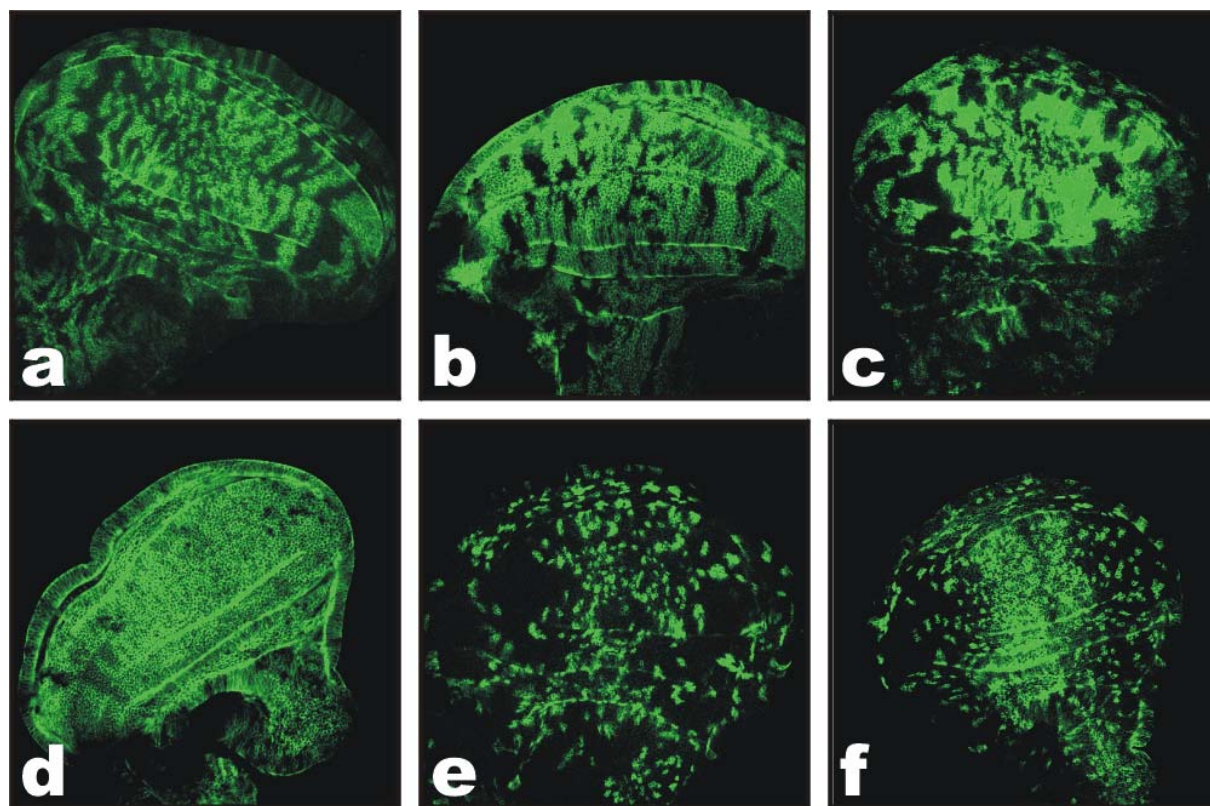


Figure 3-15: Flipping rates of wing discs 48h after 1h heatshock

a: D-MYC; b: D-DEL-1; c: D-DEL-2; d: D-DEL-3; e: D-DEL-4; f: D-DUP; all images show CD2-stainings of late 3rd instar wing discs in optical cross-section, black gaps represent flipped cell clones. Note similar clone frequency in a-c, but total different frequency in d and e+f.

All lines showed incomplete flipping, affecting not all cells after a heatshock of 1h at a temperature nearly

critical for survival of the larvae. This can be explained by a strict cell cycle dependence of the flippase, also observed by others (A. Keller, pers. com.). Also the genetic context of the integration locus might influence the rate of flipping as there are large differences in flipping-rates among the examined lines (compare figure 3-15d to 3-15e). Nevertheless, it was not possible to compare the expression rates of the ectopic DPP among different lines. Thus, the pUFWT-system was not useful for analysis of the different DPP-variants.

3.3.3 Expression-test of pUAST-constructs

The pUAST-constructs can directly be activated through any Gal4-driver. Therefore the comparison of expression levels is not dependent on any preceding event like flipping. To get high expression levels of the DPP-constructs, they were crossed to a heatshock-Gal4 line [123]. This line expresses large amounts of Gal4 subsequently after heatshock activation. Several sets of experiments revealed that preparing heads of adult flies resulted in better western blot results with lower background than preparing total adult flies or even larvae (data not shown).

Western blot analysis with a polyclonal anti-DPP-antiserum directed against denaturated immature DPP [73] resulted in three DPP-specific bands for every preparation: one band was in all variants of same height at around 50-53kD and represents the cleaved prodomain (PD) of DPP (expected MW: 48kD, see fig. 3-16c). Two bands of around 55-64kD and 85-90kD varied in height between the variants and were assigned to the polypeptide of prodomain and ligand before cleavage by the furin protease.

All three flylines in figure 3-16a show an equal amount of the cleaved prodomain (PD). The mature ligand is not properly detected by the anti-DPP-antibody (not shown), but the ratio of ligand monomer to prodomain is always 1:1. Thus it is possible to conclude from equal amounts of prodomain to equal expression levels of mature ligands. Therefore the three lines were considered as equally expressing and used for all further experiments. The large amount of noncleaved product is not a consequence of overtaxing the processing machinery. In figure 3-16b six different flylines expressing the D-DUP-variants are seen. Some of them clearly differ in the level of expression (compare lane 3 to lane 4). But even in weak expressing lines the ratio of the three bands is the same as in the strongest expressing line.

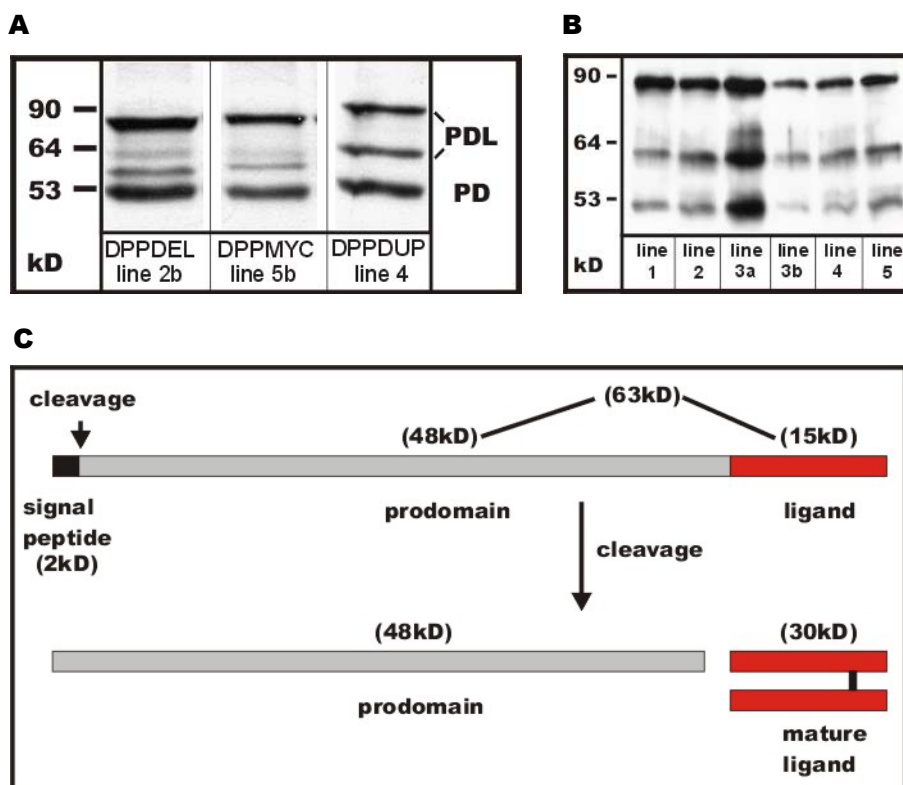


Figure 3-16: Expression of DPP-variant in stable *Drosophila* lines:

- Expression of D-DEL, D-MYC, and D-DUP lines 3h after a 45' heatshock at 37°C. Uncleaved prodomain-ligand- chain (PDL) and cleaved prodomain (PD) are indicated.
- Comparison of expression-strength of different D-DUP lines (1-5). Protein from two fly heads was separated by 10% SDS-gel under reduced conditions and detected with anti-DPP antibody in western blotting. Again the three bands for PDL and PD are shown.
- Scheme of DPP polypeptides before and after cleavage by proteases. The signal peptide is shown as a black bar, the large prodomain in grey and the ligand peptide in red. Note that the mature ligand is dimerized via a disulfid bond, but becomes

separated under reduced SDS-gel conditions. Observed bands of 55-64kD and 85-90kD in A+B cannot be assigned unambiguously within this model.

3.3.4 Clonal expression of UAS-DPP in the wing imaginal disc

With the UAS-DPP constructs, clonal analysis was only possible by generating clones through the Gal4-driver. The suitable tool for this purpose was an actin-Gal4 fly line, which contained a FRT-site flanked CD2-cassette between the actin promoter and the Gal4 gene. By crossing this line to UAS-GFP (Bloomington), a line was established, that expressed the cellular marker only in these cells, where a flippase induced recombination event flipped out the CD2-cassette and thereby activated the Gal4-driver (see fig. 3-17). This line was used in combination with the DPP-variants and a heatshock-flippase element.

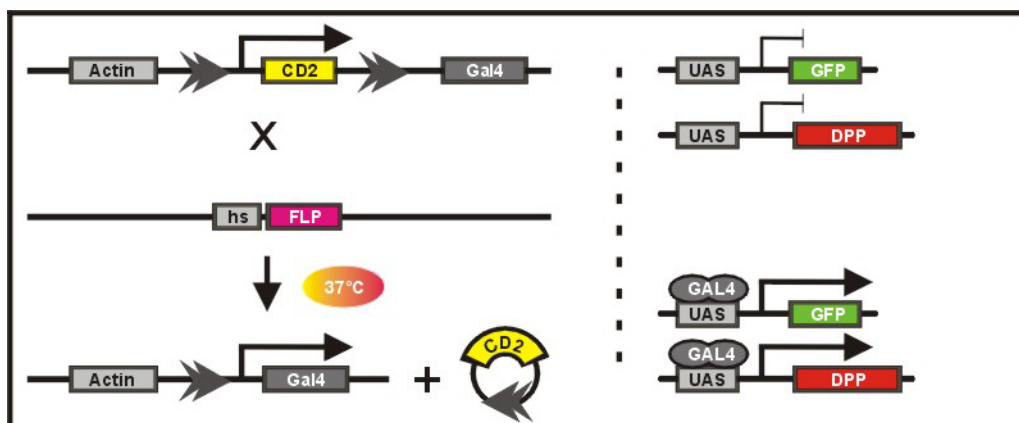


Figure 3-17: Clonal coexpression of DPP-variants and GFP through activation by actin-Gal4
Recombination event after heat shock is shown in left panel. The CD2 cassette is deleted and Gal4 becomes activated. The latter subsequently activates DPP and GFP-expression in corresponding cells (right panel). FRT sites are indicated as doublearrows.

Initial tests with drastic heat shocks (1h at 37°C) demonstrated the functionality of the system in order to generate ectopic clones of DPP expression (see figure 3-18). Mainly due to the high time- and material consumption in order to generate single clones lying in identical areas of the discs, use of the system was discontinued.

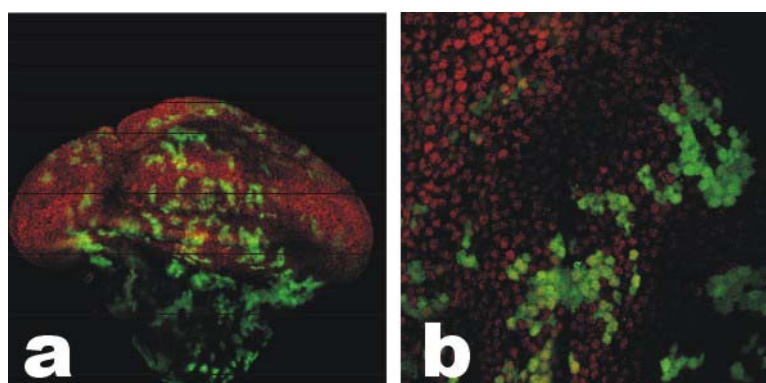


Figure 3-18: Ectopic OMB-expression results from induced clones of ectopic DPP-expression
Early 3rd instar larvae were heatshocked at 37°C for 30' and prepared after 48h. Figure shows optical cross-section through wing disc. β-galactosidase staining (resembling Omb) is shown in red, ectopic DPP producing cells coexpress GFP (green). The right panel shows 3.1 fold higher magnification of left panel.

3.3.5 Expression of DPP-variants in wing imaginal discs by various gal4-driver lines

The UAS-constructs offer the possibility to drive expression of the DPP-variants by any available Gal-4 driverline in many different tissues. Also for the wing imaginal disc there are a couple of specific or ubiquitous driver lines.

First the Gal4-driverline dpp-Gal4 [244] was used to drive expression of the DPP-variants in the endogenous DPP expression domains in imaginal disc tissues. The Gal4-UAS system is temperature-dependent resulting in low activity at low temperature (18°C), moderate activity at standard temperature (25°C) and high activity at limiting temperature (29°C). In this experiment 29°C was chosen to achieve a high ratio between DPP-variants and endogenous DPP. Superficial observations of the omb-expression pattern of 3rd instar larvae wing imaginal discs showed no differences among the three variants. As adult wings showed ectopic vein

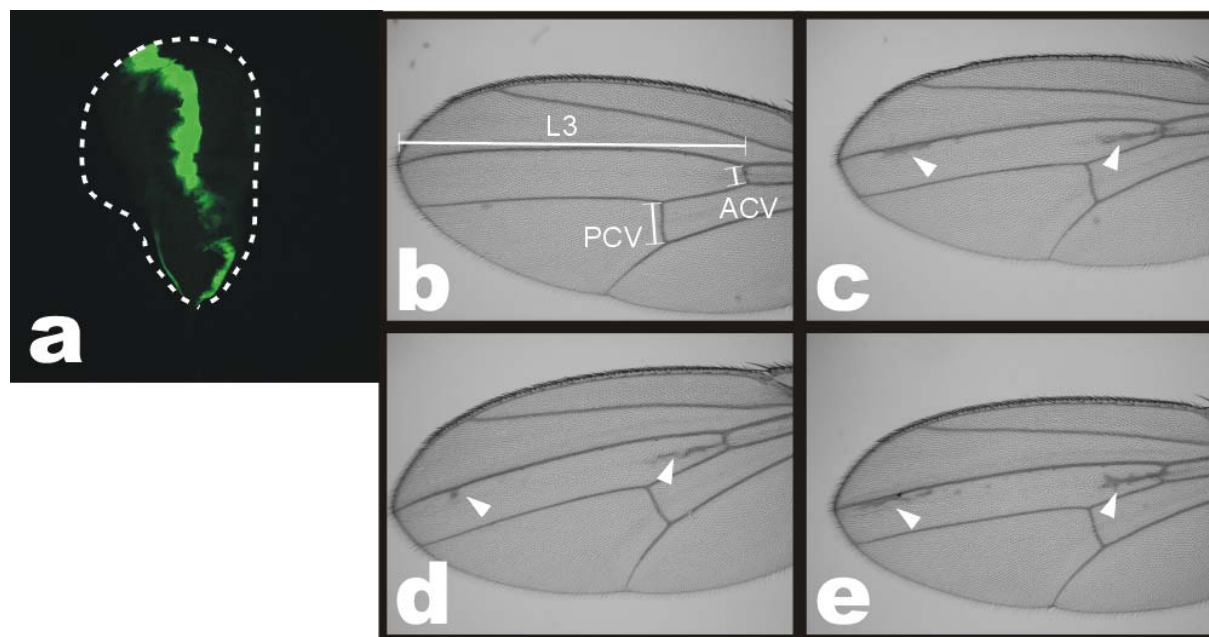


Figure 3-19: Overexpression of DPP-variants in the endogenous DPP-expression pattern

a: Wing disc of a dpp-Gal4:UAS-GFP fly showing dpp expression domain. Dashed line indicates disc margin. b-e: Cuticle preparations of adult wings from overexpression of DPP-variants by dpp-Gal4. b: wildtype wing; white lines indicate measured dimensions. c-e: overexpression of D-DEL, D-MYC and D-DUP; arrowheads indicate ectopic vein material.

patterns (see figure 3-19c-e), they were analysed in detail by measuring the lengths of the anterior crossvein (ACV), the poster crossvein (PCV) and the longitudinal vein L3 (see figure 3-19b). Overexpressing the DPP-variants showed no significant difference in the extensions of the different veins (see Table 3-4). Only the length of anterior crossvein increased slightly from D-DEL to D-DUP. In the quality and quantity of the ectopic vein material no difference could be observed.

	L3 vein (% wildtype)	ACV (% wildtype)	PCV (% wildtype)
wildtype	100 ± 2,6	100 ± 4,0	100 ± 6,6
D-DEL	98,2 ± 2,7	96,9 ± 6,0	106,6 ± 6,0
D-MYC	99,3 ± 3,3	100,2 ± 7,0	107,9 ± 4,0
D-DUP	97,3 ± 2,1	105,7 ± 6,4	102,8 ± 3,3

Table 3-4: Vein lengths shown in correlation to wildtype (n=40).

UAS-constructs were driven by dpp-Gal4 [244]. Flies were raised at 29°C to elevate GAL4 activity.

The second Gal4-driver tested in the wing was omb-Gal4 [172](see figure 3-20). Omb is a DPP target gene in the wing imaginal disc and indirectly activated through the brinker double repression mechanism [172, 175-177]. Expressing ectopic dpp through omb-Gal4 leads to an autoactivation loop. As seen in figure 3-20 even at low temperature the omb-expression domain finally covers the whole disc from the anterior to the posterior margin, equal for the ectopically expressed variants, whereas in wildtype the omb domain spans less than 50% of the disc. Measuring the dimensions of the disc and of the proximal-distal extension of the omb-domain reveals a significant increase in the anterior-posterior disc size. Among the three variants no difference was found (see figure 3-21). Astonishingly, in the proximal-distal extension the omb-domain becomes smaller through ectopical expression of the DPP-variants with significant differences between wildtype and D-MYC or D-DUP. Comparing the three variants also structural differences were observed. Whereas in D-DEL-discs there is always a maximum of omb-expression seen in the presumptive anterior wing pouch (fig. 3-20b), D-MYC- and D-DUP-disc mostly have peak levels in anterior and posterior parts of the wing pouch (fig. 3-20c). Every second D-DUP-disc additionally bears ectopic patterning or proliferation centers identified by circling rings of disc folds (fig. 3-20d). Experiments at higher temperature (25°C) lead to more extreme phenotypes with apparently stronger overproliferated discs but negligible differences between the variants. At both temperatures no adult animals were obtained.

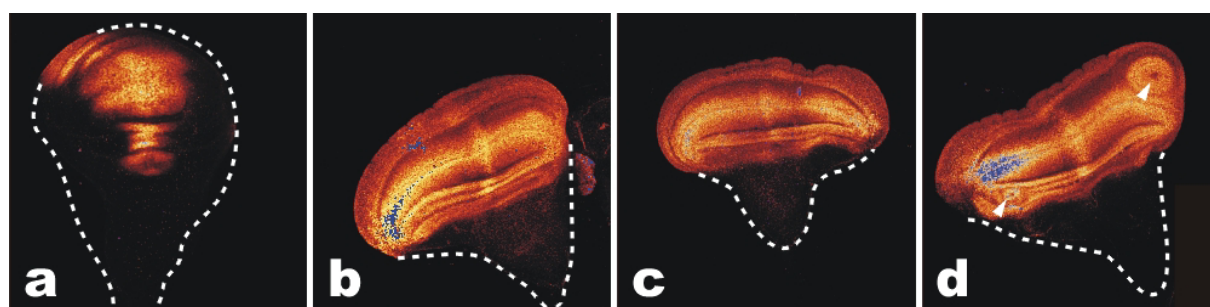


Figure 3-20: Ectopic expression of DPP-variants by omb-Gal4 at 18°C

Shown is expression of β-gal resembling the omb-expressing pattern. Red color represents weak expression, blue color highest expression. Dashed line indicates disc margin. a: wt-disc; b: D-DEL, c: D-MYC, d: D-DUP, white arrowheads mark ectopic patterning centres. All animals contained an omb-Gal4 driver. Note that in b highest expression maps to one side and in c to both sides of the disc.

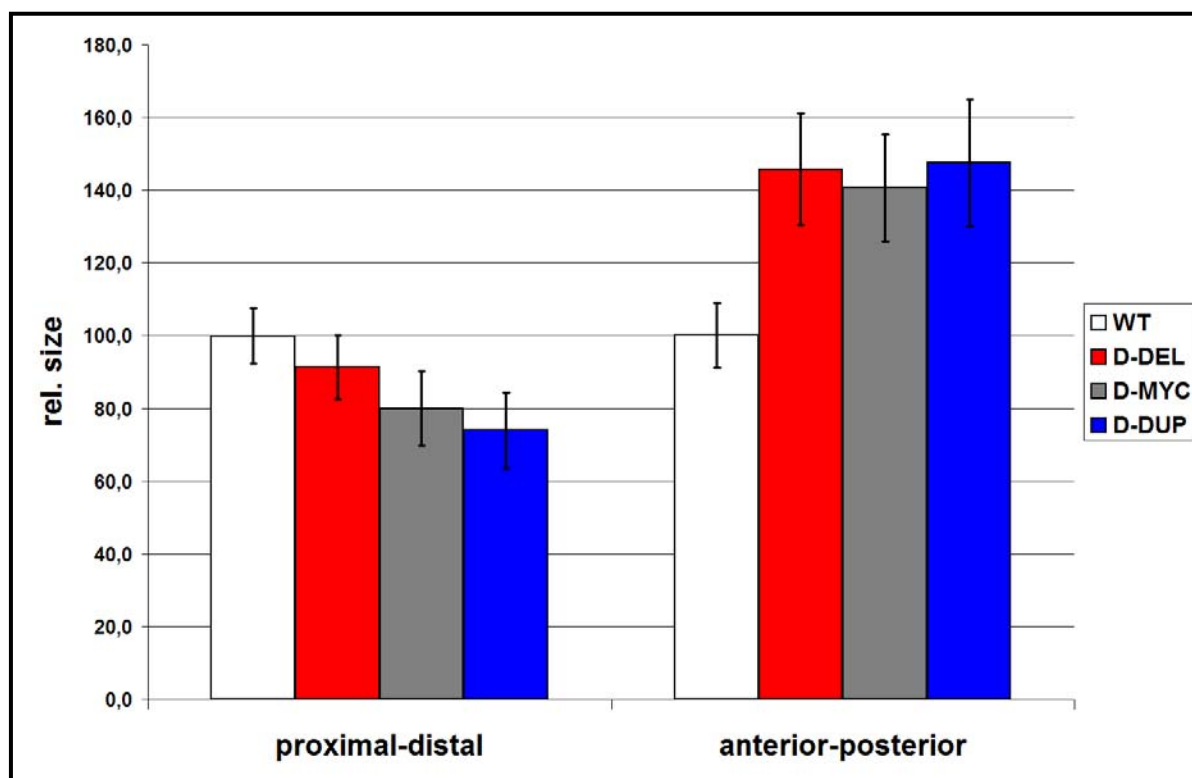


Figure 3-21: Dimensions of the omb-domain

All animals contained an omb-Gal4 driver and were raised at 18°C. All longitudinals are set in correlation to wildtype longitudinals (100%, rel. size). Left graph shows extension of OMB-expression domain in proximal-distal direction, right graph in anterior-posterior extension. Error bars indicate standard deviation.

As a third Gal4-driver line, C765-Gal4 [87] was used which is ubiquitously active in the wing disc (see figure 3-22). Female flies carrying the C765-Gal4 transgene and the X35-omb insertion were crossed to the three variants and to w^{1118} males as control. Ectopic DPP activated by C765-Gal4 resulted in differences in overproliferation and ectopic omb-expression in wing discs, depending on the variant or temperature used. At 18°C the phenotypes of the discs ranged from nearly indistinguishable from wildtype (in the case of D-DEL), to 20% overproliferation and doubling of the omb-domain for D-MYC and D-DUP (see figure 3-22 b,c,d and figure 3-23). Thus, there was a significant difference between overexpression of non-matrix-binding DPP (D-DEL) and matrix-binding DPP (D-MYC and D-DUP). This is also obvious by the percentage share of the omb-domain within the AP disc dimension. Increasing the breeding temperature to 25°C caused in all three variants a strong overproliferation phenotype and an extension of the omb-expression domain over the whole wing pouch region (see figure 3-22). Dimension-measurements as for 18°C discs were not performed as the strong proliferation along the AP-axis resulted in bending of the disc seen by the curved shape of the central folds (see figure 3-22f-h).

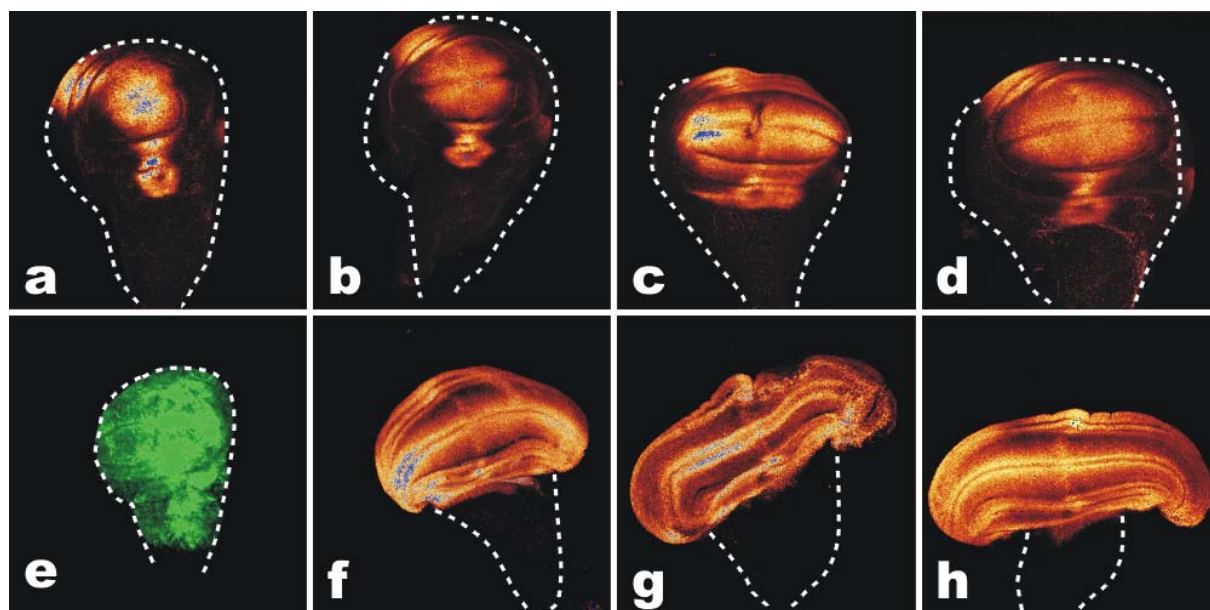


Figure 3-22: Ectopic expression of DPP-variants by C765-Gal4 at 18°C.

Again expression of omb in 3rd instar wing discs is shown by β -Gal staining. Dashed lines indicate the disc margins. All discs shown contain C765-Gal4 driver. a-d: wing discs from larvae grown at 18°C; a: wildtype; b: D-DEL; c: D-MYC; d: D-DUP. e: UAS-GFP expression through C765-Gal4 shows ubiquitous activity of Gal4-driver. f-h: wing discs from larvae grown at 25°C; f: D-DEL; g: D-MYC; h: D-DUP.

The weak structural changes of the discs at 18°C allowed adult viability in all lines. Cuticle preparations of wings were made and disturbances of normal vein structure documented (see figure 3-24 and table 3-5). Even crossing w^{1118} flies to the gal4-driver resulted in small stripes of ectopic vein material distal of PCV with 50% penetrance. D-DEL and D-MYC flies show similar phenotypes with defects in L2 vein and L5 vein. Whereas disturbances in the L2 vein show penetrances of around 50% in both variants, the L5 vein is more than twice as often disturbed in D-MYC (47%) as in D-DEL (19%). Outstanding is the phenotype of the D-DUP flies. They show loss of the distal halves of L2 and L5 veins in nearly every individual (96% and 92%, respectively). Ectopic vein material at L4 vein is also only found in D-DUP-expressing animals with a penetrance of 36%. Thus, whereas at the level of imaginal discs, surveying the omb expression, phenotypes divide into two groups: no/mild phenotypes for wildtype (i.e. X35; C765-Gal4/III) and D-DEL and strong phenotypes for D-MYC and D-DUP. Against that surveying vein patterns of adult wings reveal three phenotypical groups: wildtype (i.e. Gal4-driver) with neglectable disturbances at PCV, D-DEL and D-MYC with similar disturbances of L2 and L5 pattern and D-DUP with strong disturbances of L2/L5 and ectopic vein material adjacent to L4.

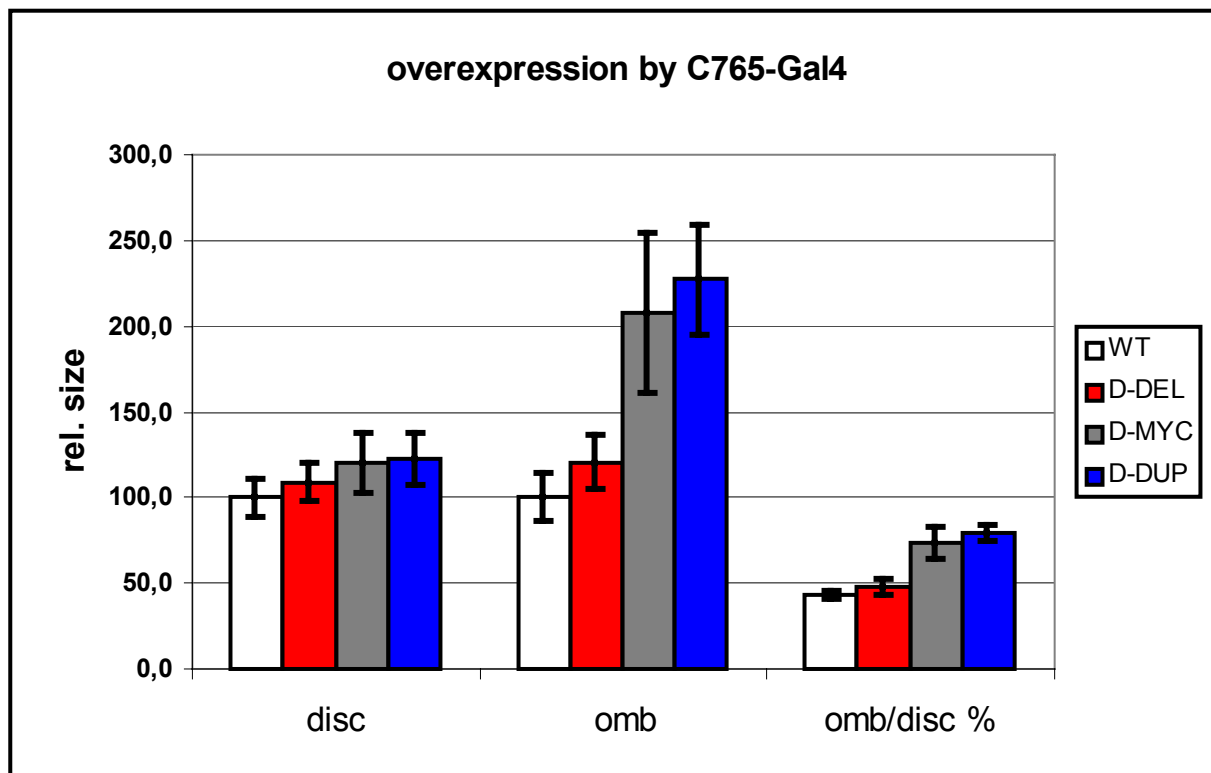


Figure 3-23: Dimensions of the wing disc and omb-domain (n=50)

All longitudes are set in correlation to wildtype longitudes (100%, rel. size) except for omb/disc correlation. All animals were raised at 18°C and contained a C765-Gal4 driver. The left graph shows AP extension of the disc, the center graph AP extension of Omb-expression, the right graph percentage of AP-Omb-extension within the whole disc. Error bars indicate standard deviation

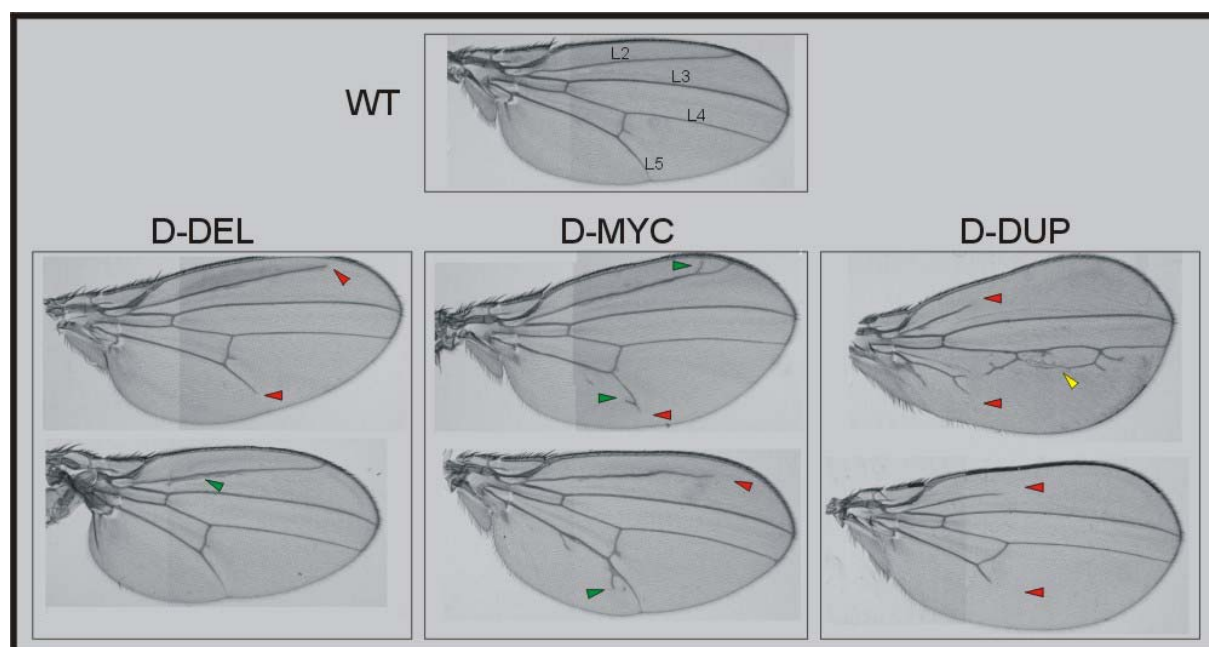


Figure 3-24: Adult wing phenotypes caused by overexpression of DPP-Variants by C765-Gal4 at 18°C

Upper panel shows wildtypw wing with longitudinal veins L2-L5 indicated. Lower panels show characteristic phenotypes resulting from ubiquitous overexpression of indicated variants driven by C765-Gal4. All animals were raised at 18°C. Red arrowheads indicate vein gaps, green arrowheads indicate ectopic vein material and yellow arrowhead mislocation or ectopic vein material.

genotype	X35; C765-Gal4 w ¹¹¹⁸	X35; C765-Gal4 D-DEL	X35; C765-Gal4 D-MYC	X35; C765-Gal4 D-DUP
ectopic PCV	52%	86%	56%	66%
Ectopic L2	0%	23%	37%	0%
L2 gap	0%	32%	21%	96%
L2 defects	0%	55%	58%	96%
Ectopic L5	0%	8%	23%	0%
L5 gap	0%	11%	24%	94%
L5 defects	0%	19%	47%	94%
Ectopic L4	0%	0%	0%	36%

Table 3-5: Vein defects caused by overexpression of DPP-variants by C765-Gal4 (n=40)

Note, that the small outgrowth of PCV is found also in the Gal4-driverline.

3.3.6 Rescue of transheterozygous dpp^{d12}/dpp^{d14} flies by DPP-Variants

Overexpression experiments shown in 3.3.5 represent the in vivo function of the DPP-variants. Nevertheless, DPP is expressed there in ectopic locations, which normally do not face high levels of DPP. Thus, to investigate the in vivo matrix binding requirement for establishing the DPP gradient in the wing disc, endogenous dpp was removed using transheterozygous combinations of dpp^{disc} alleles [89, 245-247]. These dpp^{d12}/dpp^{d14} mutant flies lack omb and sal target gene expression in the wing pouch, which is largely reduced in size ([243] + fig 3-25a), and die during early pupation [243, 245]. Rescue of the mutant phenotype with wildtype DPP generates flies which are unable to hatch from their pupal cases, but rescue efficiency can be monitored on the imaginal disc level. Flies bearing the different UAS-DPP transgenes were successively crossed to dpp^{d14} , X35, and CyO-GFP flies resulting in ($X35; dpp^{d14}, UAS-D-DEL/CyO-GFP$), ($X35; dpp^{d14}, UAS-D-MYC/CyO-GFP$) and ($X35; dpp^{d14}/CyO-GFP; UAS-D-DUP$) flies, respectively. These lines were crossed to ($dpp^{d12}/CyO-GFP; dpp-Gal4$) animals and hatching progeny 3rd instar larvae were collected. Eliminating GFP-positive and male individuals leaves only animals carrying all required genetic elements. Rescued imaginal discs were normal in size and shape of the target genes' omb-lacZ and Sal expression domains (see figure 3-25b-g). A slight tendency to larger discs is seen from b to d (D-DEL to D-DUP) and from e to g (D-DEL to D-DUP) indicating matrix dependent effects.

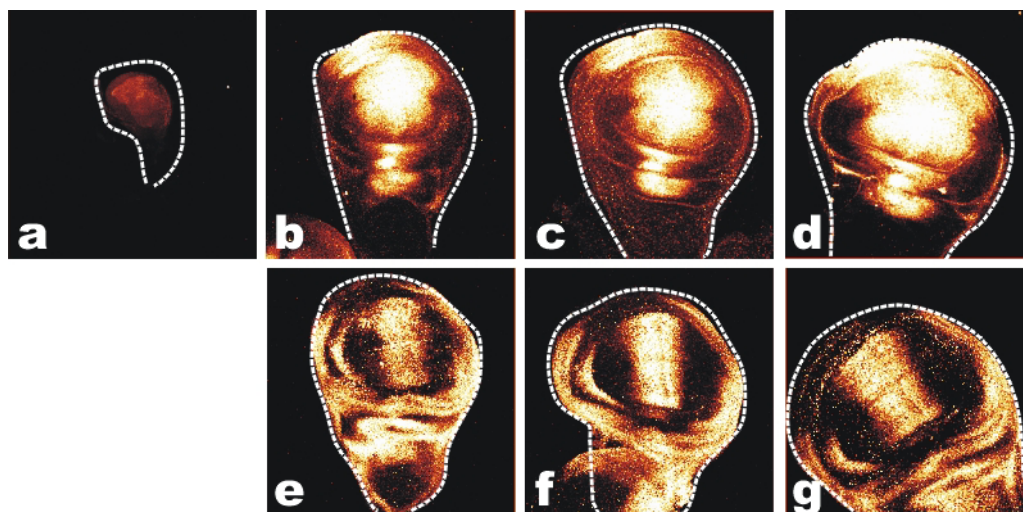


Figure 3-25: Rescue of dpp^{d12}/dpp^{d14} mutants by DPP-variants

All discs shown are dpp^{d12}/dpp^{d14} . Upper row shows anti- β -galactosidase staining (omb), lower row shows spalt staining. Discs have been rescued with D-DEL (b, e), D-MYC (c, f) and D-DUP (d, g). Note that sal expression outside the wing pouch is not influenced by DPP expression.)

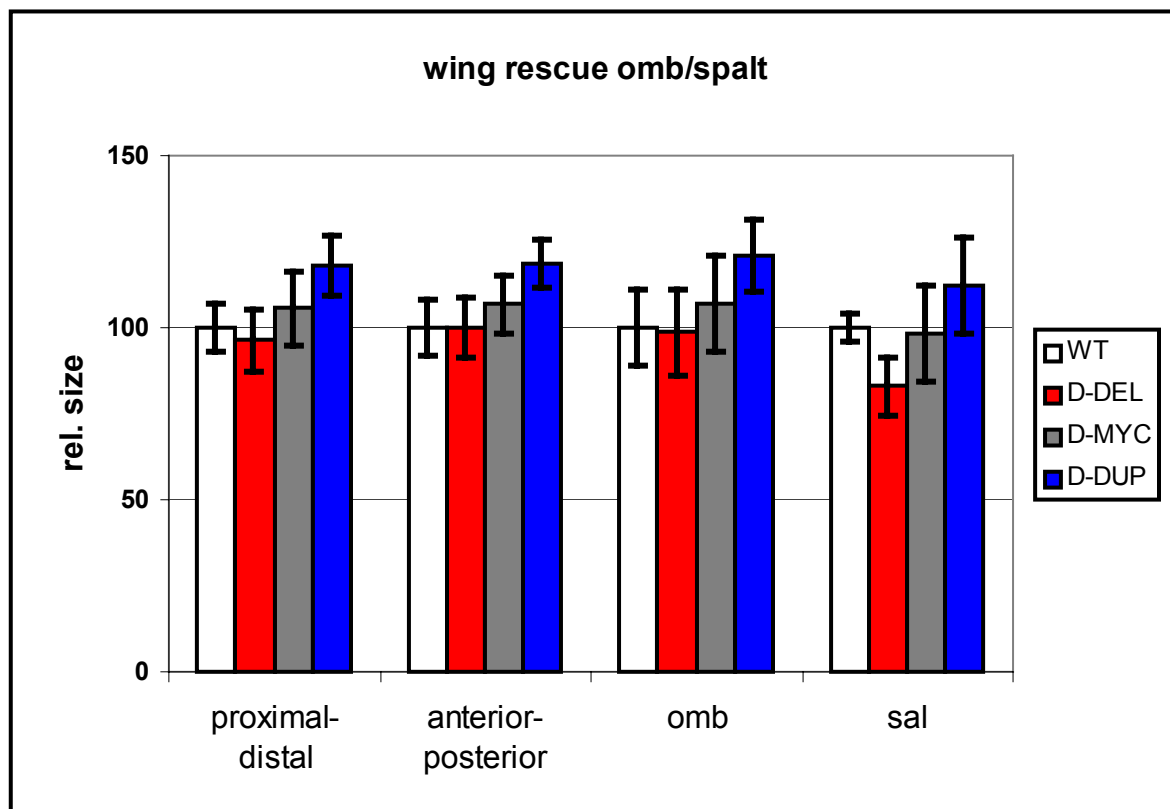


Figure 3-26: Rescue of dpp^{d12}/dpp^{d14} mutants by DPP-variants

All measures are set in correlation to wildtype (100%, rel. size); wildtype consists of genotype ($X35; dpp^{d12}; dpp-Gal4$). Flies were raised at 25°C. First two graphs show extensions of the wing pouch, the other two graphs AP extension of the target genes. Error bars indicate standard deviation.

Measurements from 40 discs of each genotype revealed slight differences in proximal-distal and anterior-posterior extensions of the disc, increasing with matrix binding potential of DPP-Variants (see fig. 3-26). All values are close to wildtype, underlining the potential of all variants to rescue endogenous DPP adequately. Only in the extension of the Sal-domain, differences between D-DEL and D-DUP are significant. The differences of the omb and sal expression are not directly a result of proliferation phenotypes since the extension of the DPP-expressing stripe of cells is regulated through Hh signaling and therefore of same size in all genotypes.

3.3.7 Expression of DPP-variants in the tracheal system

There is evidence in the literature, that the developing tracheal system is a useful investigation object for the signaling properties of the different DPP-variants. The tracheal precursor cells (TPC) are strictly limited in number (~80 cells per segment) and are highly sensitive to DPP-signals in their migration behavior [84]. Endogeneously, DPP is expressed in small stripes dorsally and ventrally of the tracheal pits. Only a subset of the cells react to the secreted DPP and organize themselves in three vertical branches: The dorsal branch (DB) and the anterior and posterior lateral trunks (aLT, pLT). Other signals like EGF and FGF direct cells into horizontal branches: the dorsal trunk (DT) and the visceral brunch (VB). Previous experiments demonstrated that ectopic expression of DPP within these tracheal pit cells itself recruits nearly all cells into vertical branches [84]. On the other hand loss of endogenous DPP-signaling results in loss of all vertical structures and development of only horizontal branches. The ectopical expression of DPP in the tracheal cells is possible by a Gal4-line consisting of a promoter-fragment of the *breathless* gene fused to Gal4 (*btl-Gal4*). This promoter-fragment taken from the FGF-receptor *breathless* is exclusively active in the TPC and the dorsal midline cells [84]. The *btl-Gal4*-driver was crossed to the UAS-DPP-Variants and to UAS-GFP_{lacZ} thereby ectopically expressing the DPP-variants in all TPC and simultaneously mark these cells by coexpression of the GFP_{lacZ}-reportergene. Figure 3-27a shows an stage 14 embryo with normally developed tracheal branches schematically drawn in fig. 3-27e. Ectopic expression of D-DEL in TPC leads only to minor changes in the branching pattern. Whereas most branches are unaffected, the dorsal branches contain more cells as seen by the double rows, compared to the one-cell-row in wildtype embryos (see figure 3-27b+f). The misarranged cells presumably derive from the dorsal trunk population, as the dorsal trunk seems at some positions reduced compared to triple to fourfold row in wildtype. More drastic are the changes in D-MYC-expressing embryos. Dorsal branches are expanded to tripple rows,

dorsal trunks are totally missing except for rare stumps, even visceral branches are reduced in cell numbers and anterior as posterior lateral trunks are slightly expanded (see figure 3-27c+g). Surprisingly the D-DUP embryos show no increase in the phenotypes compared to D-MYC. Rather, defects are identical to that seen in the D-MYC embryos. The phenotypes of D-MYC and D-DUP embryos reflect mostly the effects seen by overexpression of DPP or constitutively active DPP-receptor Tkv as described previously [84].

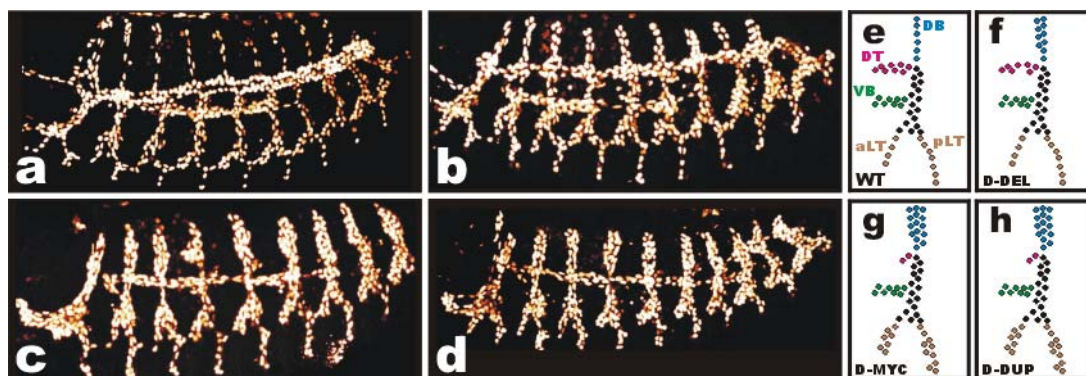


Figure 3-27: Overexpression of DPP-variants in tracheal precursor cells

a-d shows anti- β -Gal staining of stage 14 embryos. Anterior is to the left and dorsal is up. Seen are TPC and in a) also dorsal midline cells. a): btl-Gal4:UAS-GFPlacZ; b): btl-Gal4:UAS-GFPlacZ,UAS-D-DEL; c): btl-Gal4:UAS-GFPlacZ,UAS-D-MYC; d): btl-Gal4:UAS-GFPlacZ,UAS-D-DUP. e-h are schematic drawings of one segment out of a-d.

Taken together, only the ectopic expression of matrix binding DPP in the tracheal precursor cells was able to rearrange the cell migration pattern under the apparent conditions. The extend of matrix binding had no influence on the severness of the observed phenotype.

3.4 DPP-reporter systems

Several assays have been developed to investigate the signaling potency of BMP-2 and other signaling molecules. In vivo experiments demonstrated the functional homology and interchangeability of DPP/BMP-4 between *Drosophila* and *Xenopus*, i.e. invertebrates and vertebrates [84, 248, 249]. Thus, it was our aim to modify established BMP-2 reporter-assays in a manner to sensitize them to DPP signals.

The alkaline phosphatase (ALP) assay makes use of the inductive effect of BMP-2 and other similar factors on C2C12 mouse mesenchymal precursor cells [250]. Cultivating C2C12 cells in the presence of suitable amounts of BMP-2 for three days causes expression of the alkaline-phosphatase gene in an extent proportional to the applied concentration in a range of 5-100nM of ligand [234, 238, 251]. The amount of ALP is measured through turnover of the substrate para-nitrophenylphosphate, leaving a yellow coloured molecule that can be quantified by means of its absorbance at 405nm in an ELISA-reader. Several approaches to evoke the ALP-expression in C2C12 cells through DPP, even after transfection of the DPP specific receptors tkv and punt, failed [252].

Another reporter assay to study concentration dependent ligand activity is the luciferase reporter gene assay. Here, a ligand responsive promoter (enhancer) element is cloned in front of a minimal promoter followed by the luciferase gene (mostly firefly luciferase). This construct is transfected as plasmid into suitable cells and after sufficient ligand stimulation the amount of produced luciferase is measured through turnover of substrate.

The SBE reporter element [253] consists of four repeats of a Smad binding element (SBE) followed by an adenoviral minimal promoter and the firefly-luciferase gene (see fig. 3-31). Initial studies revealed a responsiveness of the SBE reporter to TGF- β , activin and BMP-2 [253]. Previous experiments in our lab showed in accord to these findings a 10- to 20fold inducibility of the SBE-reporter through stimulation with 20-50nM BMP-2 in C2C12 cells. However, even micromolar concentrations of DPP did not elicit any response [252]. These results point to an incapability of DPP to activate Smad-pathways in mammalian cell systems.

Astonishingly, not even cotransfection of receptors tkv and punt enabled DPP to evoke ALP-activity, whereas the constitutively active receptor tkvQD activates the SBE-reporter in C2C12 cells (data not shown). This might be explained by a disturbance of the regular DPP signaling complex by other mammalian receptors, which are able to sequester the ligand or to invade into the signaling complex. Thus, the aim was to stably transfect *Drosophila* S2-cells with a SBE-reporter. S2 cells nicely respond to DPP and BMP-2 by phosphorylation of the mediator Mad ([252] and see 3-32a).

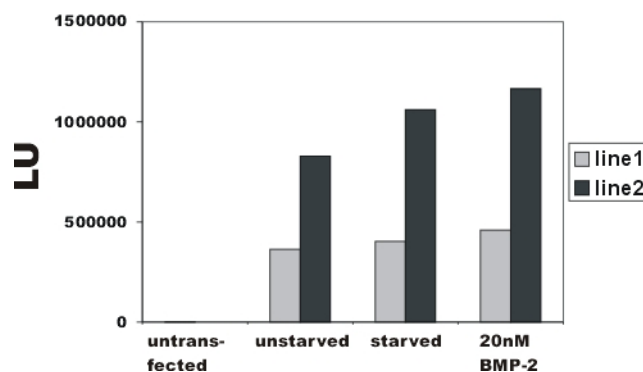


Figure 3-28: Effects of starving and BMP-2 stimulation on two S2-lines stably carrying the SBE-reporter. Stable cell lines were cultivated in growth medium or starved for 29h in starving medium or stimulated with 20nM BMP-2 in starving medium for 24h after 5h starvation.

Two stable cell lines were established and tested for luciferase activity. From the high luciferase activity already in unstimulated cells, it became evident, that both lines carried the SBE-reporter, presumably in multiple copies. Luciferase activity was 800 and 2000 times higher than in untransfected S2 cells (see figure 3-28).

Unfortunately, the high luciferase activity in unstimulated cells did not decrease under strong starving conditions (lowering FCS from 8% to 0.1%, data not shown). Even starving periods of up to 24h did not result in lower luciferase levels (data not shown). Stimulation of the cells with 20nM BMP-2 for 24h had no substantial effect. This constitutive activation of the luciferase gene might be caused by the Smad-binding elements or by the mammalian minimal promoter. To test the first possibility 12x GCCG [158], another luciferase reporter was stably transfected into S2 cells. This reporter consists of a fourfold repeat of three Mad-binding elements followed by type X collagen minimal promoter and the firefly luciferase (see figure 3-31). The Mad-binding elements have been designed as consensus-sequence from various Mad-binding sites [156, 157]. Thus, at least the Mad binding part should perfectly fit to the *Drosophila* cell culture system. Unstimulated stable cells showed high luciferase activity which was not decreased through starving. Signals were not increased through 24h stimulation with 20nM or 50nM BMP-2 and DPP, respectively (see figure 3-29). This nonappearance of

inductivity is presumably caused by the exhausting basal activation of the luciferase gene. Since it was possible that the constitutive activation of the luciferase reporter gene was caused by the mammalian minimal promoters used in the reporter constructs, alternative strategies were developed using minimal promoters derived from *Drosophila*.

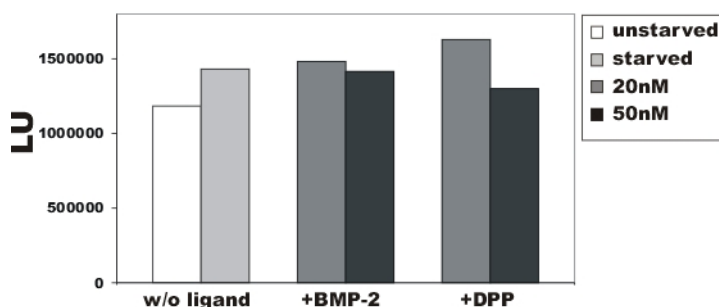


Figure 3-29: Effects of starving and BMP-2/DPP stimulation on a cell line stably carrying the 12xGCCG-reporter

Cells were starved as described above and cultivated with indicated ligand concentration for 24h.

First, the SBE-cassette of the pGL-3ti-SBE vector was XhoI-BglII excised and two preannealed oligonucleotides, pMad1 and pMad2 were ligated into the open vector. The preannealed oligonucleotides represent 3 Mad binding elements (MBE: GCCGnCGC) flanked by overhanging 5' ends, fitting to the cleaved XhoI and BglII sites of the opened vector. The resulting vector, pGL3ti-MBE, was subsequently cut with BglII and HindIII to remove the adenoviral minimal promoter (see figure 8-3).

From the large number of described promoter elements in *Drosophila*, two commonly used have been chosen: a heatshock minimal promoter was isolated from pUAST [254] and a P-element promoter was isolated from placW [255]. The latter was isolated in a short 106bp version and a long 520bp version. For isolation of the heatshock promoter two primers, pGL-M1 and pGL-M2, were designed. With these primers a 257bp fragment starting immediately downstream of the 5x UAS-sequence(pGL-M1) and ending just before the unique EcoRI site (pGL-M2) was amplified from pUAST. With these primers, flanking BglII (pGL-M1) and HindIII (pGL-M2) sites were introduced.

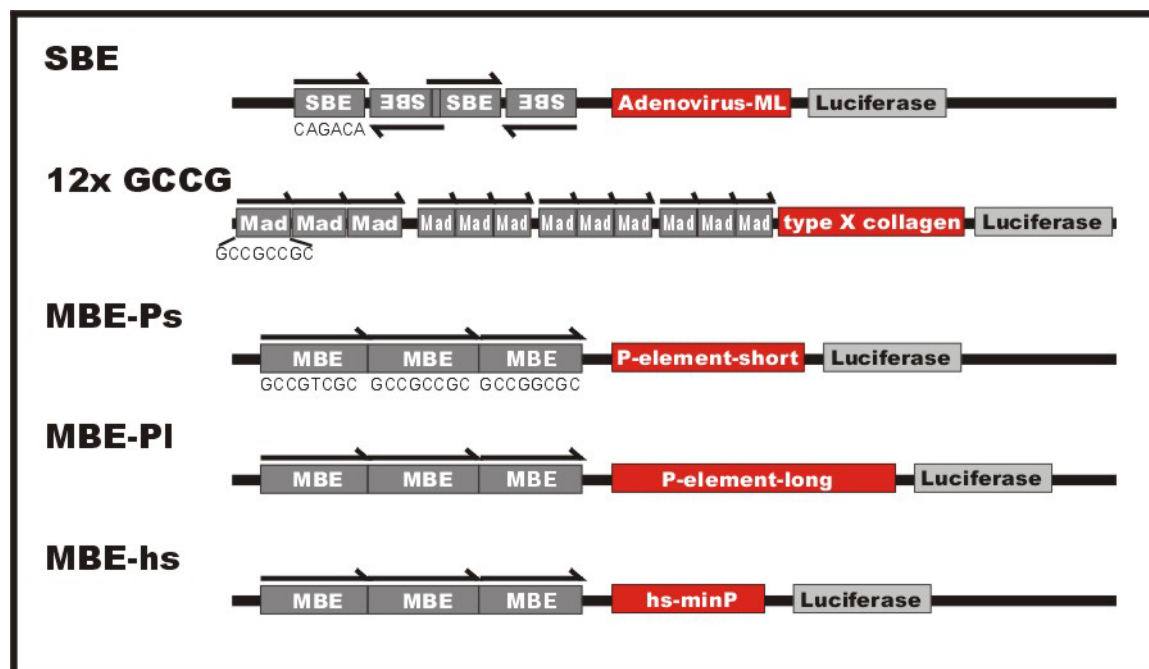


Figure 3-31: Detailed promoter comparison of all used luciferase-reporter constructs

Smad-binding elements are shown in dark grey, minimal promoters in red and luciferase gene in light grey.

DNA-sequences of Smad binding elements are shown in detail and orientation is indicated by arrows.

With the primer combinations pGL-M3/pGL-M4 and pGL-M5/pGL-M4 the 106bp fragment (bases 150 to 45) and the 520bp fragment (bases 564 to 45) were amplified from PlacW (flybase reference FBtp0000204). Again flanking BglII(pGL-M3/pGL-M5) and HindIII (pGL-M4) sites were introduced. All three fragments were

digested with BglII and HindIII and fragments were ligated into opened vector pGL3ti-MBE (for cloning details see figure 6-3)(see figure 3-31).

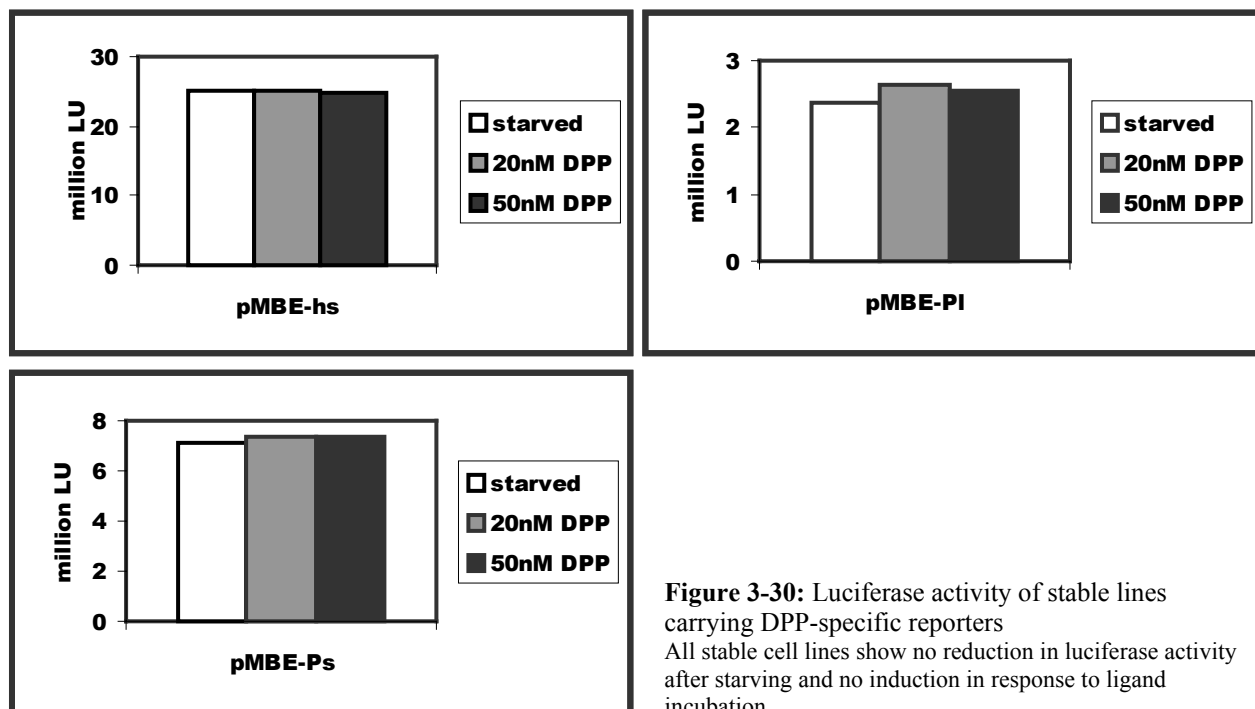


Figure 3-30: Luciferase activity of stable lines carrying DPP-specific reporters
All stable cell lines show no reduction in luciferase activity after starving and no induction in response to ligand incubation.

For each reporter construct a stable cell line was established and assayed for luciferase activity. All three lines showed high luciferase activity. This luciferase activity could not be decreased noticeably through starving for 24h (data not shown). Stimulation with 20nM/50nM DPP for 24h led to minimal (pMBE-PI, pMBE-Ps) or no (pMBE-hs) induction (see figure 3-30).

Neither use of specific Mad binding sites nor the introduction of *Drosophila* specific minimal promoter elements made it possible to generate stable S2 cell lines that could be used as DPP readout assay. The basal signals observed in all stable cell lines were high indicating a multiple insertion of the different reporter constructs. Thus, it was not possible to generate stable S2 cell lines, that carry a DPP-sensitive luciferase reporter construct. Further efforts will be made to establish a functional transient system with the constructed reporters.

3.5 Influence of DPP and its receptors on Mad phosphorylation

DPP represents the BMP-2/4 homolog in *Drosophila* and as BMP-2 it signals through a heterologous pair of receptor-serine/threonine-kinases [123, 125-127]. The common type I receptor of this pair subsequently phosphorylates the mediator Mad, which in turn transports the signal to the nucleus together with the co-mediator Medea (reviewed in [97]). In contrast to BMP-2, there is up to now no hint for any mediation of the DPP signal outside the Mad-pathway. This led us to detailed studies on the Mad activation, also in the light of two existing type I receptors were only tkv can accomplish substitution for sax and not vice versa [115, 131]. First, *Drosophila* S2 cells were tested for response to DPP. In this assays the Myc-tagged variant was used. To verify C-terminal phosphorylation of the Mad-protein, a polyclonal Phospho-Smad-1/Smad-5 antibody (obtained from P.ten Dijke) was used, which had been shown to crossreact with phosphorylated Mad in wing discs [223]. Treatment of S2 cells with DPP or BMP-2 resulted in strong phosphorylation of Mad which could not be detected in untreated cells (see figure 3-32 A).

Further experiments with various ligand concentrations and stimulation times revealed the phosphorylation state as a very quick response evoked already 5-10 minutes after ligand stimulation (see figure 3-32B). To calculate the speed of response one has to consider that after 5min of ligand incubation receptor-bound ligands might be able to activate receptors during fast centrifugation step and under beginning lysis condition. Thus, the faint band seen after 5min might correspond more to a 10min signalling period. Phosphorylation is already detectable after stimulations with 50pM (see figure 3-32 B+C).

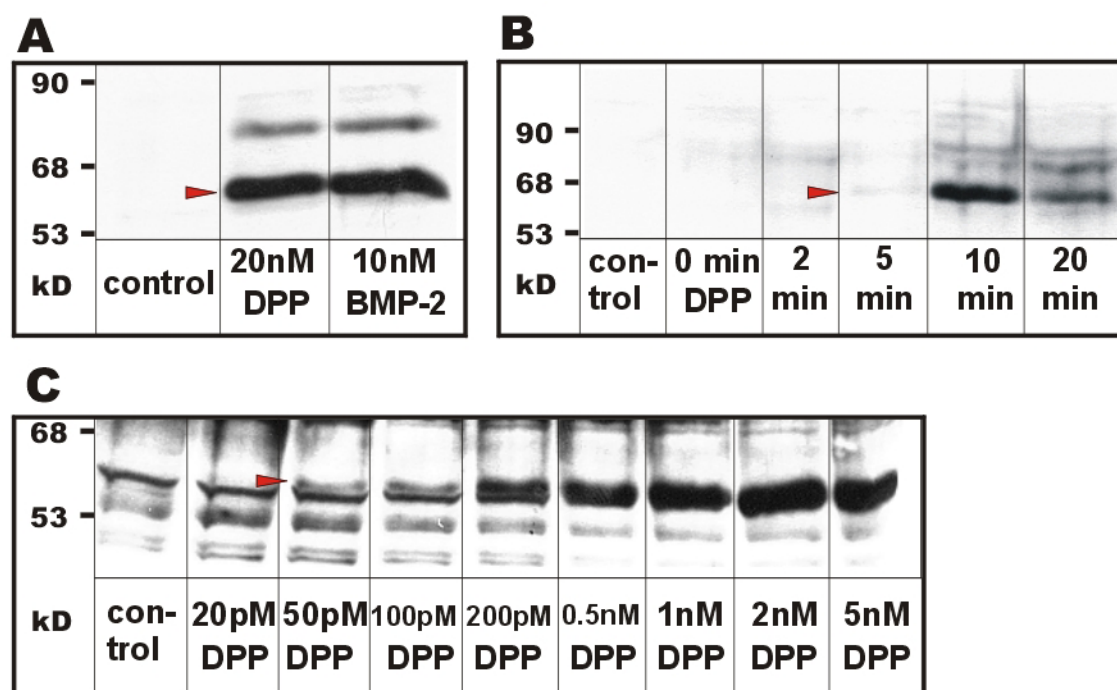


Figure 3-32: Westernblots with α P-Mad showing phosphorylation of Mad in S2 cells after ligand stimulation. All cells were starved for 6h prior to ligand incubation. A: ligand incubation 45min; B: ligand concentration 5nM DPP; C: ligand incubation 30min (DPP); red arrowheads indicate mad phosphorylation. Blot C was performed with different antibody aliquot with considerably higher background signal.

To obtain clearer insights in the capacity of the DPP receptors to transduce signals via Mad phosphorylation, stable cell lines with inducible sets of receptors were generated (for cloning details see figure 8-2). The receptors were cloned into pMT-V5, a vector containing a metallothionein promoter which allows induced expression by adding CuSO_4 to the medium. For Thick veins a highly specific and sensitive antibody was available, the other receptors were C-terminally tagged with Myc (put) or HA (sax). Induced stable cell lines were tested for receptor expression. Anti-HA antibody showed only weak signals (data not shown). Thus, the presence of Sax could not be proven directly. Antibody stainings for Tkv and Put worked well (see e.g. figure 3-33 lane 3+4 and 7+8). Coexpression of type I and type II receptor results in ligand independent induction of Smad phosphorylation and targetgene expression [87]. Only overexpression of at least one type I receptor with the type II receptor Put evoked phosphorylation of the Mad-protein (see figure 3-33 lanes 6,14,16). Coexpression of sax and put, shows sax expression indirectly through the phosphorylation of mad (lane 14) as put alone could not trigger mad phosphorylation (lane 8).

	S2 cells		tkv		tkv put		put		sax		tkv sax		sax put		tkv/sax put	
CuSO_4	-	+	-	+	-	+	-	+	-	+	-	+	-	+	-	+
Tkv																
MYC																
P-Mad																
	1	2	3	4	5	6	7	8	9	10	11	12	13	14	15	16

Figure 3-33: CuSO_4 -induced receptor expression and ligand independent mad-phosphorylation

Shown are western blots of stable cell lines uninduced or after 24h induction with 500 μ M CuSO₄. Note basal activity of pMT-promoter even in the absence of CuSO₄ (Tkv: lanes 3, 11, 15; Put: lanes 5, 7). Mad phosphorylation is only detected in the presence of at least one type I and one type II receptor (lanes 6, 14, 16). Summarized, both type I receptors have the potential to trigger Mad phosphorylation after activation through the common type II receptor punt. Conclusions from the quality of the Mad activation could not be drawn as expression levels of the different receptors could not be compared. Therefore it remains unclear, how Tkv signaling can substitute for Sax signaling in vivo, whereas the vice versa is not possible.

4 Discussion

Signaling of diffusable cytokines through specific cell surface receptors is a key event in cell to cell communication. A variety of cytokines additionally interacts with glycosamino-sidechains of extracellular matrix proteoglycans. In the recent years a host of publications described the importance of this interactions by analyses of defects in glycosaminoglycan synthesis or proteoglycan-coreproteins. However, because of the pleiotropic effects of most mutations it is difficult to study the effect of matrix interactions on distinct pathways. Thus, in the present work the potential matrix interaction sites of a well investigated cytokine, Decapentaplegic, were manipulated to study the involvement of extracellular matrix components in a single signaling pathway.

4.1 Design of Variants

DPP was chosen as object for research because of the extraordinary high homology to vertebrate BMP-2/4. Starting with the first conserved cystein of the mature ligand the aa identity reaches 75% (compare fig. 4-1). Functional homology is demonstrated by the exchangeability of DPP and BMP-4 between different species and extends further to many other members of the BMP signaling cascade (see chapter 1.4). Also the conserved mechanism of induction of ventral/dorsal non-neuronal structures in *Xenopus* and *Drosophila* by BMP-4/DPP underlines the evolutionary common origin of this pathway [101].

Recombinant BMP-2 derived from *E.coli* shows biological activity as demonstrated in alkaline phosphatase assay in C3H10T1/2 cells and in chicken limb bud assay [234]. In the latter, the activity of BMP-2 was increased by co-incubation with 30nM-3µM heparin or 50µM of a peptide containing the 17 first aa's of mature BMP-2. A BMP-2 variant, named EHBMP-2/B2m-, where the N-terminal residues 1-12 (MAKHKQRKRLKS) had been substituted by the N-terminal 13 residues from human interleukin-2 (MAPTSSSTKKTKQL), showed in contrast to BMP-2 no apparent affinity for heparin and a lower EC₅₀ value in limb bud assay [234]. Strikingly, the BMP-2 N-terminus contains much more positively charged aa's than the interleukin-2 N-terminus. These positively charged aa-sidechains represent potential interaction sites for the negatively charged sulfate groups of modified glycosaminoglycan sidechains [234, 256]. Interestingly, the two adjacent lysins in the interleukin-2 N-terminus are not sufficient for the interaction with heparin. Indeed, several heparin-binding growth factors have been identified so far (see table 1-1) and detailed analysis of interacting aa's often revealed the existence of basic aa residues clustered arrays to be responsible for matrix binding phenomena suggesting the latter to be a key feature in matrix interaction [234, 257, 258]. At the N-terminus of DPP there exist 10 basic aa's. Despite the clustered occurrence of basic aminoacids, this part of the mature DPP shows no homology to BMP-2/4.

Thus, we designed 3 variant forms of DPP with alterations in the potential matrix binding motif to examine the influence of this part of the DPP-ligand on signaling events. To generate an easy possibility to visualize the expression-levels of the variants in *Drosophila*, a myc-epitope was inserted into the flexible glycine rich part of the N-terminus. As the myc-epitope (GEQKLISEEDL) is rich in acidic aa residues, the epitope was inserted in all three variants between glu462 and gly463 thereby leaving three spacing glycine residues between epitope and matrix binding clusters. In the deletion variant D-DEL the whole region between gly465 and asn482 was deleted removing 9 out of 10 positive charges within the N-terminus. The variant D-MYC resembles wildtype DPP with an additional myc-epitope. Because of the suspected relevance of the clustered basic aminoacids, the region including lys471 to lys483 was inserted as an additional copy between ser459 and gly460 to obtain the duplication variant D-DUP (see table 3-1).

BMP-2 (human)	QAKHKQRKRLK-SSCKRHPLYVDFSDVGWN NDWIVAP
DPP	DVSGGEGGGKGGRNKRQPRRPTRRKNHDDTCRRHSLYVDFSDVGWDDWIVAP
BMP-2	PGYHAFYCHGECFPFLADHLNSTNHAIVQTLVNSVN-SKIPKACCVPT ELSA
DPP	LGYDAYYCHGKCFPLADHFNSTNHAVVQTLVNNM PGKVPKACCVPTQLDS
BMP-2	ISMLYLDENEKVVLKNYQDMVVEGCGCR
DPP	VAMLYLNDQSTVVLKNYQEMTVVCGCR

Figure 4-1: Sequences of mature BMP-2 and DPP.

Conserved AA residues of the protein core are shown in grey, basic AA residues of the flexible N-terminus in red.

4.2 Expression and purification of rekombinant DPP-Variants

The construct for recombinant DPP was derived from F. Altnauer [236]. First it was tried to purify DPP with the protocol designed for BMP-2 [234, 236], but refolded DPP, in contrast to BMP-2, was more unstable and elicited a high tendency to precipitate under the applied conditions (50mM NaOAc pH 5.0; 30% 2-propanol). Therefore, the protocol developed by J. Groppe [237] with purification by heparin-affinity chromatography in the presence of 6M urea was used. This method led to a satisfying yield in recombinant DPP. As in the case of D-DEL a drastically reduced affinity for heparin was expected, a tentacel FPLC (EMD-SO₃⁻) was used instead of heparin. Considering the low theoretical pI (4.67 according to protparam tool; www.expasy.ch) of D-DEL, the buffer system was fitted to pH 4.0. Because of problems with the purification of D-DUP by heparin-sepharose, again FPLC was the method of choice, but at pH 8.0 (pI 9.14). The purification of the four variants provided final purities of apparently >90% (see fig. 3-5). Conspicuously, the dimeric D-DUP runs faster through SDS-PAGE than dimeric D-MYC (see fig. 3-5), although the molecular weight (D-DUP 35.6kD; D-MYC 34.4kD) and positive charges (D-DUP 29; D-MYC 22) would suggest the opposite. Analysis of the efficiency of purification (see table 3-2) shows comparable yields for all variants till the level of inclusion bodies. However, the final yield of the heparin-sepharose purified variants exceed the FPLC purified variants four to sixfold. Consistently, also the elution profiles vary substantially between heparin-sepharose and FPLC (compare fig 3-3 to fig. 3-4). This raises the question, whether purification by FPLC leads to more distinct fractions since the profile shows four peaks instead of two in the case of the heparin profile. Nevertheless, DPP and D-MYC show the same homogenous migration behaviour in SDS-PAGE as D-DEL and D-DUP (see fig. 3-5).

4.3 Biochemical properties of DPP-variants

4.3.1 Heparin affinity of DPP-variants

The purified DPP-variants were designed for the purpose to demonstrate biological activity, which is on the one hand different in terms of matrix affinity and matrix dependent biological activity but on the other hand equal regarding the intrinsic signaling potential.

For BMP-2 it has been demonstrated, that under 6M urea conditions it can be only eluted in the presence of high salt concentrations (0.7M) from heparin affinity columns (244, 245). Furthermore, an apparent affinity of recombinant BMP-2 for heparin was revealed by biacore-measurements, which was under the chosen experimental conditions ~20nM [234]. BMP-variants with exchanged N-terminus (B2m-) exhibited no detectable affinity for heparin immobilized on a biacore-sensorchip. Variants with duplications of one or both basic triplets in the N-terminus showed a clearly increased affinity for heparin ([234], F. Vogel, unpublished results).

All four variants were loaded on a heparin-EMD fractogel column in the presence of 6M urea to guaranty stable conditions [237]. Elution of the proteins with a 0-1M NaCl gradient shows their different affinities to heparin. In addition to UV absorbtion the conductivity was measured to get a clear connection between protein elution and the saltgradient. As expected, the deletion variant D-DEL showed the lowest apparent affinity to heparin and is eluted at 0.15M NaCl followed by D-MYC at 0.4M NaCl and DPP at 0.5M NaCl. The highest apparent affinity was shown by the duplication variant D-DUP, which is eluted at 0.55M NaCl. Thus, the involvement of the N-terminal basic aa residues in heparin binding was proven. The difference between the wildtype DPP (0.5M) and the myc-epitope tagged variant D-MYC might be due to the myc-epitope, which carries three negative net-charges and therefore repells the negatively charged GAG-chains. Residual heparin-affinity of the deletion variant might be explained by means of 13 postively charged aa's of the coreprotein, three of them clustered directly downstream of the first conserved cystein.

4.3.2 Receptor affinity of DPP-variants

To quantify the intrinsic activity of the three generated DPP-variants, their apparent affinities for the ectodomain of the type I receptor thick veins were measured. Thick veins was identified as the high affinity type I receptor and is involved in all DPP actions investigated so far [113-115, 123-126, 132, 259, 260]. Tkv signals via a complex with the type II receptor punt ([127], reviewed in [97, 261]). Comparing the aa residues of the BMP-2 binding epitope to the BRIA receptor with residues in DPP reveals all major binding residues to be identical or conservatively exchanged (K15R, I62V, S69N). This concurrence in binding epitopes, together with the ability of BMP-2 to phosphorylate Mad in Drosophila S2-cells (see chapter 3.4) suggests a conserved type I receptor binding mechanism between BMP-2 and DPP. Taken this into account, changes in DPP's N-terminal basic aminoacid clustering should similar to BMP-2/ B2m- not affect high affinity receptor binding and signaling-complex formation and activation. Nevertheless, these interactions have been analysed by biacore-measurements with the immobilized Thick veins-ectodomain (Tkv_{EC}) and various ligand concentrations in solution. Expression of the Tkv-ectodomain in a suitable baculovirus expression system in SF-9 cells revealed two bands after purification by Ni-NTA-agarose: one, as expected 27kD in size, the other one even stronger at around 50kD.

Running the gel under reduced conditions lead to the same results thereby excluding the possibility of an incorrect cystein-bridged Tk_{vEC} -dimer. The 50kD band is also positive in His-westernblot and therefore not a Tk_{vEC} -coprecipitate. One possibility might be an unusual stable noncovalent Tk_{vEC} -dimeric structure, which should be further proved by mass spectrometry or protein sequencing. A readthrough-variant of the Tk_{v} construct seems unlikely since many other type I/II receptor constructs with identical N- and C-terminal sequences never elicited this phenomenon (J. Nickel, pers. comm.). If the 50kD band really would turn out to be a dimeric tkv -structure, this would be of great interest in the light of receptor oligomerisation mode and receptor-ligand affinities based on ectodomain dimerisation.

Further purification of the Tk_{vEC} -monomer by TMAE anion-exchange column was successful and the 27kD band eluted in high purity in one single fraction, whereas the 50kD band eluted significantly later (see fig. 3-9) Biacore measurements with the purified, biotinylated and immobilised Tk_{vEC} with ligand concentrations ranging from 15nM to 180nM revealed dissociation constants in between 14 and 25nM, which can be seen as indistinguishable due to standard deviations and limits in resonance unit resolution. Thus, as expected from preliminary BMP-2 data [234, 251], the introduced changes in DPP's N-terminus in the variants didn't influence the affinity to the extracellular domain of the Tk_{v} receptor.

4.3.3 Biological activity of DPP variants

The biological activity of all four purified variants was demonstrated in a limbbud assay. In this well established micromass cell culture test, mesenchymal stem cells react to 96h incubation with nanomolar doses of BMP-2/DPP by chondrogenic differentiation and start to produce large amounts of extracellular matrix [234-237, 262-265]. Thus, with continuing incubation time, ligands are faced to increasing amounts of extracellular matrix potentially influencing the ligands overall bioactivity. Exchanging the heparin binding sites of BMP-2 to a dummy sequence led to a 5-10fold increase in BMP's activity comparable to cocultivation with 3 μM heparin or 50 μM of a peptide resembling the 17 N-terminal aa's of mature BMP-2 [234]. In contrast, the introduction of an additional copy of one or both basic triplets in the N-terminus of BMP-2, lowered the activity of the latter (F. Vogel, unpublished results). This negative influence of matrix binding on biological activity can be explained by a simple model: Matrix binding cytokines are captured by the extracellular matrix and thereby prevented from a direct interaction with the high affinity receptors. Matrix binding deficient cytokines, on the other hand, are not impeded by means of matrix binding and thus are able to interact with receptors immediately. Thus, whereas concentrations of ligands are identical in the cell culture supernatant, these differ in the micro-milieu of the cell surface level (see fig. 4-2). At high ligand concentrations matrix occupancy becomes saturated and all ligand variants led to the same saturation value

The DPP deletion variant D-DEL showed an increase in biological activity also seen for B2m- in limbbud assay [234]. This is seen in the shift of EC_{50} from ~60nM (D-MYC) to ~5nM (D-DEL)(see fig. 3-11). In spite of the difference of the variants in heparin affinity shown by FPLC, the activity of DPP, D-MYC and D-DUP is identical. Increasing the heparin affinity by a second copy of the N-terminal basic core has no effect on the specific activity in the limbbud assay. The difference of BMP-2 and DPP duplication variants in this assay might be explained by two observations. First, heparin/heparan sulfate is a substance with heterogenous chain modifications [10]. Hence, there might be differences in heparin used for FPLC and heparan sulfate sidechains of chicken limbbud cells. These differences might result in identical affinity of the three variants (DPP, D-MYC and D-DUP) to limbbud-ECM components. For FGF e.g. it has been shown, that distinct 2-O- and 6-O-sulfate groups in a defined spacing are responsible for correct ligand-receptor complex formation [10]. In that case, minor changes in heparan sulfate modification have strong effects on matrix-ligand interactions.

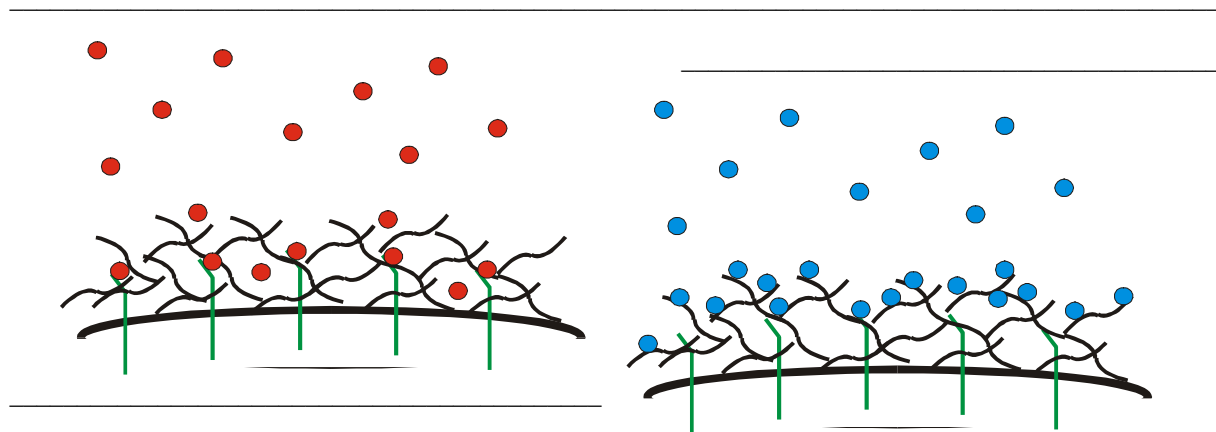


Figure 4-2: Model for ligand concentration differences in the micro-milieu caused by matrix interactions. Matrix binding deficient ligands are shown in red, matrix binding ligands in blue, cell surface receptors in green and matrix proteoglycans as black curves.

Second, the BMP matrix binding site comprises of two basic triplets separated by one aa, whereas the DPP N-terminal region contains only one basic triplet and two duplets, each spaced by two aa residues (see figure 4-1). Obviously, this difference in aa clustering can result in different binding properties to heparin and cause the differences seen in limbbud test.

Taken together, the limbbud test demonstrated bioactivity for all four purified DPP variants. The influence of the DPP matrix binding sites on signaling activity was clearly shown by means of differences between D-DEL and D-MYC/D-DUP. The deletion of the matrix binding site in DPP results in increased biological activity, as measured in chicken limbbuds.

4.4 Design of expression systems in *Drosophila melanogaster*

Reverse genetics are widespread in *Drosophila* research and provide powerful tools to examine the in vivo effects of the DPP-variants. P-Element based germline transformation allows stable integration of DNA-constructs into the *Drosophila* genome. Cloning the gene of interest after an UAS-sequence (a binding site for the yeast transcription factor Gal4, not used by *Drosophila* transcriptional activators) allows the expression of these by a large variety of tissue specific *Drosophila* Gal4-driver lines [231, 232, 254].

Among DPP's numerous developmental actions the patterning of wing imaginal discs was chosen as investigation object for several reasons. First, DPP has been reported to act as morphogen in this system activating target genes at different distances from the DPP source in a cell non-autonomous manner [87]. Second, the wing imaginal disc resembles a cell-monolayer (only covered by the peripodial membrane on the apical site) that allows to perform several staining techniques and to analyse the results unequivocally. Additionally, there are lacZ-reporterlines and specific antibodies for the target genes omb and spalt available [87, 172, 216]. Third, expression systems generating small clones of Gal4 activity have been described to be useful to ectopically express DPP in limited spatial areas [87].

The expression setup described in 3.3.2 was designed for heat shock inducible expression of the various DPP-variants. The system allows modulation of several parameters. Through the heatshock, the flippase enzyme is activated randomly in single cells. If discs are analysed at timepoints >12h after flippase induction, the "flipped" cells have divided and generated small clones ectopically expressing the DPP-variants. Thus, the timepoint of the heatshock influences the size of ectopically expressing clones. Induction during second/early third instar larvae (i.e. 60h-72h prior to analysis) revealed large clones, whereas heatshocks 24-30h prior to analysis (first detection of ectopic omb-lacZ) revealed clones only 2-4 cells in size (data not shown). The temperature during heatshock and the duration of the heatshock, in contrast, influence the frequency of clone induction. Mild heatshocks at 30°C lasting 4 to 8min result in a few clones distributed randomly throughout the disc. Shocking the larvae for 30min at 37°C leads to frequent inductions throughout the disc (see fig. 3-15). Nevertheless, the frequency of induction is not further increased with heatshocks lasting for one hour and it never occurred that all cells of one disc had activated the flippase. Consequently it was not possible to perform the recombination event in all cells of the wing disc to allow expression of the DPP-variants. Together with findings, that the flippase-construct used in this study did not work in adult tissues (A. Keller, pers. com.) this pointed to a cell cycle dependency of the flipping-event. One explanation would be the lack of directed nuclear translocation of the yeast flippase in *Drosophila*.

The aim of this experimental setup was to induce ectopic DPP-variant clones of equal size and to compare the amount of induction of the targetgenes omb and spalt. To be able to compare different variants, it was necessary to ensure that every variant was expressed at equal level. Constructs were designed largely equally, but P-elements inserted at sites with different transcriptional activities and position variegation effects were observed. The variants could only be expressed after flippase mediated recombination. To achieve equal numbers of cells expressing the DPP-variants, the larvae were shocked to a maximal extent (1h, 37°C) but unfortunately this did not result in equal flipping rates (see fig. 3-15). Thus, DPP levels were not directly comparable. A second strategy would have been to compare levels of CD2 expression in the unflipped state. But this would not rule out differences in expression caused by translation or processing. Therefore this experimental setup was rejected. In a second approach, the DPP-variants were cloned into the pUAST vector (see fig. 6-1). This directly allowed Gal4-driven expression of the targetgenes and provided an easy technique to check the expression levels of the different UAS-DPP lines. The DPP expression was determined in transheterozygous animals also carrying a hs-Gal4 element. Heatshocks lasting for 1h sufficiently activated the DPP-expression via Gal4. Recovery times lasting from 3h-6h showed no visible difference in the expression strength of the chosen lines D-DEL-2b, D-MYC-5b and D-DUP-4 (data not shown), indicating a comparable expression profile, which has not been found for other heatshock induced transgenes (M. Porsch, pers. com.). The westernblot detection of the protein of approximately two adult fly heads with a polyclonal DPP antiserum revealed three prominent bands of about 50kD, 57-63kD and 80-88kD in size (see fig. 3-16). The monomeric/dimeric ligand was not detected properly, which is consistent with the original publication, describing the expression of DPP in stably transfected *Drosophila* S2 cells [73]. The 50kD band is the only band not differing in size among variants, thus it doesn't contain the mature ligand part and represents the cleaved prodomain. In Panganiban et al. [73] the prodomain

expressed in S2-cells was found at 47kD confirming this conclusion. Confusing is the existence of two bands between 57- 63kD and 80-88kD. Both bands vary in size between the variants, reflecting the differences in the ligand part. In Panganiban et al. the full-length polypeptide was detected as double band at 68 and 70kD in size. According to the difference (to ref. [73]) in mobility observed in the prodomain (47kD in Panganiban et al. to 50kD in this publication), one would expect also the full-length peptide running slightly higher. Under these conclusion the 80-88kD band represents the whole polypeptide chain. This would designate the 57-63kD band to be an intermediate cleavage product resulting from cleavage within the prodomain. As there are no prodomain fragments of corresponding size found, this assignment remains uncertain. Another explanation supposes an extreme stability of the ligand. This could, under the experimental conditions lead to insufficient reduction of the ligand dimer. Consequently, the 57-63kD band represents one full-length chain and the 80-88kD band comprises of one full-length chain disulfid bridged to a second ligand-monomer, the latter cleaved from its prodomain. By this explanation, the two bands fit more properly to the corresponding predicted molecular weights (64-67kD and 78-85kD). Nevertheless, the assignment of the prodomain is unequivocal and the cleavage of full-length polypeptide into prodomain and mature ligand results in a 2:1 molar ratio for every variant. Thus, equal amounts of cleaved prodomains directly reflect equal amounts of mature ligands and the three fly lines analysed in fig. 3-16a show equal expression levels of the DPP-variants.

In a second flipping approach these UAS-DPP lines were combined with a flippase-induced Actin-Gal4 driver. In this setup the flipping event was transferred from the UAS-construct to the Gal-4 driver and the latter was crossed to the UAS-lines, thereby providing a genetically identical Gal-4 source for all DPP-lines. Detection of clones was achieved through incrossing of a UAS-GFP reporter element, which, in contrast to the previous system, positively marked the ectopic clones (see fig. 3-17).

While the experimental setup worked properly, it was not used for detailed clonal analysis. It turned out to be an unproportionate effort to gain sufficient numbers of clones with equal size and at identical positions in the disc. Because of the endogenous DPP-gradient and other irregularities in proteins influencing DPP-signaling like receptor or glypican expression patterns [222-224], ectopic DPP expressing clones could only be compared at identical positions. To minimize influences of the endogenous DPP and to visualize solely the effect of ectopic DPP, only clones at the periphery of the disc, outside the endogenous Omb-expression domain would be subject to analysis. Lecuit and Cohen [222] reported a high tkv expression level in this area, that limits the diffusion range of DPP and is downregulated by means of ectopic DPP expression. Thus, diffusion of DPP in this area mainly depends on tkv levels and would make it difficult to observe differences caused by increased or decreased matrix binding of the ligand. Therefore the clonal induction setup was rejected in favor of other expression systems accessible by the use of various Gal4 lines.

4.5 Moderate matrix-binding implications in DPP signaling in the wing imaginal disc

4.5.1 Overexpression of DPP-Variants in the endogenous DPP-domain

Previous studies reported strong AP-overproliferation of the wing disc and significant expansions of the Omb and Sal expression domains by means of overexpression of DPP in its endogenous expression domain [87, 88, 172]. On the basis of these results, the DPP-variants were expressed under the control of a dpp-Gal4 driverline [244]. Interestingly, this had no measurable effect on wing disc size or omb-expression domain (data not shown). In adult wings, a short ectopic vein stripe was detected with high penetrance between L3 and L4 distal to the ACV (see fig. 3-19). Nevertheless, no differences in penetrance and size of ectopic veins were detectable among the three variants. The different phenotypes of wing discs compared to published data might be due to different Gal4-driverlines used (e.g. blk-Gal4 in [87] compared to dpp-Gal4 [244] in this work) and lower expression levels of the variants compared to other UAS-DPP lines. Indistinguishable effects caused by the variants are likely to be due to heterodimer formation as the variants are expressed exclusively in the same cells as endogenous DPP. Resulting heterodimers have one (DPP/D-DEL) or three (DPP/D-DUP) matrix binding modules compared to two in wildtype DPP (DPP/DPP). This difference of only one matrix binding module might be not sufficient to cause different phenotypes.

4.5.2 Overexpression of DPP-Variants in the Omb-domain

Expression of DPP-variants by means of omb-Gal4 represents a typical feed-forward (positive feedback) system. The Omb-promoter is activated by endogenous DPP. Successively ectopic DPP is expressed in the enlarged Omb-domain and induces the Omb-promoter in ectopic and more distal regions. This again leads to an extended DPP expression. If there are any differences in targetgene activation due to matrix binding differences of the variants, these should be increased by the feed-forward mechanism. As seen in fig. 3-20, even at reduced Gal4 activity (18°C), the resulting omb-expression domain covers the whole distal part of the wing disc, which is largely increased in the AP direction. Differences among the variants in the AP extension are not detected, but this might be due to limits in proliferation. Differences are only seen in terms of disc folding. In D-DUP overexpressing discs, structural abnormalities like circular folding centres are found with low penetrance (see

fig. 3-20d, white arrowheads). These potentially represent points of extraordinary high proliferation, indicating an increased signaling capacity of D-DUP compared to the other variants. Astonishingly, the proximal-distal extension of the Omb domain decreases with overexpression of increasing matrix binding variants (see fig. 3-21). Because this effect is not seen in other overexpression systems (see fig. 3-26), this might not be a direct inhibition effect of strong DPP signaling, but is more likely to be a secondary result from the extremely high AP-proliferation phenotype. Thus, whereas overexpression of DPP-variants in the Omb-domain shows quantitative (proximal-distal) and qualitative (ectopic folding centres) differences among the three variants, the discs produce high amounts of DPP in the whole distal part evoking high responses by all three variants.

4.5.3 Ubiquitous overexpression of DPP-variants in the disc

The Gal4-driverline C765-Gal4 [87] is ubiquitously active in wing imaginal discs and visualisation via UAS-GFP elicited a uniform staining pattern of the whole disc (see fig. 3-22e). Overexpression of the three variants by means of C765-Gal4 (18°C) resulted in expanded discs with enlarged Omb-domains (compare 3-22a-d).

Dimension measurements revealed, that the disc extension along the AP axis was increased consistent with higher matrix-binding potential of the overexpressed variants, although differences were not significant (see fig. 3-23). In contrast, the Omb-expression domain varied drastically in size with significant differences between wildtype/D-DEL and D-MYC/D-DUP (see fig. 3-23). Thus, at the comparably low expression levels driven by C765 at 18°C matrix-binding DPP (but not the deletion variant) is sufficient to strongly activate omb-expression but only has a weak effect on proliferation.

Increasing the temperature to 25°C lead to similar phenotypes as overexpression via omb-Gal4 (compare fig. 3-22 to fig. 3-20). As in this cases the omb-domains reach in all variants the anterior and posterior wing disc margins, the only comparable size is the AP extension of the wing disc. But unfortunately, the discs did not extend linear along the AP axis. Comparison of the central AP fold of the discs in fig. 3-22f-h reveals, that with increasing matrix binding of the overexpressed variant, the central fold is bent to 90° or more. This unables any objective measurement of the AP extension of these discs.

The overexpression of DPP-variants at 18°C caused in contrast to 25°C no pupal lethality. Thus, also adult tissues could be analysed. Cuticle preparations of adult wings revealed severe disturbances in the formation of distinct longitudinal wing veins. The pattern of the longitudinal wing veins has been previously described as a qualitative readout system for ectopic DPP activity [90, 204]. Ectopic clones of dpp induce compartment restricted mirror duplications in the vein pattern [128] and overexpression in the endogenous domain is able to generate additional wings [172, 266]. The uniform overexpression caused by C765-Gal4 instead leads to loss or forking of distal vein regions or ectopic vein material adjacent to the regular veins (see fig. 3-24). The phenotypes observed raise the question, whether they are caused by C765-Gal4 activity in late larval stages or during puparium. It is not described so far, if C765-Gal4 expression is restricted to larval stages or persists during prepupation. The endogenous DPP expression refines in late prepupae (6-9h after pupation) from the AP border expression to a series of stripes corresponding to the vein primordia. Uniform overexpression of DPP during this stage by means of a hs-DPP construct or Gal4-580 and Gal4-1348, both active during pupariation, lead to large areas of ectopic vein tissue in intervein regions [96, 227]. Thus, as ectopic vein material is only induced adjacent to regular veins, it does not resemble DPP activity during pupariation. Another aspect, that points out the phenotypes to be results of larval DPP activity, is the occurrence of distal gaps in L2 and L5. Similar phenotypes were only observed by larval sal-overexpression [217, 219] or loss of dpp function in pupation [93, 96, 227]. In the latter case, the L4 vein was most sensitive to disturbances in DPP gene dosis, and gaps in L4 have not been observed with C765-Gal4 overexpression. From these findings it can be concluded, that the wing vein pattern modification observed, results solely from larval activity of C765-Gal4.

Comparing the effect of DPP on ectopic Omb-expression and adult wing vein pattern, a striking discrepancy becomes evident. In larval development, the effects of D-DUP and D-MYC are comparable and significantly different to effects caused by D-DEL (see fig. 3-23). Adult wings, instead, show comparable defects for D-DEL and D-MYC and drastic stronger disturbances of wing vein pattern in case of D-DUP overexpression (see table 3-5). However, Omb mutants revealed a necessity of Omb for survival of distal wing tissue and only minor involvement in formation of distal L4 and L5 [172]. Spalt/spalt related mutant clones, in contrast, have no influence on overall adult wing size, but are required for precise determination of several veins [217, 219]. Vein L2 is induced at the anterior edge of spalt expression in an area of intermediate sal expression levels. The L5 vein is induced posterior adjacent to the Sal-domain. Expression of high levels of Sal throughout the wing blade lead to a complete loss of L2 and L5 supporting the model of Sal domain edges as vein inducers. Thus, the role of Sal in defining L2 and L5 explains the defects observed in these veins caused by overexpression of the DPP-variants. In the light of this Sal-dependence of vein formation the discrepancy between larval and adult phenotypes might be explained by means of differences in the levels of Sal and Omb induction in late wing imaginal disc and it would be worth to visualize and measure also the Sal expression domain in this overexpression setup. The formation of ectopic vein material adjacent to L4 is solely observed in D-DUP overexpression. This phenotype might be explained by the general downregulation of the DPP-pathway and a predominant role of Hh signaling in patterning this area [223]. Thus, extrem high DPP-signals might interfere

with the Hh dependent pathways and provoke thereby the formation of the ectopic vein material. On the other hand, this phenotype could also reflect simply a total disorganisation of L5 vein induction, which lead to an anterior shifts of L5 vein.

4.5.4 Wing disc rescue by DPP-variants

Exchanging the endogenous DPP by the DPP-variants provides the best possibility to assess the *in vivo* importance of the matrix binding sites for DPP signaling and patterning. To achieve removal of the endogenous DPP-source, several mutations in the regulatory “disc” DPP promoter region are available [72], which in transheterozygous combinations delete DPP in imaginal tissues without affecting previous DPP functions. Commonly used combinations are dpp^{d4}/dpp^{d5} with only mild reduction or dpp^{d8}/dpp^{d12} dpp^{d8}/dpp^{d10} and dpp^{d12}/dpp^{d14} with total reduction of DPP activity [204, 217, 243, 245, 246] in wing imaginal discs. Restoring DPP function is achieved by the use of specific *dpp*-Gal4 driver-lines, which consist of small disc-promoter fragments combined with the Gal4 gene [89]. UAS-DPP elements driven by *dpp*-Gal4 are able to rescue the target gene expression pattern up to full viability [89, 243, 245, 246]. In this study the dpp^{d12}/dpp^{d14} heteroallelic combination was used to remove the endogenous DPP.

All three variants were able to restore a full-sized normal shaped wing disc with regular expression of the target-genes *Omb* and *Sal* (see fig. 3-25). Thus, full matrix binding is not necessary to establish a functional DPP gradient. Nevertheless, there were differences among the variants observed concerning the extension of the disc in AP and DV direction and the action range of the DPP ligand (see fig. 3-26). A clear tendency is seen in the proliferation, as determined by the size of the wing pouch measured along the AP and the DV boundaries, proportionally increasing with the matrix binding potential. Differences are significant between D-DEL and D-DUP. Also the AP extension of the target-genes *omb* and *sal* showed the same tendency, whereby the strongest difference (1.5 fold) is seen in *Sal* expression. In conclusion, the DPP gradient in the wing imaginal disc is formed in its full extent independently of the matrix binding ability of DPP, but the latter influences disc size and action range of DPP to some extent with most influence on DPP peak levels.

4.6 Matrix-binding requirement of DPP in the tracheal system

The branching morphogenesis of the tracheal system in *Drosophila* embryos is a process with an elaborate interplay of several signaling pathways. Each tracheal pit comprises of around 80 cells and without any further cell division six different branches are formed solely by migration in response to different signaling pathways. Whereas the Hedgehog and FGF-pathway are necessary for mobility, the EGF, Wg and DPP pathway are involved in determining cell fates of the different branches. The EGFR pathway is activated in the central part of tracheal placodes and mutants in the EGFR-pathway show defects in the dorsal trunk and visceral branch formation [84]. The Wg-pathway precisely defines the cells of the dorsal trunk [267]. DPP is expressed in ectodermal stripes above and below the tracheal pits, determining the dorsal branch and the lateral trunks [196]. The role of DPP in the specification of vertical branches has been demonstrated by loss of DPP signaling and ectopic pathway activation in the whole tracheal system. In the latter case, most cells are arranged in vertical branches and both EGFR-specified branches fail to develop [84, 196]. Thus, the branching morphogenesis is highly complex and regulated by interactions between several pathways and represents a useful system to study the potential of DPP-variants to disturb this balance.

The *bth*-Gal4 driven overexpression of DPP or the activated receptor *Tkv* has been investigated previously [84, 196]. Notably, the expression strength of the used DPP-variants is quite moderate compared to UAS-DPP lines used by other groups (data not shown). This might explain the slightly more severe phenotypes observed by these groups compared to overexpression of D-MYC (see fig. 3-27c). Matrix-binding per se is a crucial step in DPP signaling during tracheal branching, which is clearly demonstrated by the strong difference in the reorganising potential between matrix-binding and non-matrix-binding DPP variants (see fig. 3-27 b-d). Ectopic expression of the matrix binding deficient variant D-DEL causes only minor defects, notably a slight thickening of the dorsal branches and consequently reduction of cell number in the dorsal trunks. D-MYC and D-DUP in contrast cause more severe phenotypes (i.e. strong thickening of dorsal branches, nearly total loss of dorsal trunks and reduction of visceral branches) comparable to data from the literature [84, 196]. Interestingly, D-DUP is not able to cause a stronger phenotype than D-MYC. This hints towards a limit in the reorganising potential, that is even achieved by wildtype matrix binding. Experiments with elevated temperature, (29°C, data not shown) and therefore increased Gal4 activity, elicited identical phenotypes supporting this view. But this is countered by the more drastic phenotypes observed by other groups [84, 196]. Another possibility would be that only the whole N-terminus, not the “basic core” mediates matrix binding in the tracheal system. Thus the D-DUP variant under this circumstances has no increased matrix affinity compared to D-MYC. The existence of signaling-relevant HSPGs in the matrix of tracheal precursor cells has been proven by mutations in the *sulfateless* and the *dHS6ST* gene which both cause severe defects in the tracheal migration. But this phenotype is reminiscent of mutations in the FGF pathway which affect migration behaviour of all branches and therefore are not suitable to conclude on DPP-signaling defects [27, 32, 268]. The drastic effect of a simple modification (i.e.

sulfation of the 6-OH position in heparan sulfate) on the other hand demonstrates that ligand-GAG interactions are highly specific and raises the question, whether heparan sulfate sidechains are modified the same way in every tissue. This is supported by the observation that the HS-proteoglycan gene *dally* interacts with *wg* and not *dpp* in early embryogenesis and interacts on the other way round with *dpp* and not *wg* in the genitalia disc [27, 32, 65, 268], which also suggests tissue specific modifications of the *dally* GAG-chains.

4.7 Tissue specific relevance of matrix binding on DPP signaling

The analysis of mutations in GAG biosynthesis revealed an involvement of proteoglycans in several signaling pathways, i.e. Wg, DPP, Hh, and FGF. Interestingly, not every developmental process depends on matrix interactions to the same extent. One of the earliest cytokine action, the establishing of the DV-axis by combined action of DPP and Scw was not affected by any maternal and zygotic mutation in GAG synthesis or proteoglycans [26, 27, 32-34, 51, 65, 66, 268]. Later in imaginal disc patterning, there is a clear involvement of GAGs and proteoglycans in DPP signaling processes [34, 62, 64]. Other DPP dependent patterning events like branching morphogenesis in the tracheal system might also depend on matrix binding, but mutational analysis is complicated due to other matrix dependent cytokines (FGF) involved in this process [26, 27]. Consistently, Wingless signaling strongly depends on GAGs and glypicans in early embryonic patterning, whereas wing disc and genitalia disc patterning is less affected [32-34, 51, 65, 66, 268].

In this study, the effects of ectopic DPP in tracheal patterning were strongly dependent on matrix binding ability (see fig. 3-27), thus it can be considered that matrix components are also necessary for endogenous DPP function. The existence of HS-proteoglycans in this tissue is undoubted since FGF signaling in the same context was shown to be severely affected by mutations in UDP-glucose-dehydrogenase, N-deacetylase/N-sulfotransferase and HS6-O-sulfotransferase enzymes [26, 27].

DPP overexpression and rescue experiments in the wing imaginal disc showed trend effects of increased and decreased matrix binding on overall DPP signaling function (see fig. 3-19 till 3-26). However, the rescue experiment clearly demonstrated full DPP activity and complete pattern generation in the absence or presence of N-terminal matrix binding sites. One can speculate on remaining matrix binding by means of 13 basic aa residues in the core protein, but with the exception of one lysine (K63 \Rightarrow E46), these are all conserved between DPP and BMP-2. For the latter it has been shown, that removal of the basic N-terminus completely abrogates any apparent affinity to heparin under physiological conditions [234]. Thus at least HS-proteoglycan binding might also in the case of DPP solely be mediated via the flexible and basic N-terminus.

Finally, the tissue specific requirement and level of extracellular matrix binding for DPP signaling might depend on several factors. First, the overall structural orientation of DPP secreting and receiving cells requires various extents of ligand-matrix interactions. In **DV axis formation**, cells receiving the DPP signal are simultaneously the secreting cells and therefore the distance for the ligand to diffuse through the extracellular space is limited. The signaling cell-layer is covered by the perivitellin-membrane, which also limits the ligand diffusion. Thus, short distance and limited diffusion space might create a situation which allows high ligand concentrations without involvement of extracellular matrix. In **wing imaginal disc patterning**, in contrast, DPP is expressed in a small stripe of cells and signals along a cell monolayer surface over 20 cell diameters in distance [87]. Hence, DPP has to diffuse a long distance to activate *omb* at low threshold concentrations and simultaneously reach high threshold concentrations to activate the *sal* target gene. Finally, the wing imaginal disc is covered by the peripodial-membrane, which limits the diffusion space. But the overall requirement in diffusion range and gradient formation may explain the moderate involvement of matrix interaction in this case.

Second, other factors than the extracellular matrix influence the diffusion range and local ligand concentration. These can substitute the matrix function. In DV axis formation, a balanced system of the Tld agonist and the Sog and Tsg antagonists resolve the uniform DPP expression pattern to a steep activity gradient [87, 103, 106, 186]. Sog has also been discussed to influence directly DPP's diffusion range [269]. Additionally, the high affinity receptor Tkv is actively downregulated in the central part of the wing imaginal disc to elevate DPPs diffusion range [223, 224].

Third, the availability of HS-proteoglycans differs among tissues. *Dally* and *Dally-like*, the two *Drosophila* glypicans elicit a highly regulated temporal and spatial expression pattern [64]. A *dally-lacZ* reporter element shows activity only in small stripes coincident with Wg and DPP secreting cells in wing imaginal disc [64]. Coincidentally, mainly peak levels of DPP (i.e. Spalt expression) are affected in DPP rescue experiments. Notably, also HS-proteoglycan modifying enzymes, e.g. dHS6-O-sulfotransferase, show restricted expression patterns [27]. This allows the generation of tissue specifically modified GAG-chains with variation in binding properties for distinct ligands and might explain the great variation in matrix-binding influences on DPP-signaling among tissues.



Figure 5-3: Model for supporting function of matrix interactions in ligand signaling in vivo
Blue and red ellipses represent ligand secreting cells. Matrix binding deficient ligands are shown in red, matrix binding ligands in blue, cell surface receptors in green and matrix proteoglycans as black lines. Yellow stars indicate signaling events in ligand receiving cells.

4.8 Matrix binding and gradient formation

The initial aim of this work was to assess the involvement of matrix interaction in the establishing of a DPP morphogen gradient in the wing imaginal disc. Gradients of secreted factors are widespread in development, and if these factors can elicit at least three different reactions in target cells (depending on the factor concentration), they are assigned as morphogens [270]. In *Drosophila*, bicoid, Wg, Hh and DPP have been shown to act as morphogens [87, 271-273]. Instructive insights into morphogen gradient mechanisms are derived from activin mediated patterning in early *Xenopus* development (rev. in [274]). Activin induces concentration dependently at least five different cell fates in dissected *Xenopus* blastomers [275, 276]. In the course of this, concentration differences of 1.5fold can clearly induce different cell fates. The range of the activin gradient reaches at least 10 cell diameters [277] and is established in a short time period of one to several hours [278]. Interpretation of the concentration value occurs on the level of the number of occupied cell surface receptors and is further mediated via comparable differences in the amount of activated Smad proteins [279, 280]. However, Activin has never been shown to interact with GAGs or the ECM and the N-terminal sequence of *Xenopus* β -activin (GLECDG**H**TNLC) totally lacks groups of basic aa residues. Recent studies with *Xenopus* BMP-4 demonstrated an increased diffusion range of the latter after removal of the potential matrix binding sites [256]. Thus, the Activin morphogen gradient might be established differently to DPP gradients due to the inability of Activin to react with GAGs of the ECM.

Among the multiple requirements of DPP during development, DPP has been identified to act as morphogen in two processes, namely establishing of the DV axis in early embryogenesis and wing imaginal disc patterning in late larval development. In DV axis formation, DPP signaling thresholds define at least three areas of gene expression: dorsalmost the amnioserosa-group genes like *Race* and *hindsight*, more lateral expanding *u-shaped* and *tailup*, and finally covering the whole ectoderm are *pannier*, *rhomboid* and d-GATAc [184]. The graded expression in the lateral regions is achieved by the *brinker* repression mechanism, whereas high threshold level genes are regulated synergistically through DPP/Screw peak-levels [184, 281]. DPP and Screw are expressed ubiquitously throughout the dorsalmost 40% and the whole embryo-circumference, respectively. They are inhibited laterally and enriched dorsally by the SOG/TSG-TLD repression-reactivation mechanism [103, 106, 282]. This redistribution of DPP/Screw to a steep gradient occurs about 2h after fertilisation and is seen as a 20 cell-broad stripe of Mad-phosphorylation, that rapidly resolves to an intensive dorsal stripe of p-Mad, only 8 cells in diameter, that persists for about one hour [269, 281]. Recent publications postulated and experimentally demonstrated DPP to be largely immobile without the action of SOG. Thus, the concentration gradient is established not by diffusion of DPP itself, but through the action of SOG/TSG allowing long range DPP diffusion ([269], fig. 4-4). This raises the question, why DPP occurs largely immobile, as it has been shown to be active in wing discs without the help of SOG more than 20 cell diameters away from its source [87]. One possibility of DPP immobilisation would be extensive matrix binding. However, maternal and zygotic mutations in glypicans or GAG synthesizing and modifying enzymes elicited no kind of disturbance in DV axis formation, largely ruling out this explanation [26, 27, 32-34, 51, 65, 66, 268]. The absence of matrix effects in DV-DPP signaling might be simply due to lacking of relevant levels of HS-proteoglycans. These are tightly temporally and spatially regulated during embryogenesis and have not been shown to be present in very early embryogenesis [65, 66, 268]. DPP is restricted in motion more likely by means of its type I receptor Thick veins. During disc patterning Tkv is downregulated throughout the main DPP activity domain [223, 224] and overexpression of Tkv leads to a reduced DPP action range [222-224]. Thus, as DPP is expressed in low levels during embryonic stage 5 [281] and Tkv is expressed during DV-axis formation uniformly throughout the DPP action range, the ligand might without SOG action be trapped locally by its own signaling receptor.

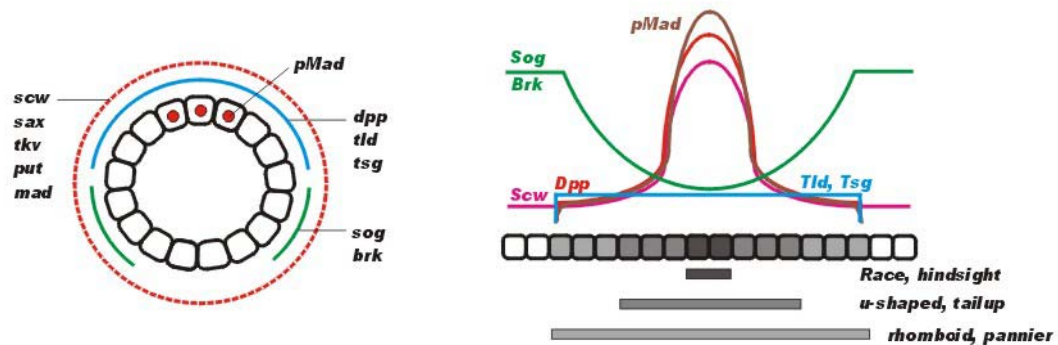


Figure 4-4: Establishing of a DPP activity gradient in DV-axis formation (adopted from [281], fig. 7)
Left panel shows gene expression of gradient establishing factors at Drosophila embryonic stage 5; right panel shows resulting protein distribution and below DPP targetgene expression in greyscales.

A different scenario appears during establishing of the DPP wing disc gradient. Whereas the DPP gradient in early embryogenesis forms within minutes and lasts for about one hour, DPP is expressed during the whole third larval stage in the wing imaginal disc, thereby acting for more than 48h to induce target genes and patterning the disc [89]. In the course of this, the disc proliferates quite strongly and increases largely in size, nevertheless the DPP source remains stable in its AP extension due to the Hedgehog short range inducing mechanism [204, 212]. The target-genes of DPP are to a large extent regulated by means of the brinker repressor, in this fashion translating the threshold levels, similar to DV-axis determination [176, 181, 221]. The DPP gradient establishes via immediate diffusion of DPP, which was directly visualized as a GFP-fusionprotein [245, 246]. Agonists/antagonists like Sog or Tld are not involved in this process [102, 191]. Experiments demonstrated an influence of vesicle trafficking on the DPP diffusion range, thereby suggesting transcytosis to play a role in long range gradient formation [245]. However, the major postulated mechanism to establish the DPP long range diffusion is the downregulation of Tkv throughout the central part of the wing disc [222-224]. This is based on at least three regulatory mechanisms. The masters of thick veins (*mtv*) gene product represses *tkv* expression and is expressed at high levels in DPP expressing cells by activation via Hedgehog. In more posterior regions, *mtv* is activated at moderate levels by means of engrailed function. In more anterior regions, *mtv* is slightly more active than in posterior regions. This lateral inhibition of *tkv* might be mediated by DPP signaling itself [222, 224], as DPP has been shown to downregulate *Tkv* significantly in ectopic DPP expression clones outside the endogenous DPP range. This *Tkv* regulation mechanism has been postulated to evoke two different effects on

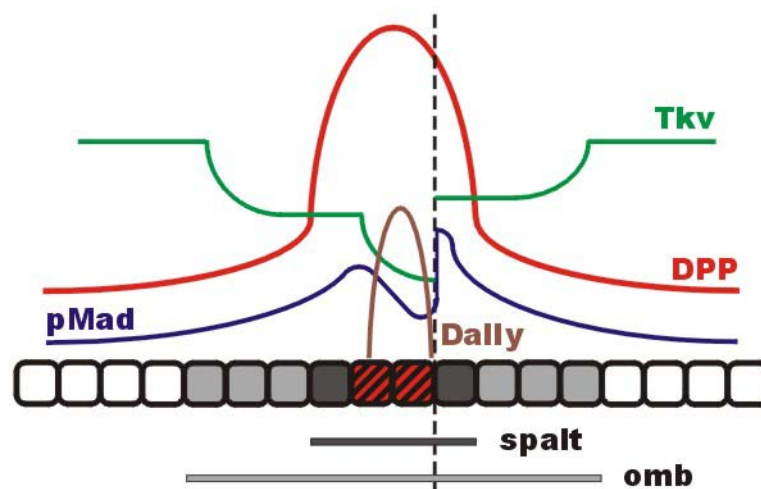


Figure 4-5: Establishing of a DPP-gradient in wing disc patterning
Expression levels (*Tkv*, *Dally*), mediator activation (*pMad*) and ligand distribution (*DPP*) are shown in coloured curves. DPP expressing cells (red) and targetgene expression in wing disc cell layer (black⇒*spalt*, grey⇒*omb*) are shown below.

DPP-signaling. First, the downregulation of Tkv in the central disc regions allows DPP diffusion into lateral region. However, DPP concentrations in these regions are high enough to activate target-genes also via reduced numbers of DPP receptors. Second, the elevated receptors at the border of the DPP action range enable low levels of DPP to signal in sufficient amounts to activate target-genes [222]. In addition to receptor regulation, a second BMP-ligand, GBB, also plays a role during patterning events. While overexpression data suggested a clear separation in two pathways, DPP/Tkv and GBB/Sax [115, 132], mutational analysis also supported a Sax role independent of GBB, presumably mediated via Tkv [116, 226].

Both *Drosophila* glypicans have been shown to be expressed in the wing disc. Dally has been reported to interact with DPP-signaling in several imaginal discs [62]. In the wing disc, dally has been shown to be expressed in a broad stripe covering the DV compartment border and in a small stripe identical to DPP expressing cells. Later in prepupae, dally expression is found in wing vein primordia consistent with a defect in distal L5 vein observed in dally mutants. Curiously, the interaction is synergistic in eye-antenna, and genitalia disc, whereas it seems to be opposing in wing disc. However, overexpression experiments in wing discs also demonstrated a positive correlation between dally and DPP-signaling. The other *Drosophila* glypican, dally-like, has been demonstrated to affect Wg signaling in embryonic and wing disc development [51]. The expression pattern in the wing is uniform without any data on expression levels compared to dally. As no dally-like mutant has been described so far, the effect of the latter on DPP signaling remains unknown.

Both, overexpression and rescue experiments demonstrated a positive correlation of matrix binding ability and DPP signaling strength in *Drosophila* wing imaginal disc (see 3-20 to 3-26), suggesting an interaction of DPP with HS-proteoglycans. The only proteoglycans known so far to be expressed in wing discs are the two glypicans dally and dally-like protein.

By means of the rescue experiment it was clearly demonstrated, that the DPP gradient forms to a large extent independently of matrix interactions. However, the greatest differences among the rescue by the three variants were found in the Sal expression domain (see fig. 3-25 and 3-26). Consequently, the peak levels of DPP are most effected by changes in matrix binding. This coincides with the expression pattern of dally. Thus, to achieve peak levels of DPP signaling in regions with lowest receptor distribution, the additional support of a locally expressed HS proteoglycan might be necessary (see fig. 4-5). The effects of DPP-variants on Omb expression in lateral regions of the disc (see fig. 3-22 a-d) can't be explained by a DPP-dally interaction due to the fact that dally-expression is limited to the DV and AP compartment boundaries [64]. Thus another proteoglycan might be involved in signaling of the ectopically expressed DPP. A candidate for this interaction would be dally-like, which is uniformly expressed in wing discs [51].

In conclusion, the two DPP morphogen gradients established during DV-axis formation and wing imaginal disc patterning are organized by different mechanisms. Whereas the former appears to form without any ligand-matrix interaction, the involvement of matrix binding in the correct shaping of the gradient could be demonstrated for the wing disc morphogen gradient.

4.9 DPP signaling in cell culture assays

One of the aims during this work was the generation of a quantitative readout system for DPP activity. The only biological reporter system working so far is the limbbud-assay (238, & see fig 3-12). Several aspects in the limbbud assay are limiting its usefulness: It's time effort (7 days), and handling with radioactivity. Additionally, the micromass cell culture contains a large amount of ECM influencing ligand activity and not allowing measurements of intrinsic ligand activity (basic ligand-receptor signaling). Attempts to activate alkaline phosphatase in C2C12 or MC3T3 cells, as described for BMP-2, failed [252]. Therefore, the luciferase reporter system was chosen to be adopted to *Drosophila* cell culture. Several BMP-2 sensitive reporters are described so far [252, 253]. The strategy was to generate stable *Drosophila* S2-cell lines containing multiple copies of the luciferase reporter element. All stable cell-lines, that were generated, showed high basal activities and insensitivity to starving or ligand incubation (see fig. 3-28 to 3-30). High basal activities, caused by the Mad-binding elements or minimal promoters, were largely excluded. Finally, two possibilities might explain the observed phenomenon. First, the luciferase gene itself could contain promoter sequences, which are active in *Drosophila*. Second, the highly efficient method to generate stable cell-lines with multiple insertions of the plasmid results with high probability in insertions of the reporter constructs into transcriptionally active genes. The latter case should be excluded in transient transfection assays. This might lead to a general usage of the luciferase reporter system in *Drosophila* cell culture.

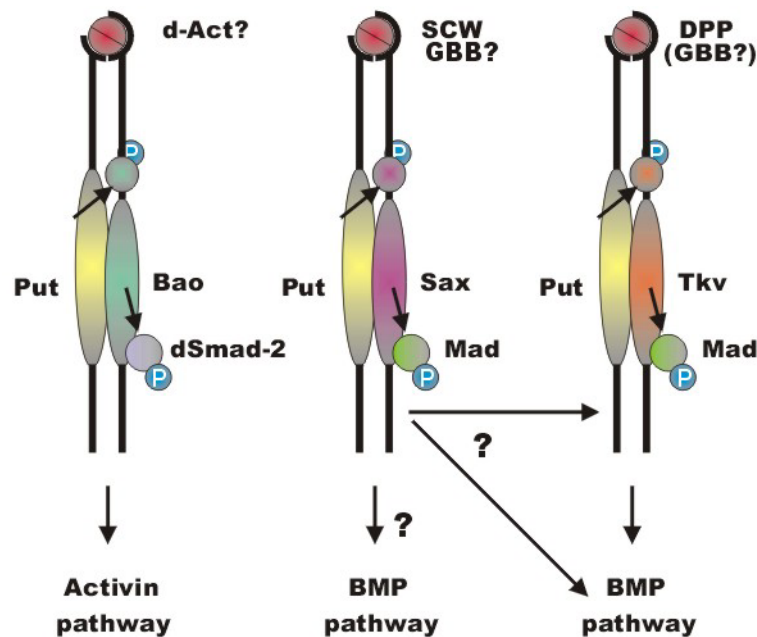


Figure 4-6: TGF-beta signaling pathways in *Drosophila*

In a second cell culture approach, the ability of Thick veins and Saxophone was tested to induce the downstream signaling cascade ligand-independently. Initial experiments demonstrated, as expected, a clear concentration and time dependence of Mad-phosphorylation in response to DPP incubation (see fig. 3-32). Thus the Mad-phosphorylation serves as visualisation tool for DPP signaling cascade activity.

Several studies claimed Saxophone to convey other ligand signals than DPP. In early embryogenesis, Sax clearly transduces exclusively Screw signals, whereas Thick veins mediates DPP signaling [113, 114, 131]. Whereas loss of Scw/Sax signaling was compensated by means of overexpressing DPP/Tkv, the latter could not be substituted by Scw/Sax. This implied a converging pathway which is dominated by Tkv downstream signaling. Similar results were found in wing disc development with Gbb as ligand for Sax, but additionally, Gbb showed activity independent of Sax more likely to be mediated by Tkv [115, 132, 226]. Taken together, this raised the question of the level of Sax/Tkv convergence and how the one-way substitution is molecularly organized. In this work, only DPP was available as ligand. Thus, data were only obtained for ligand independent receptor activation. The inducible stable cell lines, produced in various combinations of the three involved receptors Sax, Tkv and Put, clearly showed, that overexpression of at least one type I and the type II receptor is needed to mediate Mad-phosphorylation (see fig 3-33). As the levels of expressed receptors were not comparable due to different epitope tags, no conclusion could be drawn in terms of the efficiency of Mad-phosphorylation concerning Tkv and Sax. Given similar receptor activation potentials of the three ligands SCW, GBB and DPP, no differences are obvious on the level of Mad activation, which is definitely a converging point for Sax and Tkv pathways. Involvement of a second BMP-Smad in *Drosophila*, which might be also detected by the anti-phospho Mad antibody, could be excluded. Since the *Drosophila* genome is completely sequenced for years and extensive searches, based on the highly conserved MH2 domain, revealed only the existence of activin-pathway restricted dSmad-2 [159, 283], there is an agreement on the existence of only two R-Smads in *Drosophila*. Crossreactions of the antibody with dSmad-2 is largely unlikely due to large differences around the SSXS-sequence (dSmad-2: RLPCSSMS; hSmad-1: HNPISSVS; Mad: HNAISSVS).

Taken together, the ability of Sax to phosphorylate Mad seems equal to Tkv. Consequently, the differences concerning Sax and Tkv to compensate for each other must be assigned to the ligand-receptor interactions or to Mad-independent signal mediation. The former possibility is largely excluded by the inability of constitutively active Sax to elicit Tkv-act like phenotypes [115]. But unequivocally conclusions might be drawn only from cell culture and in-vitro ligand-receptor interactions performed with DPP, GBB and Screw (see figure 4-6).

5 References

1. Stryer, L., *Biochemistry*. 3rd ed. 1988, New York City: W.H. Freeman and Company.
2. Alberts, B., Lewis, B., Raff, M., Roberts and Watson, *Molecular Biology of The Cell*. 3rd ed. 1994, New York: Garland Publishing Inc.
3. Lodish, B., Zipursky, R., Matsudaira, M., Baltimore and Darnell, *Molecular Cell Biology*. 4th ed. 2000, New York City: W.H. Freeman and Company.
4. Cross, P.C.a.M., Lynne K., *Cell and tissue Ultrastructure*. 1993, New York City: W.H. Freeman and Company.
5. David, G., *Integral membrane heparan sulfate proteoglycans*. *Faseb J*, 1993. **7**(11): p. 1023-30.
6. Kjellen, L. and U. Lindahl, *Proteoglycans: structures and interactions*. *Annu Rev Biochem*, 1991. **60**: p. 443-75.
7. Yanagishita, M. and V.C. Hascall, *Cell surface heparan sulfate proteoglycans*. *J Biol Chem*, 1992. **267**(14): p. 9451-4.
8. Salmivirta, M., K. Lidholt, and U. Lindahl, *Heparan sulfate: a piece of information*. *Faseb J*, 1996. **10**(11): p. 1270-9.
9. Varki, A., *Six blind men and the elephant--the many faces of heparan sulfate*. *Proc Natl Acad Sci U S A*, 2002. **99**(2): p. 543-5.
10. Esko, J.D. and S.B. Selleck, *Order out of chaos: assembly of ligand binding sites in heparan sulfate*. *Annu Rev Biochem*, 2002. **71**: p. 435-71.
11. Bernfield, M., et al., *Biology of the syndecans: a family of transmembrane heparan sulfate proteoglycans*. *Annu Rev Cell Biol*, 1992. **8**: p. 365-93.
12. Olwin, B.B. and A. Rapraeger, *Repression of myogenic differentiation by aFGF, bFGF, and K-FGF is dependent on cellular heparan sulfate*. *J Cell Biol*, 1992. **118**(3): p. 631-9.
13. Rapraeger, A.C., A. Krufka, and B.B. Olwin, *Requirement of heparan sulfate for bFGF-mediated fibroblast growth and myoblast differentiation*. *Science*, 1991. **252**(5013): p. 1705-8.
14. Yayon, A., et al., *Cell surface, heparin-like molecules are required for binding of basic fibroblast growth factor to its high affinity receptor*. *Cell*, 1991. **64**(4): p. 841-8.
15. Schlessinger, J., I. Lax, and M. Lemmon, *Regulation of growth factor activation by proteoglycans: what is the role of the low affinity receptors?* *Cell*, 1995. **83**(3): p. 357-60.
16. Mason, I.J., *The ins and outs of fibroblast growth factors*. *Cell*, 1994. **78**(4): p. 547-52.
17. Spivak-Kroizman, T., et al., *Heparin-induced oligomerization of FGF molecules is responsible for FGF receptor dimerization, activation, and cell proliferation*. *Cell*, 1994. **79**(6): p. 1015-24.
18. DiGabriele, A.D., et al., *Structure of a heparin-linked biologically active dimer of fibroblast growth factor*. *Nature*, 1998. **393**(6687): p. 812-7.
19. Faham, S., et al., *Heparin structure and interactions with basic fibroblast growth factor*. *Science*, 1996. **271**(5252): p. 1116-20.
20. Ornitz, D.M., et al., *FGF binding and FGF receptor activation by synthetic heparan-derived di- and trisaccharides*. *Science*, 1995. **268**(5209): p. 432-6.
21. Venkataraman, G., et al., *Preferential self-association of basic fibroblast growth factor is stabilized by heparin during receptor dimerization and activation*. *Proc Natl Acad Sci U S A*, 1996. **93**(2): p. 845-50.
22. Plotnikov, A.N., et al., *Structural basis for FGF receptor dimerization and activation*. *Cell*, 1999. **98**(5): p. 641-50.
23. Schlessinger, J., et al., *Crystal structure of a ternary FGF-FGFR-heparin complex reveals a dual role for heparin in FGFR binding and dimerization*. *Mol Cell*, 2000. **6**(3): p. 743-50.
24. Guimond, S., et al., *Activating and inhibitory heparin sequences for FGF-2 (basic FGF). Distinct requirements for FGF-1, FGF-2, and FGF-4*. *J Biol Chem*, 1993. **268**(32): p. 23906-14.
25. Pye, D.A., et al., *Heparan sulfate oligosaccharides require 6-O-sulfation for promotion of basic fibroblast growth factor mitogenic activity*. *J Biol Chem*, 1998. **273**(36): p. 22936-42.
26. Lin, X., et al., *Heparan sulfate proteoglycans are essential for FGF receptor signaling during Drosophila embryonic development*. *Development*, 1999. **126**(17): p. 3715-23.
27. Kamimura, K., et al., *Drosophila heparan sulfate 6-O-sulfotransferase (dHS6ST) gene. Structure, expression, and function in the formation of the tracheal system*. *J Biol Chem*, 2001. **276**(20): p. 17014-21.
28. Reichsman, F., L. Smith, and S. Cumberledge, *Glycosaminoglycans can modulate extracellular localization of the wingless protein and promote signal transduction*. *J Cell Biol*, 1996. **135**(3): p. 819-27.
29. Aviezer, D. and A. Yayon, *Heparin-dependent binding and autophosphorylation of epidermal growth factor (EGF) receptor by heparin-binding EGF-like growth factor but not by EGF*. *Proc Natl Acad Sci U S A*, 1994. **91**(25): p. 12173-7.

30. Zioncheck, T.F., et al., *Sulfated oligosaccharides promote hepatocyte growth factor association and govern its mitogenic activity*. J Biol Chem, 1995. **270**(28): p. 16871-8.
31. Hempel, J., et al., *UDP-glucose dehydrogenase from bovine liver: primary structure and relationship to other dehydrogenases*. Protein Sci, 1994. **3**(7): p. 1074-80.
32. Hacker, U., X. Lin, and N. Perrimon, *The Drosophila sugarless gene modulates Wingless signaling and encodes an enzyme involved in polysaccharide biosynthesis*. Development, 1997. **124**(18): p. 3565-73.
33. Binari, R.C., et al., *Genetic evidence that heparin-like glycosaminoglycans are involved in wingless signaling*. Development, 1997. **124**(13): p. 2623-32.
34. Haerry, T.E., et al., *Defects in glucuronate biosynthesis disrupt Wingless signaling in Drosophila*. Development, 1997. **124**(16): p. 3055-64.
35. Bellaiche, Y., I. The, and N. Perrimon, *Tout-velu is a Drosophila homologue of the putative tumour suppressor EXT-1 and is needed for Hh diffusion*. Nature, 1998. **394**(6688): p. 85-8.
36. Toyoda, H., A. Kinoshita-Toyoda, and S.B. Selleck, *Structural analysis of glycosaminoglycans in Drosophila and Caenorhabditis elegans and demonstration that tout-velu, a Drosophila gene related to EXT tumor suppressors, affects heparan sulfate in vivo*. J Biol Chem, 2000. **275**(4): p. 2269-75.
37. The, I., Y. Bellaiche, and N. Perrimon, *Hedgehog movement is regulated through tout velu-dependent synthesis of a heparan sulfate proteoglycan*. Mol Cell, 1999. **4**(4): p. 633-9.
38. Lind, T., et al., *The putative tumor suppressors EXT1 and EXT2 are glycosyltransferases required for the biosynthesis of heparan sulfate*. J Biol Chem, 1998. **273**(41): p. 26265-8.
39. Selleck, S.B., *Proteoglycans and pattern formation: sugar biochemistry meets developmental genetics*. Trends Genet, 2000. **16**(5): p. 206-12.
40. Lin, X. and N. Perrimon, *Role of heparan sulfate proteoglycans in cell-cell signaling in Drosophila*. Matrix Biol, 2000. **19**(4): p. 303-7.
41. Filmus, J., *Glypicans in growth control and cancer*. Glycobiology, 2001. **11**(3): p. 19R-23R.
42. David, G., et al., *Molecular cloning of a phosphatidylinositol-anchored membrane heparan sulfate proteoglycan from human lung fibroblasts*. J Cell Biol, 1990. **111**(6 Pt 2): p. 3165-76.
43. Stipp, C.S., E.D. Litwack, and A.D. Lander, *Cerebroglycan: an integral membrane heparan sulfate proteoglycan that is unique to the developing nervous system and expressed specifically during neuronal differentiation*. J Cell Biol, 1994. **124**(1-2): p. 149-60.
44. Filmus, J., J.G. Church, and R.N. Buick, *Isolation of a cDNA corresponding to a developmentally regulated transcript in rat intestine*. Mol Cell Biol, 1988. **8**(10): p. 4243-9.
45. Watanabe, K., H. Yamada, and Y. Yamaguchi, *K-glypican: a novel GPI-anchored heparan sulfate proteoglycan that is highly expressed in developing brain and kidney*. J Cell Biol, 1995. **130**(5): p. 1207-18.
46. Veugelers, M., et al., *Characterization of glypican-5 and chromosomal localization of human GPC5, a new member of the glypican gene family*. Genomics, 1997. **40**(1): p. 24-30.
47. Saunders, S., S. Paine-Saunders, and A.D. Lander, *Expression of the cell surface proteoglycan glypican-5 is developmentally regulated in kidney, limb, and brain*. Dev Biol, 1997. **190**(1): p. 78-93.
48. Veugelers, M., et al., *Glypican-6, a new member of the glypican family of cell surface heparan sulfate proteoglycans*. J Biol Chem, 1999. **274**(38): p. 26968-77.
49. Paine-Saunders, S., B.L. Viviano, and S. Saunders, *GPC6, a novel member of the glypican gene family, encodes a product structurally related to GPC4 and is colocalized with GPC5 on human chromosome 13*. Genomics, 1999. **57**(3): p. 455-8.
50. Nakato, H., T.A. Futch, and S.B. Selleck, *The division abnormally delayed (dally) gene: a putative integral membrane proteoglycan required for cell division patterning during postembryonic development of the nervous system in Drosophila*. Development, 1995. **121**(11): p. 3687-702.
51. Baeg, G.H., et al., *Heparan sulfate proteoglycans are critical for the organization of the extracellular distribution of Wingless*. Development, 2001. **128**(1): p. 87-94.
52. De Cat, B. and G. David, *Developmental roles of the glypicans*. Semin Cell Dev Biol, 2001. **12**(2): p. 117-25.
53. Pilia, G., et al., *Mutations in GPC3, a glypican gene, cause the Simpson-Golabi-Behmel overgrowth syndrome*. Nat Genet, 1996. **12**(3): p. 241-7.
54. Hughes-Benzie, R.M., et al., *Simpson-Golabi-Behmel syndrome: genotype/phenotype analysis of 18 affected males from 7 unrelated families*. Am J Med Genet, 1996. **66**(2): p. 227-34.
55. Lindsay, S., et al., *Large scale deletions in the GPC3 gene may account for a minority of cases of Simpson-Golabi-Behmel syndrome*. J Med Genet, 1997. **34**(6): p. 480-3.
56. Veugelers, M., et al., *Mutational analysis of the GPC3/GPC4 glypican gene cluster on Xq26 in patients with Simpson-Golabi-Behmel syndrome: identification of loss-of-function mutations in the GPC3 gene*. Hum Mol Genet, 2000. **9**(9): p. 1321-8.
57. Xuan, J.Y., R.M. Hughes-Benzie, and A.E. MacKenzie, *A small interstitial deletion in the GPC3 gene causes Simpson-Golabi-Behmel syndrome in a Dutch-Canadian family*. J Med Genet, 1999. **36**(1): p. 57-8.

58. Cano-Gauci, D.F., et al., *Glypican-3-deficient mice exhibit developmental overgrowth and some of the abnormalities typical of Simpson-Golabi-Behmel syndrome*. J Cell Biol, 1999. **146**(1): p. 255-64.
59. Eggenschwiler, J., et al., *Mouse mutant embryos overexpressing IGF-II exhibit phenotypic features of the Beckwith-Wiedemann and Simpson-Golabi-Behmel syndromes*. Genes Dev, 1997. **11**(23): p. 3128-42.
60. Paine-Saunders, S., et al., *glypican-3 controls cellular responses to Bmp4 in limb patterning and skeletal development*. Dev Biol, 2000. **225**(1): p. 179-87.
61. Grisaru, S., et al., *Glypican-3 modulates BMP- and FGF-mediated effects during renal branching morphogenesis*. Dev Biol, 2001. **231**(1): p. 31-46.
62. Jackson, S.M., et al., *dally, a Drosophila glypican, controls cellular responses to the TGF- beta-related morphogen, Dpp*. Development, 1997. **124**(20): p. 4113-20.
63. Tsuda, M., S. Izumi, and H. Nakato, *Transcriptional and posttranscriptional regulation of the gene for Dally, a Drosophila integral membrane proteoglycan*. FEBS Lett, 2001. **494**(3): p. 241-5.
64. Fujise, M., et al., *Regulation of dally, an integral membrane proteoglycan, and its function during adult sensory organ formation of Drosophila*. Dev Biol, 2001. **235**(2): p. 433-48.
65. Tsuda, M., et al., *The cell-surface proteoglycan Dally regulates Wingless signalling in Drosophila*. Nature, 1999. **400**(6741): p. 276-80.
66. Khare, N. and S. Baumgartner, *Dally-like protein, a new Drosophila glypican with expression overlapping with wingless*. Mech Dev, 2000. **99**(1-2): p. 199-202.
67. Massague, J., *The transforming growth factor-beta family*. Annu Rev Cell Biol, 1990. **6**: p. 597-641.
68. Padgett, R.W., R.D. St Johnston, and W.M. Gelbart, *A transcript from a Drosophila pattern gene predicts a protein homologous to the transforming growth factor-beta family*. Nature, 1987. **325**(6099): p. 81-4.
69. Arora, K., M.S. Levine, and M.B. O'Connor, *The screw gene encodes a ubiquitously expressed member of the TGF-beta family required for specification of dorsal cell fates in the Drosophila embryo*. Genes Dev, 1994. **8**(21): p. 2588-601.
70. Gatti, M. and B.S. Baker, *Genes controlling essential cell-cycle functions in Drosophila melanogaster*. Genes Dev, 1989. **3**(4): p. 438-53.
71. Novitzki, E.a.R., SA, PIAS, 1938. **47**: p. 256-260.
72. Spencer, F.A., F.M. Hoffmann, and W.M. Gelbart, *Decapentaplegic: a gene complex affecting morphogenesis in Drosophila melanogaster*. Cell, 1982. **28**(3): p. 451-61.
73. Panganiban, G.E., et al., *Biochemical characterization of the Drosophila dpp protein, a member of the transforming growth factor beta family of growth factors*. Mol Cell Biol, 1990. **10**(6): p. 2669-77.
74. Wharton, K., et al., *Molecular lesions associated with alleles of decapentaplegic identify residues necessary for TGF-beta/BMP cell signaling in Drosophila melanogaster*. Genetics, 1996. **142**(2): p. 493-505.
75. Scheufler, C., W. Sebal, and M. Hulsmeier, *Crystal structure of human bone morphogenetic protein-2 at 2.7 Å resolution*. J Mol Biol, 1999. **287**(1): p. 103-15.
76. Irish, V.F. and W.M. Gelbart, *The decapentaplegic gene is required for dorsal-ventral patterning of the Drosophila embryo*. Genes Dev, 1987. **1**(8): p. 868-79.
77. Wharton, K.A., R.P. Ray, and W.M. Gelbart, *An activity gradient of decapentaplegic is necessary for the specification of dorsal pattern elements in the Drosophila embryo*. Development, 1993. **117**(2): p. 807-22.
78. Ray, R.P., et al., *The control of cell fate along the dorsal-ventral axis of the Drosophila embryo*. Development, 1991. **113**(1): p. 35-54.
79. Panganiban, G.E., et al., *A Drosophila growth factor homolog, decapentaplegic, regulates homeotic gene expression within and across germ layers during midgut morphogenesis*. Development, 1990. **110**(4): p. 1041-50.
80. Hursh, D.A., R.W. Padgett, and W.M. Gelbart, *Cross regulation of decapentaplegic and Ultrabithorax transcription in the embryonic visceral mesoderm of Drosophila*. Development, 1993. **117**(4): p. 1211-22.
81. Thuringer, F., S.M. Cohen, and M. Bienz, *Dissection of an indirect autoregulatory response of a homeotic Drosophila gene*. Embo J, 1993. **12**(6): p. 2419-30.
82. Staehling-Hampton, K., et al., *dpp induces mesodermal gene expression in Drosophila*. Nature, 1994. **372**(6508): p. 783-6.
83. Frasch, M., *Induction of visceral and cardiac mesoderm by ectodermal Dpp in the early Drosophila embryo*. Nature, 1995. **374**(6521): p. 464-7.
84. Wappner, P., L. Gabay, and B.Z. Shilo, *Interactions between the EGF receptor and DPP pathways establish distinct cell fates in the tracheal placodes*. Development, 1997. **124**(22): p. 4707-16.
85. Campbell, G., T. Weaver, and A. Tomlinson, *Axis specification in the developing Drosophila appendage: the role of wingless, decapentaplegic, and the homeobox gene aristaless*. Cell, 1993. **74**(6): p. 1113-23.

86. Capdevila, J., et al., *The Drosophila segment polarity gene patched interacts with decapentaplegic in wing development*. *Embo J*, 1994. **13**(1): p. 71-82.
87. Nellen, D., et al., *Direct and long-range action of a DPP morphogen gradient*. *Cell*, 1996. **85**(3): p. 357-68.
88. Lecuit, T., et al., *Two distinct mechanisms for long-range patterning by Decapentaplegic in the Drosophila wing*. *Nature*, 1996. **381**(6581): p. 387-93.
89. Masucci, J.D., R.J. Miltenberger, and F.M. Hoffmann, *Pattern-specific expression of the Drosophila decapentaplegic gene in imaginal disks is regulated by 3' cis-regulatory elements*. *Genes Dev*, 1990. **4**(11): p. 2011-23.
90. Morimura, S., et al., *decapentaplegic overexpression affects Drosophila wing and leg imaginal disc development and wingless expression*. *Dev Biol*, 1996. **177**(1): p. 136-51.
91. Heberlein, U., T. Wolff, and G.M. Rubin, *The TGF beta homolog dpp and the segment polarity gene hedgehog are required for propagation of a morphogenetic wave in the Drosophila retina*. *Cell*, 1993. **75**(5): p. 913-26.
92. Ma, C., et al., *The segment polarity gene hedgehog is required for progression of the morphogenetic furrow in the developing Drosophila eye*. *Cell*, 1993. **75**(5): p. 927-38.
93. Segal, D. and W.M. Gelbart, *Shortvein, a new component of the decapentaplegic gene complex in Drosophila melanogaster*. *Genetics*, 1985. **109**(1): p. 119-43.
94. Kaphingst, K. and S. Kunes, *Pattern formation in the visual centers of the Drosophila brain: wingless acts via decapentaplegic to specify the dorsoventral axis*. *Cell*, 1994. **78**(3): p. 437-48.
95. Twombly, V., et al., *The TGF-beta signaling pathway is essential for Drosophila oogenesis*. *Development*, 1996. **122**(5): p. 1555-65.
96. Yu, K., et al., *The Drosophila decapentaplegic and short gastrulation genes function antagonistically during adult wing vein development*. *Development*, 1996. **122**(12): p. 4033-44.
97. Raftery, L.A. and D.J. Sutherland, *TGF-beta family signal transduction in Drosophila development: from Mad to Smads*. *Dev Biol*, 1999. **210**(2): p. 251-68.
98. Cui, Y., et al., *BMP-4 is proteolytically activated by furin and/or PC6 during vertebrate embryonic development*. *Embo J*, 1998. **17**(16): p. 4735-43.
99. Constam, D.B. and E.J. Robertson, *Regulation of bone morphogenetic protein activity by pro domains and proprotein convertases*. *J Cell Biol*, 1999. **144**(1): p. 139-49.
100. Cui, Y., et al., *The activity and signaling range of mature BMP-4 is regulated by sequential cleavage at two sites within the prodomain of the precursor*. *Genes Dev*, 2001. **15**(21): p. 2797-802.
101. Nakayama, T., Y. Cui, and J.L. Christian, *Regulation of BMP/Dpp signaling during embryonic development*. *Cell Mol Life Sci*, 2000. **57**(6): p. 943-56.
102. Francois, V., et al., *Dorsal-ventral patterning of the Drosophila embryo depends on a putative negative growth factor encoded by the short gastrulation gene*. *Genes Dev*, 1994. **8**(21): p. 2602-16.
103. Ross, J.J., et al., *Twisted gastrulation is a conserved extracellular BMP antagonist*. *Nature*, 2001. **410**(6827): p. 479-83.
104. Graff, J.M., *Embryonic patterning: to BMP or not to BMP, that is the question*. *Cell*, 1997. **89**(2): p. 171-4.
105. Thomsen, G.H., *Antagonism within and around the organizer: BMP inhibitors in vertebrate body patterning*. *Trends Genet*, 1997. **13**(6): p. 209-11.
106. Marques, G., et al., *Production of a DPP activity gradient in the early Drosophila embryo through the opposing actions of the SOG and TLD proteins*. *Cell*, 1997. **91**(3): p. 417-26.
107. Piccolo, S., et al., *Cleavage of Chordin by Xolloid metalloprotease suggests a role for proteolytic processing in the regulation of Spemann organizer activity*. *Cell*, 1997. **91**(3): p. 407-16.
108. Oelgeschlager, M., et al., *The evolutionarily conserved BMP-binding protein Twisted gastrulation promotes BMP signalling*. *Nature*, 2000. **405**(6788): p. 757-63.
109. Scott, I.C., et al., *Homologues of Twisted gastrulation are extracellular cofactors in antagonism of BMP signalling*. *Nature*, 2001. **410**(6827): p. 475-8.
110. Chang, C., et al., *Twisted gastrulation can function as a BMP antagonist*. *Nature*, 2001. **410**(6827): p. 483-7.
111. Israel, D.I., et al., *Heterodimeric bone morphogenetic proteins show enhanced activity in vitro and in vivo*. *Growth Factors*, 1996. **13**(3-4): p. 291-300.
112. Nishimatsu, S. and G.H. Thomsen, *Ventral mesoderm induction and patterning by bone morphogenetic protein heterodimers in Xenopus embryos*. *Mech Dev*, 1998. **74**(1-2): p. 75-88.
113. Neul, J.L. and E.L. Ferguson, *Spatially restricted activation of the SAX receptor by SCW modulates DPP/TKV signaling in Drosophila dorsal-ventral patterning*. *Cell*, 1998. **95**(4): p. 483-94.
114. Nguyen, M., et al., *Interpretation of a BMP activity gradient in Drosophila embryos depends on synergistic signaling by two type I receptors, SAX and TKV*. *Cell*, 1998. **95**(4): p. 495-506.
115. Haerry, T.E., et al., *Synergistic signaling by two BMP ligands through the SAX and TKV receptors controls wing growth and patterning in Drosophila*. *Development*, 1998. **125**(20): p. 3977-87.

116. Khalsa, O., et al., *TGF-beta/BMP superfamily members, Gbb-60A and Dpp, cooperate to provide pattern information and establish cell identity in the Drosophila wing*. Development, 1998. **125**(14): p. 2723-34.
117. Wrana, J.L., et al., *TGF beta signals through a heteromeric protein kinase receptor complex*. Cell, 1992. **71**(6): p. 1003-14.
118. Liu, F., et al., *Human type II receptor for bone morphogenetic proteins (BMPs): extension of the two-kinase receptor model to the BMPs*. Mol Cell Biol, 1995. **15**(7): p. 3479-86.
119. Nohno, T., et al., *Identification of a human type II receptor for bone morphogenetic protein-4 that forms differential heteromeric complexes with bone morphogenetic protein type I receptors*. J Biol Chem, 1995. **270**(38): p. 22522-6.
120. Nohe, A., et al., *The mode of bone morphogenetic protein (BMP) receptor oligomerization determines different BMP-2 signaling pathways*. J Biol Chem, 2002. **277**(7): p. 5330-8.
121. Attisano, L. and J.L. Wrana, *Signal transduction by members of the transforming growth factor-beta superfamily*. Cytokine Growth Factor Rev, 1996. **7**(4): p. 327-39.
122. Kingsley, D.M., *The TGF-beta superfamily: new members, new receptors, and new genetic tests of function in different organisms*. Genes Dev, 1994. **8**(2): p. 133-46.
123. Ruberte, E., et al., *An absolute requirement for both the type II and type I receptors, punt and thick veins, for dpp signaling in vivo*. Cell, 1995. **80**(6): p. 889-97.
124. Brummel, T.J., et al., *Characterization and relationship of Dpp receptors encoded by the saxophone and thick veins genes in Drosophila*. Cell, 1994. **78**(2): p. 251-61.
125. Nellen, D., M. Affolter, and K. Basler, *Receptor serine/threonine kinases implicated in the control of Drosophila body pattern by decapentaplegic*. Cell, 1994. **78**(2): p. 225-37.
126. Penton, A., et al., *Identification of two bone morphogenetic protein type I receptors in Drosophila and evidence that Brk25D is a decapentaplegic receptor*. Cell, 1994. **78**(2): p. 239-50.
127. Letsou, A., et al., *Drosophila Dpp signaling is mediated by the punt gene product: a dual ligand-binding type II receptor of the TGF beta receptor family*. Cell, 1995. **80**(6): p. 899-908.
128. Brummel, T., et al., *The Drosophila activin receptor baboon signals through dSmad2 and controls cell proliferation but not patterning during larval development*. Genes Dev, 1999. **13**(1): p. 98-111.
129. Marques, G., et al., *The Drosophila BMP type II receptor Wishful Thinking regulates neuromuscular synapse morphology and function*. Neuron, 2002. **33**(4): p. 529-43.
130. Wharton, K.A., G.H. Thomsen, and W.M. Gelbart, *Drosophila 60A gene, another transforming growth factor beta family member, is closely related to human bone morphogenetic proteins*. Proc Natl Acad Sci U S A, 1991. **88**(20): p. 9214-8.
131. Podos, S.D. and E.L. Ferguson, *Morphogen gradients: new insights from DPP*. Trends Genet, 1999. **15**(10): p. 396-402.
132. Singer, M.A., et al., *Signaling through both type I DPP receptors is required for anterior- posterior patterning of the entire Drosophila wing*. Development, 1997. **124**(1): p. 79-89.
133. Wieser, R., J.L. Wrana, and J. Massague, *GS domain mutations that constitutively activate T beta R-I, the downstream signaling component in the TGF-beta receptor complex*. Embo J, 1995. **14**(10): p. 2199-208.
134. Wang, X.F., et al., *Expression cloning and characterization of the TGF-beta type III receptor*. Cell, 1991. **67**(4): p. 797-805.
135. Tsukazaki, T., et al., *SARA, a FYVE domain protein that recruits Smad2 to the TGFbeta receptor*. Cell, 1998. **95**(6): p. 779-91.
136. Xu, L., Y.G. Chen, and J. Massague, *The nuclear import function of Smad2 is masked by SARA and unmasked by TGFbeta-dependent phosphorylation*. Nat Cell Biol, 2000. **2**(8): p. 559-62.
137. Bennett, D. and L. Alphey, *PP1 binds Sara and negatively regulates Dpp signaling in Drosophila melanogaster*. Nat Genet, 2002. **31**(4): p. 419-23.
138. Raftery, L.A., et al., *Genetic screens to identify elements of the decapentaplegic signaling pathway in Drosophila*. Genetics, 1995. **139**(1): p. 241-54.
139. Sekelsky, J.J., et al., *Genetic characterization and cloning of mothers against dpp, a gene required for decapentaplegic function in Drosophila melanogaster*. Genetics, 1995. **139**(3): p. 1347-58.
140. Baker, J.C. and R.M. Harland, *A novel mesoderm inducer, Madr2, functions in the activin signal transduction pathway*. Genes Dev, 1996. **10**(15): p. 1880-9.
141. Eppert, K., et al., *MADR2 maps to 18q21 and encodes a TGFbeta-regulated MAD-related protein that is functionally mutated in colorectal carcinoma*. Cell, 1996. **86**(4): p. 543-52.
142. Graff, J.M., A. Bansal, and D.A. Melton, *Xenopus Mad proteins transduce distinct subsets of signals for the TGF beta superfamily*. Cell, 1996. **85**(4): p. 479-87.
143. Hoodless, P.A., et al., *MADR1, a MAD-related protein that functions in BMP2 signaling pathways*. Cell, 1996. **85**(4): p. 489-500.
144. Lechleider, R.J., et al., *Serine phosphorylation, chromosomal localization, and transforming growth factor-beta signal transduction by human bsp-1*. J Biol Chem, 1996. **271**(30): p. 17617-20.

145. Liu, F., et al., *A human Mad protein acting as a BMP-regulated transcriptional activator*. Nature, 1996. **381**(6583): p. 620-3.
146. Yingling, J.M., et al., *Mammalian dwarfs are phosphorylated in response to transforming growth factor beta and are implicated in control of cell growth*. Proc Natl Acad Sci U S A, 1996. **93**(17): p. 8940-4.
147. Zhang, Y., et al., *Receptor-associated Mad homologues synergize as effectors of the TGF- beta response*. Nature, 1996. **383**(6596): p. 168-72.
148. Massague, J., et al., *TGF-beta receptors and TGF-beta binding proteoglycans: recent progress in identifying their functional properties*. Ann N Y Acad Sci, 1990. **593**: p. 59-72.
149. Attisano, L. and J.L. Wrana, *Mads and Smads in TGF beta signalling*. Curr Opin Cell Biol, 1998. **10**(2): p. 188-94.
150. Massague, J., *TGF-beta signal transduction*. Annu Rev Biochem, 1998. **67**: p. 753-91.
151. Newfeld, S.J., et al., *Mothers against dpp encodes a conserved cytoplasmic protein required in DPP/TGF-beta responsive cells*. Development, 1996. **122**(7): p. 2099-108.
152. Newfeld, S.J., et al., *Mothers against dpp participates in a DDP/TGF-beta responsive serine- threonine kinase signal transduction cascade*. Development, 1997. **124**(16): p. 3167-76.
153. Wiersdorff, V., et al., *Mad acts downstream of Dpp receptors, revealing a differential requirement for dpp signaling in initiation and propagation of morphogenesis in the Drosophila eye*. Development, 1996. **122**(7): p. 2153-62.
154. Wisotzkey, R.G., et al., *Medea is a Drosophila Smad4 homolog that is differentially required to potentiate DPP responses*. Development, 1998. **125**(8): p. 1433-45.
155. Maduzia, L.L. and R.W. Padgett, *Drosophila MAD, a member of the Smad family, translocates to the nucleus upon stimulation of the dpp pathway*. Biochem Biophys Res Commun, 1997. **238**(2): p. 595-8.
156. Kim, J., et al., *Drosophila Mad binds to DNA and directly mediates activation of vestigial by Decapentaplegic*. Nature, 1997. **388**(6639): p. 304-8.
157. Xu, X., et al., *Smad proteins act in combination with synergistic and antagonistic regulators to target Dpp responses to the Drosophila mesoderm*. Genes Dev, 1998. **12**(15): p. 2354-70.
158. Kusanagi, K., et al., *Characterization of a bone morphogenetic protein-responsive Smad- binding element*. Mol Biol Cell, 2000. **11**(2): p. 555-65.
159. Das, P., et al., *Drosophila dSmad2 and Atr-I transmit activin/TGFbeta signals*. Genes Cells, 1999. **4**(2): p. 123-34.
160. Hudson, J.B., et al., *The Drosophila Medea gene is required downstream of dpp and encodes a functional homolog of human Smad4*. Development, 1998. **125**(8): p. 1407-20.
161. Das, P., et al., *The Drosophila gene Medea demonstrates the requirement for different classes of Smads in dpp signaling*. Development, 1998. **125**(8): p. 1519-28.
162. Tsuneizumi, K., et al., *Daughters against dpp modulates dpp organizing activity in Drosophila wing development*. Nature, 1997. **389**(6651): p. 627-31.
163. Inoue, H., et al., *Interplay of signal mediators of decapentaplegic (Dpp): molecular characterization of mothers against dpp, Medea, and daughters against dpp*. Mol Biol Cell, 1998. **9**(8): p. 2145-56.
164. Staehling-Hampton, K., A.S. Laughon, and F.M. Hoffmann, *A Drosophila protein related to the human zinc finger transcription factor PRDII/MBP1/HIV-EP1 is required for dpp signaling*. Development, 1995. **121**(10): p. 3393-403.
165. Arora, K., et al., *The Drosophila schnurri gene acts in the Dpp/TGF beta signaling pathway and encodes a transcription factor homologous to the human MBP family*. Cell, 1995. **81**(5): p. 781-90.
166. Grieder, N.C., et al., *Schnurri is required for Drosophila Dpp signaling and encodes a zinc finger protein similar to the mammalian transcription factor PRDII-BF1*. Cell, 1995. **81**(5): p. 791-800.
167. Matunis, E., et al., *punt and schnurri regulate a somatically derived signal that restricts proliferation of committed progenitors in the germline*. Development, 1997. **124**(21): p. 4383-91.
168. Torres-Vazquez, J., R. Warrior, and K. Arora, *schnurri is required for dpp-dependent patterning of the Drosophila wing*. Dev Biol, 2000. **227**(2): p. 388-402.
169. Dai, H., et al., *The zinc finger protein schnurri acts as a Smad partner in mediating the transcriptional response to decapentaplegic*. Dev Biol, 2000. **227**(2): p. 373-87.
170. Udagawa, Y., et al., *Schnurri interacts with Mad in a Dpp-dependent manner*. Genes Cells, 2000. **5**(5): p. 359-69.
171. Marty, T., et al., *Schnurri mediates Dpp-dependent repression of brinker transcription*. Nat Cell Biol, 2000. **2**(10): p. 745-9.
172. Grimm, S. and G.O. Pflugfelder, *Control of the gene optomotor-blind in Drosophila wing development by decapentaplegic and wingless*. Science, 1996. **271**(5255): p. 1601-4.
173. Sun, B., et al., *Ultrabithorax protein is necessary but not sufficient for full activation of decapentaplegic expression in the visceral mesoderm*. Embo J, 1995. **14**(3): p. 520-35.
174. Immergluck, K., P.A. Lawrence, and M. Bienz, *Induction across germ layers in Drosophila mediated by a genetic cascade*. Cell, 1990. **62**(2): p. 261-8.

175. Campbell, G. and A. Tomlinson, *Transducing the Dpp morphogen gradient in the wing of Drosophila: regulation of Dpp targets by brinker*. Cell, 1999. **96**(4): p. 553-62.
176. Jazwinska, A., C. Rushlow, and S. Roth, *The role of brinker in mediating the graded response to Dpp in early Drosophila embryos*. Development, 1999. **126**(15): p. 3323-34.
177. Minami, M., et al., *brinker is a target of Dpp in Drosophila that negatively regulates Dpp- dependent genes*. Nature, 1999. **398**(6724): p. 242-6.
178. Saller, E. and M. Bienz, *Direct competition between Brinker and Drosophila Mad in Dpp target gene transcription*. EMBO Rep, 2001. **2**(4): p. 298-305.
179. Zhang, H., M. Levine, and H.L. Ashe, *Brinker is a sequence-specific transcriptional repressor in the Drosophila embryo*. Genes Dev, 2001. **15**(3): p. 261-6.
180. Kirkpatrick, H., K. Johnson, and A. Laughon, *Repression of dpp targets by binding of brinker to mad sites*. J Biol Chem, 2001. **276**(21): p. 18216-22.
181. Sivasankaran, R., et al., *Direct transcriptional control of the Dpp target omb by the DNA binding protein Brinker*. Embo J, 2000. **19**(22): p. 6162-72.
182. Hasson, P., et al., *Brinker requires two corepressors for maximal and versatile repression in Dpp signalling*. Embo J, 2001. **20**(20): p. 5725-36.
183. St Johnston, R.D. and W.M. Gelbart, *Decapentaplegic transcripts are localized along the dorsal-ventral axis of the Drosophila embryo*. Embo J, 1987. **6**(9): p. 2785-91.
184. Ashe, H.L., M. Mannervik, and M. Levine, *Dpp signaling thresholds in the dorsal ectoderm of the Drosophila embryo*. Development, 2000. **127**(15): p. 3305-12.
185. von Ohlen, T. and C.Q. Doe, *Convergence of dorsal, dpp, and egfr signaling pathways subdivides the drosophila neuroectoderm into three dorsal-ventral columns*. Dev Biol, 2000. **224**(2): p. 362-72.
186. Ashe, H.L. and M. Levine, *Local inhibition and long-range enhancement of Dpp signal transduction by Sog*. Nature, 1999. **398**(6726): p. 427-31.
187. Ferguson, E.L. and K.V. Anderson, *Localized enhancement and repression of the activity of the TGF-beta family member, decapentaplegic, is necessary for dorsal-ventral pattern formation in the Drosophila embryo*. Development, 1992. **114**(3): p. 583-97.
188. Piccolo, S., et al., *Dorsoventral patterning in Xenopus: inhibition of ventral signals by direct binding of chordin to BMP-4*. Cell, 1996. **86**(4): p. 589-98.
189. Zimmerman, L.B., J.M. De Jesus-Escobar, and R.M. Harland, *The Spemann organizer signal noggin binds and inactivates bone morphogenetic protein 4*. Cell, 1996. **86**(4): p. 599-606.
190. Iemura, S., et al., *Direct binding of follistatin to a complex of bone-morphogenetic protein and its receptor inhibits ventral and epidermal cell fates in early Xenopus embryo*. Proc Natl Acad Sci U S A, 1998. **95**(16): p. 9337-42.
191. Yu, K., et al., *Processing of the Drosophila Sog protein creates a novel BMP inhibitory activity*. Development, 2000. **127**(10): p. 2143-54.
192. Bienz, M., *Endoderm induction in Drosophila: the nuclear targets of the inducing signals*. Curr Opin Genet Dev, 1997. **7**(5): p. 683-8.
193. Hoppler, S. and M. Bienz, *Two different thresholds of wingless signalling with distinct developmental consequences in the Drosophila midgut*. Embo J, 1995. **14**(20): p. 5016-26.
194. Reuter, R., et al., *Homeotic genes regulate the spatial expression of putative growth factors in the visceral mesoderm of Drosophila embryos*. Development, 1990. **110**(4): p. 1031-40.
195. Manning, G.a.K., M.A., *Development of the Drosophila tracheal system*, in *The development of Drosophila*, M.a.M.-A. Bate, A., Editor. 1993, Cold Spring Harbour Laboratory Press: Cold Spring Harbour, New York. p. 609-685.
196. Vincent, S., et al., *DPP controls tracheal cell migration along the dorsoventral body axis of the Drosophila embryo*. Development, 1997. **124**(14): p. 2741-50.
197. Affolter, M., et al., *Multiple requirements for the receptor serine/threonine kinase thick veins reveal novel functions of TGF beta homologs during Drosophila embryogenesis*. Development, 1994. **120**(11): p. 3105-17.
198. Sutherland, D., C. Samakovlis, and M.A. Krasnow, *branchless encodes a Drosophila FGF homolog that controls tracheal cell migration and the pattern of branching*. Cell, 1996. **87**(6): p. 1091-101.
199. Cohen, S.M., *Imaginal disc development*, in *The Development of Drosophila melanogaster*, M.a.M.-A. Bate, A., Editor. 1993, Cold Spring Harbour Laboratory Press: Cold Spring Harbour, New York. p. 747-841.
200. Morata, G. and P.A. Lawrence, *Control of compartment development by the engrailed gene in Drosophila*. nature, 1975. **225**(5510): p. 614-617.
201. John, A., S.T. Smith, and J.B. Jaynes, *Inserting the Ftz homeodomain into engrailed creates a dominant transcriptional repressor that specifically turns off Ftz target genes in vivo*. Development, 1995. **121**(6): p. 1801-13.
202. Lawrence, P.A. and G. Morata, *Compartments in the wing of Drosophila: a study of the engrailed gene*. developmental biology, 1976. **50**(2): p. 321-337.

203. Kornberg, T., et al., *The engrailed locus of Drosophila: in situ localization of transcripts reveals compartment-specific expression*. Cell, 1985. **40**(1): p. 45-53.
204. Zecca, M., K. Basler, and G. Struhl, *Sequential organizing activities of engrailed, hedgehog and decapentaplegic in the Drosophila wing*. Development, 1995. **121**(8): p. 2265-78.
205. Basler, K. and G. Struhl, *Compartment boundaries and the control of Drosophila limb pattern by hedgehog protein*. Nature, 1994. **368**(6468): p. 208-14.
206. Tabata, T. and T.B. Kornberg, *Hedgehog is a signaling protein with a key role in patterning Drosophila imaginal discs*. Cell, 1994. **76**(1): p. 89-102.
207. Aza-Blanc, P., et al., *Proteolysis that is inhibited by hedgehog targets Cubitus interruptus protein to the nucleus and converts it to a repressor*. Cell, 1997. **89**(7): p. 1043-53.
208. Chen, Y. and G. Struhl, *Dual roles for patched in sequestering and transducing Hedgehog*. Cell, 1996. **87**(3): p. 553-63.
209. Marigo, V., et al., *Biochemical evidence that patched is the Hedgehog receptor*. Nature, 1996. **384**(6605): p. 176-9.
210. Alcedo, J., et al., *The Drosophila smoothened gene encodes a seven-pass membrane protein, a putative receptor for the hedgehog signal*. Cell, 1996. **86**(2): p. 221-32.
211. Stone, D.M., et al., *The tumour-suppressor gene patched encodes a candidate receptor for Sonic hedgehog*. Nature, 1996. **384**(6605): p. 129-34.
212. Aza-Blanc, P. and T.B. Kornberg, *Ci: a complex transducer of the hedgehog signal*. Trends Genet, 1999. **15**(11): p. 458-62.
213. Methot, N. and K. Basler, *Hedgehog controls limb development by regulating the activities of distinct transcriptional activator and repressor forms of Cubitus interruptus*. Cell, 1999. **96**(6): p. 819-31.
214. Ohlmeyer, J.T. and D. Kalderon, *Hedgehog stimulates maturation of Cubitus interruptus into a labile transcriptional activator*. Nature, 1998. **396**(6713): p. 749-53.
215. Dominguez, M., et al., *Sending and receiving the hedgehog signal: control by the Drosophila Gli protein Cubitus interruptus*. Science, 1996. **272**(5268): p. 1621-5.
216. Kuhnlein, R.P., et al., *spalt encodes an evolutionarily conserved zinc finger protein of novel structure which provides homeotic gene function in the head and tail region of the Drosophila embryo*. Embo J, 1994. **13**(1): p. 168-79.
217. de Celis, J.F., R. Barrio, and F.C. Kafatos, *A gene complex acting downstream of dpp in Drosophila wing morphogenesis*. Nature, 1996. **381**(6581): p. 421-4.
218. Sturtevant, M.A., et al., *The spalt gene links the A/P compartment boundary to a linear adult structure in the Drosophila wing*. Development, 1997. **124**(1): p. 21-32.
219. de Celis, J.F. and R. Barrio, *Function of the spalt/spalt-related gene complex in positioning the veins in the Drosophila wing*. Mech Dev, 2000. **91**(1-2): p. 31-41.
220. De Celis, J.F., *Positioning and differentiation of veins in the Drosophila wing*. Int J Dev Biol, 1998. **42**(3): p. 335-43.
221. Affolter, M., et al., *Nuclear interpretation of Dpp signaling in Drosophila*. Embo J, 2001. **20**(13): p. 3298-305.
222. Lecuit, T. and S.M. Cohen, *Dpp receptor levels contribute to shaping the Dpp morphogen gradient in the Drosophila wing imaginal disc*. Development, 1998. **125**(24): p. 4901-7.
223. Tanimoto, H., et al., *Hedgehog creates a gradient of DPP activity in Drosophila wing imaginal discs*. Mol Cell, 2000. **5**(1): p. 59-71.
224. Funakoshi, Y., M. Minami, and T. Tabata, *mtv shapes the activity gradient of the Dpp morphogen through regulation of thickveins*. Development, 2001. **128**(1): p. 67-74.
225. Mullor, J.L., et al., *Hedgehog activity, independent of decapentaplegic, participates in wing disc patterning*. Development, 1997. **124**(6): p. 1227-37.
226. Ray, R.P. and K.A. Wharton, *Context-dependent relationships between the BMPs gbb and dpp during development of the Drosophila wing imaginal disk*. Development, 2001. **128**(20): p. 3913-25.
227. de Celis, J.F., *Expression and function of decapentaplegic and thick veins during the differentiation of the veins in the Drosophila wing*. Development, 1997. **124**(5): p. 1007-18.
228. Conley, C.A., et al., *Crossveinless 2 contains cysteine-rich domains and is required for high levels of BMP-like activity during the formation of the cross veins in Drosophila*. Development, 2000. **127**(18): p. 3947-59.
229. Ishisaki, A., et al., *Differential inhibition of Smad6 and Smad7 on bone morphogenetic protein- and activin-mediated growth arrest and apoptosis in B cells*. JBC, 1999. **274**: p. 13637-13642.
230. Laemmli, U.K., *Cleavage of structural proteins during the assembly of the head of bacteriophage T4*. nature, 1970. **227**: p. 680-685.
231. Santamaria, *Injecting Eggs, in Drosophila. A practical approach*, D. Roberts, Editor. 1986, IRL press: Oxford. p. 159-173.
232. Spradling, *P-element mediated transformation, in Drosophila. A practical approach*, D. Roberts, Editor. 1986, IRL press: Oxford. p. 175-198.

233. Rio, D.C. and G.M. Rubin, *Transformation of cultured Drosophila melanogaster cells with a dominant selectable marker*. Mol Cell Biol, 1985. **5**(8): p. 1833-8.
234. Ruppert, R., E. Hoffmann, and W. Sebald, *Human bone morphogenetic protein 2 contains a heparin-binding site which modifies its biological activity*. Eur J Biochem, 1996. **237**(1): p. 295-302.
235. Roth, M., *Die Rolle der Decapentaplegic-Proteoglykanbindungsdomänen in der Morphogenese von Drosophila melanogaster*, in *Diplomarbeit*. 1998, Physiological Chemistry II: Würzburg.
236. Altnauer, F., *Klonierung, Expression und erstmalige Aufreinigung von biologisch aktivem DPP - einem Mitglied der TGF- β Superfamilie*, in *Schriftliche Hausarbeit für erste Lehramtsstaatsprüfung*. 1997, Physiological Chemistry II: Würzburg.
237. Groppe, J., et al., *Biochemical and biophysical characterization of refolded Drosophila DPP, a homolog of bone morphogenetic proteins 2 and 4*. J Biol Chem, 1998. **273**(44): p. 29052-65.
238. Kirsch, T., J. Nickel, and W. Sebald, *BMP-2 antagonists emerge from alterations in the low-affinity binding epitope for receptor BMPR-II*. Embo J, 2000. **19**(13): p. 3314-24.
239. Nickel, J., et al., *The crystal structure of the BMP-2:BMPR-IA complex and the generation of BMP-2 antagonists*. J Bone Joint Surg Am, 2001. **83-A**(Suppl 1(Pt 1)): p. S7-14.
240. Ahrens, P.B., M. Solursh, and R.S. Reiter, *Stage-related capacity for limb chondrogenesis in cell culture*. developmental biology, 1977. **60**(1): p. 69-82.
241. Lennon, D.P., et al., *Isolation and characterization of chondrocytes and non-chondrocytes from high-density chick limb bud cell cultures*. journal of Craniofacial Genetics and Developmental Biology, 1983. **3**(3): p. 235-251.
242. Carrington, J.L. and A.H. Reddi, *Temporal changes in the response of chick limb bud mesodermal cells to transforming growth factor beta-type 1*. Exp Cell Res, 1990. **186**(2): p. 368-73.
243. Lecuit, T. and S.M. Cohen, *Proximal-distal axis formation in the Drosophila leg*. Nature, 1997. **388**(6638): p. 139-45.
244. Hazelett, D.J., et al., *decapentaplegic and wingless are regulated by eyes absent and eyegone and interact to direct the pattern of retinal differentiation in the eye disc*. Development, 1998. **125**(18): p. 3741-51.
245. Entchev, E.V., A. Schwabedissen, and M. Gonzalez-Gaitan, *Gradient formation of the TGF-beta homolog Dpp*. Cell, 2000. **103**(6): p. 981-91.
246. Teleman, A.A. and S.M. Cohen, *Dpp gradient formation in the Drosophila wing imaginal disc*. Cell, 2000. **103**(6): p. 971-80.
247. Bryant, P.J., *Localized cell death caused by mutations in a Drosophila gene coding for a transforming growth factor-beta homolog*. Dev Biol, 1988. **128**(2): p. 386-95.
248. Padgett, R.W., J.M. Wozney, and W.M. Gelbart, *Human BMP sequences can confer normal dorsal-ventral patterning in the Drosophila embryo*. Proc Natl Acad Sci U S A, 1993. **90**(7): p. 2905-9.
249. Holley, S.A., et al., *A conserved system for dorsal-ventral patterning in insects and vertebrates involving sog and chordin*. Nature, 1995. **376**(6537): p. 249-53.
250. Katagiri, T., et al., *The non-osteogenic mouse pluripotent cell line, C3H10T1/2, is induced to differentiate into osteoblastic cells by recombinant human bone morphogenetic protein-2*. Biochem Biophys Res Commun, 1990. **172**(1): p. 295-9.
251. Knaus, P. and W. Sebald, *Cooperativity of binding epitopes and receptor chains in the BMP/TGFbeta superfamily*. Biol Chem, 2001. **382**(8): p. 1189-95.
252. Wittstadt, E., *Untersuchungen zur Liganden-Rezeptor-Interaktion von DPP in verschiedenen Modellsystemen*, in *Diplomarbeit*. 2001, Physiological Chemistry II: Würzburg.
253. Jonk, L.J., et al., *Identification and functional characterization of a Smad binding element (SBE) in the JunB promoter that acts as a transforming growth factor-beta, activin, and bone morphogenetic protein-inducible enhancer*. J Biol Chem, 1998. **273**(33): p. 21145-52.
254. Brand, A.H. and N. Perrimon, *Targeted gene expression as a means of altering cell fates and generating dominant phenotypes*. Development, 1993. **118**(2): p. 401-15.
255. Bier, E., et al., *Searching for pattern and mutation in the Drosophila genome with a P- lacZ vector*. Genes Dev, 1989. **3**(9): p. 1273-87.
256. Ohkawara, B., et al., *Action range of BMP is defined by its N-terminal basic amino acid core*. Curr Biol, 2002. **12**(3): p. 205-9.
257. Meagher, J.L., et al., *Role of arginine 132 and lysine 133 in heparin binding to and activation of antithrombin*. J Biol Chem, 1996. **271**(46): p. 29353-8.
258. Aoyama, H., et al., *Isolation and conformational analysis of fragment peptide corresponding to the heparin-binding site of hepatocyte growth factor*. Biochemistry, 1997. **36**(33): p. 10286-91.
259. Burke, R. and K. Basler, *Dpp receptors are autonomously required for cell proliferation in the entire developing Drosophila wing*. Development, 1996. **122**(7): p. 2261-9.
260. Terracol, R. and J.A. Lengyel, *The thick veins gene of Drosophila is required for dorsoventral polarity of the embryo*. Genetics, 1994. **138**(1): p. 165-78.

261. ten Dijke, P., K. Miyazono, and C.H. Heldin, *Signaling via hetero-oligomeric complexes of type I and type II serine/threonine kinase receptors*. Curr Opin Cell Biol, 1996. **8**(2): p. 139-45.
262. Carrington, J.L., et al., *Osteogenin (bone morphogenetic protein-3) stimulates cartilage formation by chick limb bud cells in vitro*. Dev Biol, 1991. **146**(2): p. 406-15.
263. Chen, P., et al., *Chick limb bud mesodermal cell chondrogenesis: inhibition by isoforms of platelet-derived growth factor and reversal by recombinant bone morphogenetic protein*. Exp Cell Res, 1992. **200**(1): p. 110-7.
264. Chen, P., Y.M. Yu, and A.H. Reddi, *Chondrogenesis in chick limb bud mesodermal cells: reciprocal modulation by activin and inhibin*. Exp Cell Res, 1993. **206**(1): p. 119-27.
265. Roark, E.F. and K. Greer, *Transforming growth factor-beta and bone morphogenetic protein-2 act by distinct mechanisms to promote chick limb cartilage differentiation in vitro*. Dev Dyn, 1994. **200**(2): p. 103-16.
266. Staehling-Hampton, K., et al., *Specificity of bone morphogenetic protein-related factors: cell fate and gene expression changes in Drosophila embryos induced by decapentaplegic but not 60A*. Cell Growth Differ, 1994. **5**(6): p. 585-93.
267. Chihara, T. and S. Hayashi, *Control of tracheal tubulogenesis by Wingless signaling*. Development, 2000. **127**(20): p. 4433-42.
268. Lin, X. and N. Perrimon, *Dally cooperates with Drosophila Frizzled 2 to transduce Wingless signalling*. Nature, 1999. **400**(6741): p. 281-4.
269. Eldar, A., et al., *Robustness of the BMP morphogen gradient in Drosophila embryonic patterning*. Nature, 2002. **419**(6904): p. 304-8.
270. Wolpert, L., *Positional information revisited*. Development, 1989. **107**(Suppl): p. 3-12.
271. Driever, W. and C. Nusslein-Volhard, *A gradient of bicoid protein in Drosophila embryos*. Cell, 1988. **54**(1): p. 83-93.
272. Zecca, M., K. Basler, and G. Struhl, *Direct and long-range action of a wingless morphogen gradient*. Cell, 1996. **87**(5): p. 833-44.
273. Struhl, G., D.A. Barbash, and P.A. Lawrence, *Hedgehog acts by distinct gradient and signal relay mechanisms to organise cell type and cell polarity in the Drosophila abdomen*. Development, 1997. **124**(11): p. 2155-65.
274. McDowell, N. and J.B. Gurdon, *Activin as a morphogen in Xenopus mesoderm induction*. Semin Cell Dev Biol, 1999. **10**(3): p. 311-7.
275. Green, J.B., H.V. New, and J.C. Smith, *Responses of embryonic Xenopus cells to activin and FGF are separated by multiple dose thresholds and correspond to distinct axes of the mesoderm*. Cell, 1992. **71**(5): p. 731-9.
276. Green, J.B. and J.C. Smith, *Graded changes in dose of a Xenopus activin A homologue elicit stepwise transitions in embryonic cell fate*. Nature, 1990. **347**(6291): p. 391-4.
277. Gurdon, J.B., et al., *Activin signalling and response to a morphogen gradient*. Nature, 1994. **371**(6497): p. 487-92.
278. Gurdon, J.B., A. Mitchell, and D. Mahony, *Direct and continuous assessment by cells of their position in a morphogen gradient*. Nature, 1995. **376**(6540): p. 520-1.
279. Dyson, S. and J.B. Gurdon, *The interpretation of position in a morphogen gradient as revealed by occupancy of activin receptors*. Cell, 1998. **93**(4): p. 557-68.
280. Shimizu, K. and J.B. Gurdon, *A quantitative analysis of signal transduction from activin receptor to nucleus and its relevance to morphogen gradient interpretation*. Proc Natl Acad Sci U S A, 1999. **96**(12): p. 6791-6.
281. Dorfman, R. and B.Z. Shilo, *Biphasic activation of the BMP pathway patterns the Drosophila embryonic dorsal region*. Development, 2001. **128**(6): p. 965-72.
282. Decotto, E. and E.L. Ferguson, *A positive role for Short gastrulation in modulating BMP signaling during dorsoventral patterning in the Drosophila embryo*. Development, 2001. **128**(19): p. 3831-41.
283. Henderson, K.D. and D.J. Andrew, *Identification of a novel Drosophila SMAD on the X chromosome*. Biochem Biophys Res Commun, 1998. **252**(1): p. 195-201.

6 Summary

In the last years it became evident that many cytokines do not only bind to their specific cell surface receptors but also interact with components of the extracellular matrix. Mainly in *Drosophila*, several enzymes were identified, that are involved in glycosaminoglycan synthesis. Mutations in these enzymes mostly result in disturbances of several signaling pathways like hedgehog, wingless, FGF or dpp. In most cases it was, due to these pleiotropic effects, not possible to examine the relevance of matrix interactions for single pathways.

The aim of this work was to examine the relevance of matrix interactions for the TGF- β superfamily member DPP. Based on the fact that DPP is highly homologous to human BMP-2, the basic N-terminus of mature DPP was mutated, which has been shown to contain a heparin-binding site in BMP-2. Thus, a wildtype variant (D-MYC), a deletion variant (D-DEL), which lacked the whole basic part of the N-terminus and a duplication variant (D-DUP), which contained a second copy of the basic core motif, were generated.

In order to characterise the variants biochemically, they were expressed in *E.coli* and refolded in a bioactive form. In chicken limb bud assay, the deletion variant was much more active than the wildtype variant, comparable to data of BMP-2. By means of biacore measurements with the immobilised ectodomain of the high affinity type I receptor thick veins, it could be demonstrated, that the variants differ only in matrix binding and not in their receptor affinity. Different matrix binding was shown by Heparin FPLC.

The biological relevance of the matrix interaction of DPP was examined in transgenic flies. To allow expression of the different variants under the control of various Gal4 driver lines, they were cloned behind an UAS-promoter site.

In early tracheal development, a strong dependence of DPP signaling on matrix binding was observed. While ectopic expression of the deletion variant caused only minor defects, the branching pattern was strongly disturbed by overexpression of wildtype and duplication variant.

Ubiquitous expression of the variants in the wing imaginal disc caused overproliferation of the disc and expansion of the omb target gene expression. The extent of phenotypes correlated with the matrix binding ability of the variants. Corresponding disturbances of the wing vein pattern was observed in adult flies.

By the crossing of different dpp alleles, transheterozygous animals were created, that lack dpp only in imaginal discs. Expression of the variants under the control of a suitable dpp-Gal4 driver line revealed insights into the biological relevance of matrix binding on DPP gradient formation and specific target gene activation in wing imaginal discs. It was shown, that all variants were able to generate a functional DPP gradient with correct expression of the target genes omb and spalt. Again a correlation between extent of target gene domains and matrix binding ability of the corresponding variants was found.

Thus by mutating the N-terminus of DPP, it could be shown that this is responsible for DPP's matrix interaction. Also the relevance of matrix binding of DPP in different tissues was examined. It turned out, that the reorganisation of tracheal branching by DPP strongly depends on matrix interactions whereas the establishing of a gradient in wing imaginal discs depends only gradually on matrix interactions.

Based on these data a model for the action of DPP/TGF β s as morphogens was established. While a deletion of matrix binding leads to a decrease in specific bioactivity of the cytokine, the latter is increased by additional matrix binding sites.

6 Zusammenfassung

In den letzten Jahren wurde deutlich, daß viele Zytokine nicht nur mit ihren spezifischen Zelloberflächen-Rezeptoren interagieren, sondern auch Affinität zu Komponenten der Extrazellulären Matrix zeigen. Vor allem in *Drosophila* konnten viele Enzyme zur Synthese von Glukosaminoglykanen identifiziert werden. Mutationen in diesen Enzymen führen in der Regel zu Störungen verschiedener Signalwege, wie z.B. hedgehog, wingless, FGF oder dpp. Aufgrund dieser pleiotropen Effekte, war es meist nicht möglich, die Bedeutung der Matrix-Interaktionen für bestimmte Zytokine zu untersuchen.

In dieser Arbeit sollte die Bedeutung der Matrix-Interaktion für das TGF- β -Superfamilienmitglied DPP untersucht werden. Ausgehend von der hohen Homologie zwischen humanem BMP-2 und DPP wurde der basische N-Terminus von DPP, der im BMP-2 für die Heparininteraktion verantwortlich ist, verändert. Es wurde neben einer Wildtypvariante (D-MYC) eine Deletionsvariante (D-DEL) generiert, die keine basischen Aminosäuren im N-Terminus aufweist, sowie eine Duplikationsvariante (D-DUP), die eine zweite Kopie des basischen Hauptmotivs im N-Terminus enthält.

Zur biochemischen Charakterisierung wurden die Varianten sowie wildtypisches DPP in *E. coli* exprimiert und in eine bioaktive Form zurückgefaltet. Im Limb-Test zeigte sich vergleichbar zum BMP-2 eine stark erhöhte Aktivität der Deletionsvariante gegenüber Wildtyp-DPP. Durch Biacore-Messungen an der immobilisierten Ektodomäne des hochaffinen DPP TypI-Rezeptors Thick veins konnte gezeigt werden, daß alle Varianten gleiche Rezeptoraffinität haben und sich nur in der Matrixbindung unterscheiden. Letzteres wurde durch eine analytische FPLC mit Heparin als Matrix gezeigt.

Die biologische Relevanz der Matrixbindung wurde in transgenen Fliegen untersucht. Hierbei wurden die DPP-Varianten hinter einen UAS-Promoter kloniert, um jene unter der Kontrolle verschiedener Gal4-Treiberlinien exprimieren zu können.

In der frühen Tracheenentwicklung zeigte sich eine sehr starke Matrix-Abhängigkeit der DPP-Wirkung.

Während ektopische Expression der Deletionsvariante fast keine Störung der Zellmigration verursachte, war das Muster der Tracheenäste bei ektopischer Expression von D-MYC als auch D-DUP massiv gestört.

Ubiquitäre Expression der Varianten in der Flügelimaginalscheibe verursachte Überproliferation und eine Ausdehnung der Expressionsdomäne des omb-Genes. Die Stärke der Phänotypen korrelierte dabei mit der Matrixbindung der Varianten. Entsprechende Störungen des Venenmusters konnten in Flügeln adulter Tiere festgestellt werden.

Durch Kreuzung zweier dpp-Allele konnten transheterozygote Fliegen gewonnen werden, die keine dpp-Expression in den Imaginalscheiben zeigen. Die Expression der Varianten unter Kontrolle eines geeigneten dpp-Gal4-Treibers in diesen Fliegen gab Aufschluß über die tatsächliche Relevanz der DPP-Matrix-Interaktion für die Ausbildung eines DPP-Gradienten und spezifische Aktivierung verschiedener Targetgene in der Flügelscheibe. Es wurde gezeigt, daß alle Varianten dazu in der Lage sind, einen DPP-Gradienten mit entsprechender Expression der Targetgene omb und spalt zu erzeugen. Wieder wurde eine Korrelation zwischen Ausdehnung der Targetgen-Domänen und der Matrixbindung der Varianten beobachtet.

Somit konnte durch Mutation des N-Terminus des DPP-Proteins gezeigt werden, daß dieser für die Matrixinteraktion von DPP verantwortlich ist. Auch wurde Aufschluß über die Bedeutung der Matrixinteraktion an verschiedenen DPP-Wirkungsorten gewonnen. Die Abhängigkeit des DPP-Signals von der Matrixbindung differiert zwischen verschiedenen Gewebetypen. Während die Wirkung von DPP in der Restrukturierung der trachealen Migration sehr stark von einer Matrixbindung abhängt, sieht man bei der Proliferation und Musterbildung in der Imaginalscheibe nur graduelle Effekte.

Diese Daten führten zur Etablierung eines Modells für den Wirkungsmechanismus von DPP/TGF β Molekülen als morphogene Faktoren. Während eine Deletion von Matrixbindung zu einem Verlust der spezifischen biologischen Aktivität führt, wird durch zusätzliche Matrixbindung eine erhöhte Aktivität erreicht.

7 Abbreviations

A	anterior
Aa	aminoacid
AP	anterior-posterior
β -Gal	β -galactosidase
BSA	bovine serum albumine
BMP	bone morphogenetic protein
CHAPS	3-[(3-Cholamidopropyl)-dimethylammonio]-1-propansulfonate
CLSM	confocal laser scanning microscopy
CM	carboxymethyl
D. melanogaster	Drosophila melanogaster
Dad	daughters against dpp
DMSO	dimethylsulfoxide
Dpp	decapentaplegic
DV	dorsal-ventral
E.coli	Escherichia coli
en	engrailed
ER	endoplasmatic reticulum
FBS	fetal bovine serum
FPLC	fast protein liquid chromatography
GAG	glucosaminoglycans
Gbb	glass bottom boat
GuCl	guanidine hydrochloride
H ₂ O	water
HBS	hepes buffered saline
Hh	hedgehog
HPLC	high pressure liquid chromatography
hs	heat shock
HS	heparan sulfate
HSPG	heparan sulfate proteoglycans
IPTG	isopropyl- β -thiogalactopyranoside
Mad	mothers against dpp
Medea	maternal enhancer of decapentaplegic
M	molar
mM	milimolar
nM	nanomolar
mtv	masters of thick veins
MTT	thiazolyl blue
MV	molecular weight
NaCl	sodium chloride
NaOAc	sodium acetate
Omb	optomotor blind
P	posterior
PAGE	polyacrylamide gel electrophoresis
PBS	phosphate buffered saline
PBT	PBS + Tris
PCR	polymerase chain reaction
PLP	periodate-lysin-phosphate
ptc	patched
Put	punt
rpm	rounds per minute
RT	room temperature
sal	spalt
Sax	saxophone
Scw	screw
SDS	sodium dodecylsulfate
Smo	smoothened
SOG	short gastrulation
TGF β	transforming growth factor β
TMAE	tri-methyl-amino-ethane

Tkv	thick veins
Tld	tolloid
Tris	Tris-(hydroxymethyl)-aminomethane
Tsg	twisted gastrulation
Wg	wingless

8 Appendix

A Constructs list

vector name	backbone	cloning sites	culture number	derived from	used for
pcDNA1		--	143	invitrogen	cloning
pcDNA3		--	(220)	invitrogen	cloning
pUAST		--	272	N.Perrimon	cloning
pET-3d		--	148	invitrogen	cloning
pMT/V5		--	264	invitrogen	cloning
pMT/BiP/V5		--	382	invitrogen	cloning
pAc5.1		--	370	invitrogen	cloning
pAcGP67/HT	pAcGP	--	386	J.Nickel	cloning
pGL2-basic		--	283	promega	cloning
pcDNA1-dppmyc	pcDNA1	BamHI, EcoRI	111	M.Roth	subcloning
pcDNA3-dpp	pcDNA3	BamHI, EcoRI	262	M.Roth	subcloning
pcDNA3-d-myc	pcDNA3	NotI, XbaI	234, 271	M.Roth	subcloning
pcDNA3-d-del	pcDNA3	NotI, XbaI	305	M.Roth	subcloning
pcDNA3-d-dup	pcDNA3	NotI, XbaI	342	M.Roth	subcloning
pUAST-d-myc	pUAST	NotI	298	M.Roth	germline transform.
pUAST-d-del	pUAST	NotI	300	M.Roth	germline transform.
pUAST-d-dup	pUAST	NotI	349	M.Roth	germline transform.
pUAST-d-comp43	pUAST	NotI	430	M.Roth	germline transform.
pUAST-d-comp44	pUAST	NotI	428	M.Roth	germline transform.
pMT-V5-d-myc	pMT/V5	KpnI, NotI	277	M.Roth	S2 expression
pMT-BiP-V5-d-myc	pMT/BiP/V5	BglII, NotI	276,340	M.Roth	S2 expression
pMT-Kosak-V5-d-myc	pMT/V5	KpnI, NotI	344	M.Roth	S2 expression
pET-3d-dpp	pET-3d	NcoI, BamHI	82, 12	F. Altnauer	E.coli expression
pET-3d-d-myc	pET-3d	NcoI, BamHI	377	M.Roth	E.coli expression
pET-3d-d-del	pET-3d	NcoI, BamHI	99	M.Roth	E.coli expression
pET-3d-d-dup	pET-3d	NcoI, BamHI	362	M.Roth	E.coli expression
pcDNA3-tkv	pcDNA3	NotI, XhoI	257	M.Roth	cell culture
pcDNA3-tkvHA	pcDNA3	NotI, XhoI	242	M.Roth	cell culture
pcDNA3-sax	pcDNA3	EcoRI, XhoI	252	M.Roth	cell culture
pcDNA3-saxHA	pcDNA3	EcoRI, XhoI	258	M.Roth	cell culture
pcDNA3-saxFLAG	pcDNA3	EcoRI, XhoI	503	M.Roth	cell culture
pcDNA3-put	pcDNA3	NotI, XhoI	251	M.Roth	cell culture
pcDNA3-putMYC	pcDNA3	NotI, XhoI	259	M.Roth	cell culture
pcDNA3-tkvQD-HA	pcDNA3	NotI, XhoI	441	M.Roth	cell culture
pcDNA3-saxQD-HA	pcDNA3	EcoRI, XhoI	501	M.Roth	cell culture
pcDNA3-mad	pcDNA3	BamHI, XhoI	330	M.Roth	cell culture
pcDNA3-medea	pcDNA3	XhoI, XbaI	331	M.Roth	cell culture
pMT-V5-tkv	pMT/V5	NotI, XhoI	336	M.Roth	cell culture
pMT-V5-tkvHA	pMT/V5	NotI, XhoI	315	M.Roth	cell culture
pMT-V5-sax	pMT/V5	EcoRI, XhoI	335	M.Roth	cell culture
pMT-V5-saxHA	pMT/V5	EcoRI, XhoI	314	M.Roth	cell culture
pMT-V5-put	pMT/V5	NotI, XhoI	337	M.Roth	cell culture
pMT-V5-putMYC	pMT/V5	NotI, XhoI	316	M.Roth	cell culture
pMT-V5-tkvQD-HA	pMT/V5	NotI, XhoI	442	M.Roth	cell culture

pAc5.1-tkv	pAc5.1	NotI, XhoI	400	M.Roth	cell culture
pAc5.1-tkvHA	pAc5.1	NotI, XhoI	493	M.Roth	cell culture
pAc5.1-saxHA	pAc5.1	EcoRI, XhoI	401	M.Roth	cell culture
pAc5.1-putMYC	pAc5.1	NotI, XhoI	402	M.Roth	cell culture
pAc5.1-tkvQD-HA	pAc5.1	NotI, XhoI	443	M.Roth	cell culture
pHT-tkvEX	pAcGP	BamHI	410	M.Roth	SF9 expression
pHT-saxEX	pAcGP	BamHI	502	M.Roth	SF9 expression
pHT-putEX	pAcGP	BamHI	524	M.Roth	SF9 expression
pMT-BiP-tkvEX	pAcGP	BglII, KpnI	531	M.Roth	S2 expression
pSBE	pGL2-basic	XhoI, BglII, HindIII	189		luc reporter
pGL2-12xCGGC-luc	pGL2-basic	XhoI, BglII, HindIII	486		luc reporter
pGL2-mad-12	pGL2-basic	XhoI, BglII, HindIII	508	M.Roth	luc reporter
pGL2-mad-34	pGL2-basic	XhoI, BglII, HindIII	509	M.Roth	luc reporter
pGL2-mad-45	pGL2-basic	XhoI, BglII, HindIII	530	M.Roth	luc reporter
pcDNA3-lacZ	pcDNA3	--	243, 341	invitrogen	cell culture
pMT-V5-lacZ	pMT/V5	--	263	invitrogen	cell culture
pAc5.1-lacZ	pAc5.1	--	368	invitrogen	cell culture
pCo-hygro	pCo	--	261	invitrogen	selection
pUFWT				O'Kane	cloning
pUFWT-CD2	pUFWT	SphI	174	M.Roth	subcloning
pUFWT-CD2-dmyc	pUFWT	NotI	186	M.Roth	germline transform.
pUFWT-CD2-dmyc1	pUFWT	NotI	1-01	M.Roth	germline transform.
pUFWT-CD2-dmyc2	pUFWT	NotI	256	M.Roth	germline transform.
pUFWT-CD2-dmyc3	pUFWT	NotI	187	M.Roth	germline transform.
pUFWT-CD2-dmyc4	pUFWT	NotI	1-02	M.Roth	germline transform.
pUFWT-CD2-dmyc5	pUFWT	NotI	1-03	M.Roth	germline transform.
pUFWT-CD2-dmyc6	pUFWT	NotI	1-04	M.Roth	germline transform.

B Primer list

Primer name	Sequence	Purpose	Source
T7	AATACGACTCACTATAGG	vector sequencing	Interaktiva
SP-6	ATTTAGGTGACACTATAG	vector sequencing	Interaktiva
T3	AATTAACCCTCACTAAAGGG	vector sequencing	Interaktiva
BGH-revers	TAGAAGGCACAGTCGAGG	vector sequencing	Interaktiva
MT-forward	CATCTCAGTGCAACTAAA	vector sequencing	MWG
pACGP-down	GCAAGATGGTAAGCGCTA	vector sequencing	MWG
pACGP-up	GGATCATTATGCTCCGTG	vector sequencing	MWG
pGL-M6	CCGGGAGGTACCGAG	vector sequencing	Interaktiva
pGL-M7	TTTTTGCGTCTTCC	vector sequencing	Interaktiva
DM-1	GCTACCATGGCCCCAGGAGAGCAGAAGCTTATCTCTGAGGAGGACCTGGGAGGAG GAGCGAGACGGCTACGAGGCGCAAGAAC	variant D-DEL1	Interaktiva
DM-2	GCTACCATGGCCCCAGGAGAGCAGAAGCTTATCTCTGAGGAGGACCTGGGAGGAG	variant D-DEL	Interaktiva

	GAAACCACGACGACACCTGCCGGCGGCAC		
DM-4	GGAGAGCAGAAGCTTATCTCTGAGGAGGACCTGGGCGGTGGCAAGGGCGGCCGGAACAAG	MYC-epitope (DPP) 5'	Interaktiva
DM-5	GAATTGGAATTCGAATCTATCGACAGCCACAGCCCACCACGG	EcoRI-site 3'-DPP	Interaktiva
DM-6	ACACAAAGATAGTAAATCGA	reverse primer to DM-5	Interaktiva
DM-7	CAGGTCCTCCTCAGAGATAAGCTTCTGCTCTCCCTCTCCGCCAGACACGTCCCGAATGGA	MYC-epitope (DPP) 3'	Interaktiva
DM-8	GGATCCGGATCCATGCGCGCATGGCTTCTACTCCTC	BamHI-site 5'-DPP	Interaktiva
DM-9	CGATGGCTTTTATCACTATCA	reverse primer to DM-8	Interaktiva
DM-10	ATGAAGCGACCGCCCA	NotI-deletion 5' dpp	Interaktiva
DM-11	TGGGCGGTGCTTCAT	NotI-deletion 3' dpp	Interaktiva
DM-12	ATTCACATGCGGCCGCACGCGTGGATCCATGCGCGCATGGCTTCTACTC	NotI/MluI-sites 5' dpp	Interaktiva
DM-13	GCTACCATGGCCCCAGGAGAGCAGAAGCTTATCTCTGAGGAGGACCTGGGAGGAGGATGCGCGGCGCGTCTGCTGACGTGGACTTCTCGGACGTG	variant D-DEL4	Interaktiva
DM-14	TCTCTCTCCGGACACGTCCCGAA	Kpn2I-site 3'	Interaktiva
DM-15	TTCGGGACGTGTCCGGAGGAGAG	Kpn2I-site 5'	Interaktiva
DM-16	GCTACCATGGCCCCAGACGTGTCCGGAGGCGGCAAG	pET-3d-D-MYC 5'	Interaktiva
DM-17	CCGGAGGCGGCAAGCGGCAGCCGAGACGGCCTACGAGGCGCAAGT	D-DUP cassette 5'	Interaktiva
DM-18	CCGGACTTGCGCGTGGTAGGCCGTCTCGGCTGCCGCTTGCCGCCT	D-DUP cassette 3'	Interaktiva
DM-19	TGACTAGAATTCCTACACGTACAGCGAGTGCCGCCG	competition peptide 5'	ROTH
DM-20	AATATGCATCGTAGCCAGA	sequencing	Interaktiva
DM-21	AGCACAAGCAGCCGCTCCTGT	sequencing	Interaktiva
DM-22	CAAAAGCATTTAATCCATTC	sequencing	Interaktiva
DM-23	CCATCGCAGCCACCAGCAA	sequencing	Interaktiva
DM-24	TGATCTCGGCGTAGAGCTTC	sequencing	Interaktiva
DM-25	GCTACCATGGCCCCAGGAGAGCAGAAGCTTATCTCTGAGGAGGACCTGGGAGGAGGAAACGAGGCGCAAGAACCACGACGACACCTGCCG	variant D-DEL2	Interaktiva
DM-26	CGCGCCTTGTGCCGCCCGTC	sequencing	Interaktiva
DM-27	GTCTTTGGTACCAGATCTACCGAGGATATATCCAGAGA	pMT-BiP-DPP 5'	Interaktiva
DM-28	TACTCTGGTACCATGGCACGCGCATGGCTTCTACTCCTCGCA	pMT-BiP-DPP 5' (Kosak)	Interaktiva
DM-29	GCTACCATGGCCCCAGACGTGTCCGGAGGCGGCAAG	pET-3d-D-DUP 5' (V2)	Interaktiva
DM-30	CAAGGATCCTATCGACAGCCACAGCCCACC	sequencing pET-3d 3'	Interaktiva
DM-31	GGCGGCCGGAACGGAGGGCAGCCGGGAGGGCTACGGGAGGCAAGAACCACCGAC	variant D-del 5'	Interaktiva
DM-32	GTCGTGGTTCTTGCCCTCCCGTAGGCCCTCCCGGCTGCCCTCCGTTCCGGCCGCC	variant D-del 3'	Interaktiva
DM-33	GGCGGTGGCAAGGGCGGCGGGAACGGAGGGCAGCCGGGAGGGCCTACGGGAGGCGGCAACCACGACGACACCTGC	variant D-del 5'	Interaktiva
DM-34	GCAGGTGTCGTGCTGGTTGCCGCCTCCCGTAGGCCCTCCCGGCTGCCCTCCGTTCCGCCGCCCTTGCCACCGCC	variant D-del 3'	Interaktiva
DM-35	GCTACCATGGCCCCAGACGTGTCCGGAGGAGAGGGCGGT	pET-3d-D-MYC 5'	Interaktiva
DM-36	GTCACCATGGCCCCAGACGTGTCTGGCGGAGAGGGA	pET-3d-D-MYC 5'	Interaktiva
DM-37	CACGACGACACGTGCCGGCGGCACTCG	Eco72I in dpp 5'	MWG
DM-38	CGAGTGCCGCCGGCACGTGTGCTGCTG	Eco72I in dpp 3'	MWG
DM-39	CTAAGGAGATCTGACGTGTCTGGCGGAGAGGGC	peptide 5'	MWG
DM-40	CCGGAGGAGAAGGCGGTGGCAAGGGCGGCGGAAACGGCGGACAGCCGGGCGGCCCCACGGGAGGCGGTAAACCACGACGACAC	D-del insert 5'	MWG
DM-41	GTGTCGTGCTGGTTACCGCCTCCCGTAGGGCCGCCGGCTGTCCGCCGTTTCCGC	D-del insert 3'	MWG

	CGCCCTTGCCACCGCCCTCTCCT		
DM-42	TCAACCCTCGAGGATCTCAATATGAAGTTATGC	DPP-pMT-BiP	MWG
DM-43	TCAAGGGAATTCCTACACGTACAGCGAGTGCCGCCGGCA	short peptide 3'	MWG
DM-44	TCAAGGGAATTCCTAGGTGTCGTCGTGGTTCTT	long peptide 3'	MWG
tkv-1	TACAACCTCGGAACCTG	reverse primer to tkv-2	MWG
tkv-2	TCACATCTCGAGTTAGGCGTAGTCTGGGACGTCGTATGGGTAGACAATCTTAATG GGCACATC	TKV-HA 3'	MWG
tkv-3	ATGGAAATGGGATCT	sequencing	Interaktiva
tkv-4	TTTACGATGAGACGA	sequencing	Interaktiva
tkv-5	TTATGTTTCACCTAC	sequencing	Interaktiva
tkv-6	CAATATCTTGGGCTT	sequencing	Interaktiva
tkv-7	ATCTCTGGATCCGAATTCAGTGCGAATGTTTCAG	ectodomain 5'	MWG
tkv-8	ATCTCTGGATTCCGTGTGTAGGGACTCGCTGCT	ectodomain 3'	MWG
tkv-9	AATGCCAAGGATATTCAGATG	tkvQD 5'	Interaktiva
tkv-10	CATCTGAATATCCTTGGCAAT	tkvQD 3'	Interaktiva
tkv-11	CTGCATGGCAAGAACATT	sequencing	MWG
tkv-12	AACTCAATGTGCAACTCA	sequencing	MWG
tkv-13	TAATATAGATCTGAATTCAGTGCGAATGTTTCAG	ectodomain 5' pMT-BiP	Interaktiva
tkv-14	TATTATGGTACCTTAGTGATGGTGATGGTGATGGCTTCCCGTGTGTAGGGACTCG CTGCT	ectodomain 3' pMT-BiP	Interaktiva
sax-1	AAAGTGGGCACCAAG	reverse primer to sax-2	MWG
sax-2	TCATAACTCGAGCTAGGCGTAGTCTGGGACGTCGTATGGGTAAACGCAGACCTCG TCGAAGTC	SAX-HA 3'	MWG
sax-3	GTGCTGGAATTCGGCACGATGGAGTCCAAT	ATG-5'	Interaktiva
sax-4	TGACTCCTGCACCTG	reverse primer to sax-3	Interaktiva
sax-5	CACACGCGATGCCGA	sequencing	Interaktiva
sax-6	TGACCATCTTCTTCA	sequencing	Interaktiva
sax-7	TCAGTCGCGACGAGG	sequencing	Interaktiva
sax-8	AGTCAAAGAATATAC	sequencing	Interaktiva
sax-9	CTAGCCAAAGATGTCAACCTG	saxQD 5'	Interaktiva
sax-10	CAGGGTGACATGTTTGGCTAG	saxQD 3'	Interaktiva
sax-11	CCTTGTAATCCTCTGCTA	sequencing	MWG
sax-12	GCAAGCCAAGCCAGCTAT	sequencing	MWG
sax-13	ATCTCTGGATCCAGAGCCGAAATCAGCGATCAT	ectodomain 5'	Interaktiva
sax-14	ATCTCTGGATCCTATGCTACTGGTATCCGCGGT	ectodomain 3'	Interaktiva
sax-15	CCCTGTCGGGACCCCTATGAG	BamHI remove 5'	MWG
sax-16	CTCATAGGGGTCCCGACAGGG	BamHI remove 3'	MWG
sax-17	CGGGCGCTCGAGCTACTTGTCATCATCGTCTTTGTAGACAACGCAGACCTCGTCG AAGTC	sax-FLAG 3'	MWG
put-1	ATACACACGGTCAAG	reverse primer to put-2	Interaktiva
put-2	TACTGTCGAGCTACAGGTCTCCTCAGAGATAAGCTTCTGCTCTCCTAAGCAAT TCGTAGATTCCTT	PUT-MYC 3'	Interaktiva
put-3	TCCTATGCGGCCGCACAATGTCCAAATACGATC	ATG-5'	Interaktiva
put-4	TTGATGCGCAGGATGCCC	reverse primer to put-3	Interaktiva
put-5	GCATAGACGTCTACGCATGCGGCCTAGTCTCTGGG	reverse primer to put-6	Interaktiva
put-5B	GACCAAGTGCAGAGCC	sequencing	Interaktiva
put-6	CTTTACCTCGAGCTACAGGTCTCCTCAGAGATAAGCTTCTGCTCTCCTAAGCAA TTGCTAGATTCTTGGCGTC	PUT-MYC 3'	Interaktiva
put-6B	GTCCCATTCAGCTGC	sequencing	Interaktiva
put-7	CGCTGAGTCCATGGC	sequencing	Interaktiva
put-8	TATTATGGATCCTCTATTTGCCCGGAAGTCAT	ectodomain 5'	Interaktiva
put-9	TATTATGGATCCATTGCTGCCGTCCTGCGTCTT	ectodomain 3'	Interaktiva
			Interaktiva

bao-1	TTGATGCGCAGGATGCCC	reverse primer to bao-2	Interaktiva
bao-2	TCTCGGCTCGAGTCAGGCGTAGTCTGGGACGTCGTATGGGTAGTTCTTGACCTTGTCCTCCAC	BAO-HA 3'	Interaktiva
pMAD1	TCGAGGCCGTCGCGCCCGCGCCGCGGCGCA	3x MBE 5'	Interaktiva
pMAD2	GATCTGCGCCGGCGCGGCGCGCGACGGCC	3x MBE 3' - BglII	Interaktiva
pMAD3	AGCTTGCGCCGGCGCGGCGCGCGACGGCC	3x MBE 3' - HindIII	Interaktiva
pGL-M1	AATATTAGATCTGAGCGCCGAGTATAAATAGAGGC	pUAST-5' min-prom	Interaktiva
pGL-M2	TATTATAAGCTTCCAATTCCTATTAGAGTTC	pUAST-3' min-prom	Interaktiva
pGL-M3	TATTATAAGCTTTTTTATTCCACGTAAGGG	placW 3' short min-prom	Interaktiva
pGL-M4	TATTATAGATCTACCGAAGTATACACTTAAATT	placW 5' min-prom	Interaktiva
pGL-M5	TATTATAAGCTTTTCGTACTCAAAGTACGAAT	placW 3' long min-prom	Interaktiva
Not-Box1	TCGATAAGCGGCCGCAAC	NotI between ClaI/PvuII	MWG
Not-Box2	AGCTGTTGCGGCCGCTTA	NotI between ClaI/PvuII	MWG
Not-Box3	TCGAGTAAGCGGCCGCTCA	NotI between XhoI/HindIII	Interaktiva
Not-Box4	AGCTTGAGCGGCCGCTTAC	NotI between XhoI/HindIII	Interaktiva
Nhe-I	CATGCTAGCTGG	NheI-site in pAC5.1	Interaktiva
Nhe-2	AATTCAGCTAGCATGGTAC	NheI-site in pAC5.1	Interaktiva

C Fly stocks

Stock	description	from	GOP stock #
hs-flp (I)	heat shock induceable flippase		267
hs-Gal4 (III)	heat shock induceable Gal4		796
C765-Gal4 (III)	imaginal disc Gal4-driver	K. Basler	5
act<CD2>Gal4	flippase activated Gal4 driver		640
omb ^{P2-3} L3/FM7	omb driver/reporter		387
X35 (I)	omb-lacZ		82
btl-Gal4, UAS-GFPlacZ (III)	tracheal driver/reporter line		crossed from
UAS-GFPlacZ (III)	GFP and lacZ reporter		
UAS- <i>tkv</i> QD		K. Basler	
UAS-dpp	dpp wildtype	K. Basler	242
UAS-D-DEL	dpp deletion variant	M. Roth	
UAS-D-MYC/gla	dpp wildtype variant	M. Roth	
UAS-D-DUP/TM3	dpp duplication variant	M. Roth	
TM3/TM6	third chromosome balancer		
CyO/Sco	second chromosome balancer		
ScO/Sco	second chromosome balancer		
TM3-GFP/	third chromosome balancer (GFP marked)		
CyO-GFP/Sco	second chromosome balancer (GFP marked)		
dpp ^{d8}	hypomorphic dpp mutation		602
dpp ^{d12}	hypomorphic dpp mutation		
dpp ^{d14}	hypomorphic dpp mutation		600
dpp-Gal4	dpp imaginal disc Gal4 driver	K. Basler	225
dpp-Gal4	dpp imaginal disc Gal4 driver	Treisman	647

crossed stocks			
hs-flp, C765-Gal4	pUFWT-activation		
X35; CyO-GFP/Sco			
X35; TM3/TM6			
X35; D-DEL			
X35; D-MYC/CyO			
X35; D-DUP/TM6			
X35; D-DEL, dpp ^{d14} /CyO-GFP	wing rescue experiment		
X35; D-MYC, dpp ^{d14} /CyO-GFP	wing rescue experiment		
X35; dpp ^{d14} /CyO-GFP; D-DUP	wing rescue experiment		
dpp ^{d12} /CyO-GFP; dpp-Gal4	wing rescue experiment		(Gal4: from 647)

D Cloning details

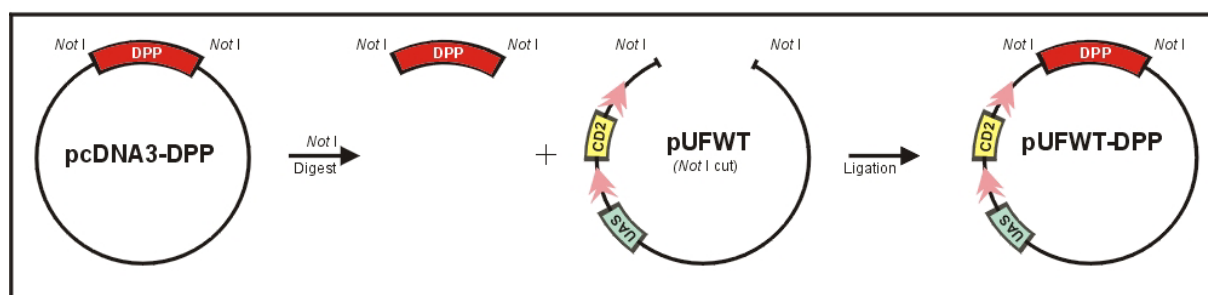


Fig 8-1: Cloning of pUFWT constructs

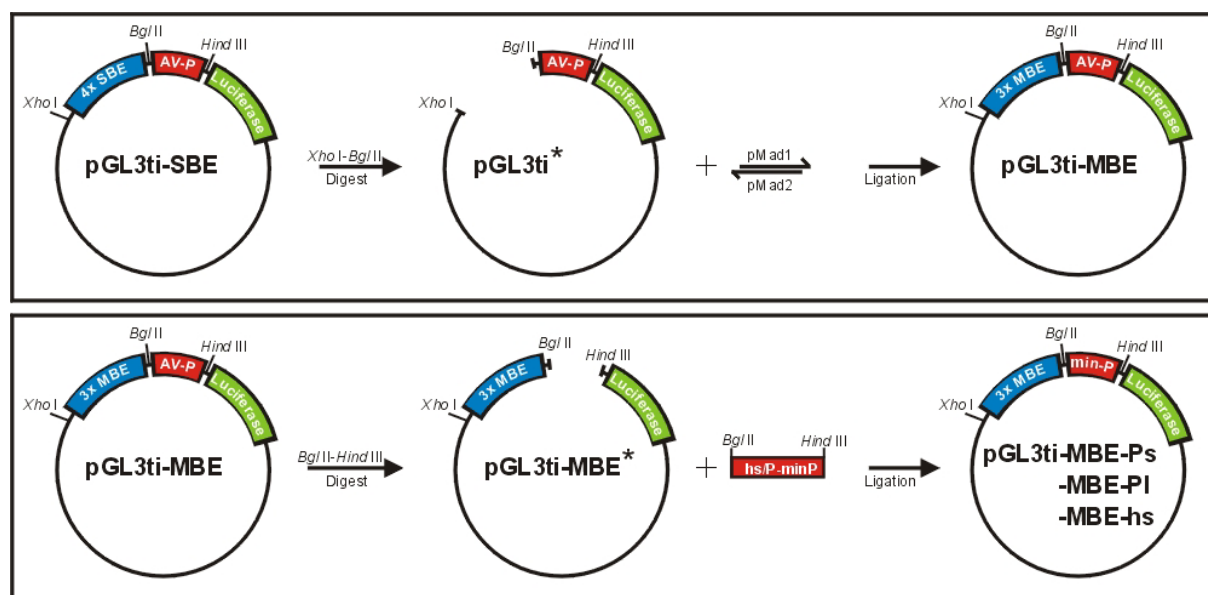


Fig 8-2: Cloning of pGL3ti-reporter

Publikationen

Journals

Rotzer, D., **Roth, M.**, Lutz, M., Lindemann, D., Sebald, W. and Knaus, P. (2001). *Type III TGF- β receptor independent signaling of TGF- β 2 via T β RIIB, an alternatively spliced TGF- β type II receptor*. EMBO J. 20(3): 480-490

Hassel, S., Schmitt, S., Hartung, A., **Roth, M.**, Nohe, A., Peterson, N., Henis, Y., Sebald, W. and Knaus, P. (2003) *Initiation of Smad-dependent and Smad independent Signaling via Distinct BMP-receptor complexes*. (Review) eingereicht bei: Journal of Bone and Joint Surgery

Roth, M. et al. Tissue specific Implication of matrix binding in DPP signaling (2003)
in Vorbereitung für: Current Biology

Veröffentlichte Abstracts

Rotzer, D., **Roth, M.**, Lutz, M., Sebald, W. and Knaus, P. (2000) *Identifizierung und Charakterisierung eines TGF- β 2 Rezeptors in Osteoblasten*. Osteologie, 9, Suppl. 1, 94

Rotzer, D., **Roth, M.**, Lutz, M., Lindemann, D., Sebald, W. and Knaus, P. (2000) *Type III TGF- β receptor independent signaling of TGF- β 2 via T β RIIB, an alternatively spliced TGF- β type II receptor*. Signal Transduction 1, Suppl. 1, 89

Lebenslauf

Persönliche Daten

Martin Roth
geboren am 29. Oktober 1971 in Würzburg
ledig

Schul Ausbildung

1978-1981	Grundschule Randersacker
1981-1982	Volksschule Schillingsfürst
1982-1991	Reichsstadt-Gymnasium Rothenburg o.d.Tauber
06/1991	Abitur

Wehr/Zivildienst

09/1991-12/1992	Zivildienst in der Sozialstation Fürth
-----------------	--

Hochschulausbildung

WS 1992/1993	Luft- und Raumfahrttechnik an der Universität Stuttgart
WS 1993/1994- WS 1997/1998	<p>Studium der Biologie an der Bayerischen Julius-Maximilians-Universität Würzburg</p> <p>Schwerpunkte: Genetik, Zoologie (Zell- und Entwicklungsbiologie), Immunologie und Virologie, Physiologische Chemie</p> <p>Diplomarbeit: am Lehrstuhl für Physiologische Chemie II und am Lehrstuhl für Genetik der Universität Würzburg Thema: Die Rolle der Decapentaplegic-Proteoglykan-bindungsdomänen in der Morphogenese von <i>Drosophila melanogaster</i></p>
seit 04/ 1998	<p>Promotion am Lehrstuhl für Genetik und Neurobiologie sowie am Lehrstuhl für Physiologische Chemie II der Universität Würzburg</p> <p>Thema: Functional and developmental characterisation of matrix binding sites in <i>decapentaplegic</i></p>

Erklärung

Erklärungen gemäß §4 Absatz 3 der Promotionsordnung der Fakultät für Biologie der Bayerischen Universität Würzburg vom 15. März 1999.

1. Ich erkläre ehrenwörtlich, die vorliegende Dissertation selbständig angefertigt zu haben und keine anderen als die von mir angegebenen Quellen und Hilfsmittel benutzt zu haben.
2. Ich erkläre desweiteren, daß die vorliegende Arbeit weder in gleicher noch ähnlicher form bereits in einem anderen Prüfungsverfahren vorgelegen hat.
3. Ich erkläre weiterhin, daß ich früher keine akademischen Grade erworben habe oder zu erwerben versucht habe.

Würzburg, den 24.02.2003

Martin Roth

Danksagungen

An erster Stelle möchte ich Walter Sebald danken, der mich für dieses Projekt begeistert hat, meine Arbeit stets aufgeschlossen und mit großem Interesse verfolgt hat und mir bestmögliche Unterstützung hat zukommen lassen.

Zu sehr großem Dank bin ich meinen beiden weiteren Betreuern, Petra Knaus und Gert O. Pflugfelder verpflichtet für Ihre große Unterstützung und Ihre vielen hilfreichen Ideen und Vorschläge, aber auch für die Freiheiten, die ich genossen habe. Auch konnten Sie mich stets motivieren und mich durch lange Durststrecken der Misserfolge führen.

Besonderer Dank gilt auch Sylke Hassel und Matthias Porsch, die nicht nur sehr hilfreiche und diskussionsfreudige Laborkollegen, sondern auch gute Freunde für den nötigen Freizeitausgleich waren.

Spätestens hier gilt der Dank der fast einmaligen (es kann nur zwei geben!) Pottsau Sebastian Scharf, ohne die ich nicht wüßte, was ein Labor wirklich lebenswert macht.



Spezielle Hilfestellungen habe ich erfahren von Joachim Nickel bei der Virenexpression, der Rezeptoraufreinigung und der Biacoremessung, von Nicole Hopf bei der Ligandenaufreinigung, von Thomas Müller und Markus Klein bei der analytischen FPLC und von Maike Gottermeier bei den Kristallisationsversuchen. Ihnen allen gilt mein besonderer Dank, den Kellerasseln auch für gelegentliches Asyl mit kulinarischer Versorgung.

Ein großes Dankeschön gilt Evelyn Wittstadt, die sich auf das Wagnis DPP mit eingelassen hat und für 9 Monate eine große Bereicherung und Leidensgenosse bei Fliege, Crosslink und S2-Zellen war.

Dankbar bin ich auch den vier F-Praktikanten Tim, Christiane, Sebastian und Anja, die ich betreuen durfte. Ihr Engagement und Ihre Geduld bei meinen häufigen Abwesenheiten sind dabei besonders hervorzuheben.

Desweiteren danke ich Wolfgang Hädelt, Nadine Hemmrich, Yvonne Kehl, Tanja Lutz und Simone Schmitt, deren kleine und große technische Hilfen meine Arbeit sehr unterstützt haben.



Außerdem danke ich allen meinen weiteren LaborkollegInnen Aditya, Anja, Anke, Britta, Diana, Elke, Florian & Florian, Gaby, Kerstin, Kristina, Markus, Marion, Sammar, Simone G., Sören und Tobias für eine harmonische Laboratmosphäre, wertvolle Diskussionen und auch sehr erinnerungswürdige Erfahrungen außerhalb des Biozentrums sowie allen weiteren ehemaligen und jetzigen Kollegen der Lehrstühle für Genetik und Neurobiologie sowie für Physiologische Chemie für konstruktive Zusammenarbeit und eine immer angenehme Atmosphäre.

Meiner Fitneß-crew bestehend aus Sascha, Joachim, Christian, Nicole, Nadine, Uschi, Sören und Isabell, die stets dafür sorgen, daß ich einen Ausgleich für das viele Treppensteigen bekomme.

Mein Dank gilt auch Martin Heisenberg und Erich Buchner für unkomplizierte Überbrückungen von Finanzierungslücken und Andrea Wizenmann für stetigen Nachschub an „Mini-chicks“.

Der letzte und größte Dank gilt meinen Eltern und Freunden, deren voller Unterstützung ich mir immer sicher sein konnte und die mich nie haben vergessen lassen, daß es ein sehr viel schöneres Leben außerhalb des Labores gibt.